ABSTRACT

Title of Dissertation: THE INFLUENCE OF VIMENTIN INTERMEDIATE FILAMENTS ON HUMAN MESENCHYMAL STEM CELL RESPONSE TO PHYSICAL STIMULI

Poonam Sharma, Doctor of Philosophy, 2017

Dissertation directed by: Associate Professor Dr. Adam H. Hsieh, Fischell Department of Bioengineering

Mesenchymal stem cells (MSCs) are increasingly being investigated as a therapeutic cell population for a variety of diseases. However, these therapies are limited by an imperfect understanding of how MSCs interact with and respond to their physical environment. Cell response to external stimuli is mediated by the cytoskeleton. Of the cytoskeletal proteins, understanding of vimentin intermediate filaments' influence on MSC behavior is still lacking, despite increasing evidence that they are involved in many cellular processes. In this work, we investigated the influence of vimentin intermediate filaments in modulating MSC characteristics and behavior by using lentiviral shRNA transduction to decrease vimentin levels in MSCs through RNA interference.

First, the contribution of vimentin intermediate filaments to the deformability of MSCs within agarose hydrogels was examined. Vimentin-deficient MSCs were found

to be less deformable than control cell populations and this resistance to deformation may be due to the compensatory role of actin microfilaments. Next, to determine how vimentin affects the ability of MSCs to interact with various microenvironments, we examined cell spreading on different extracellular matrix proteins, multiple substrate stiffness', and in response to fluid shear stress. An intact vimentin network was found to be necessary for unimpaired spreading on fibronectin, but only on stiffer substrates. Further, vimentin appears to be involved in resisting cell area changes in response to low fluid shear stress. Vimentin's physical interaction with focal adhesions, rather than an impact at the transcriptional or translational level, may contribute to the cell spreading response observed. Finally, in the third part of this work, we examined the influence of vimentin on chondrogenic differentiation of MSC populations. Unexpectedly, we found that vimentin may not be involved in chondrogenic differentiation in late stage chondrogenic cultures. Instead, the culture condition-dependent microenvironment may have a greater impact, particularly in gene expression of matrix degrading enzymes and the αV integrin subunit. Altogether, these studies indicate a role for vimentin in the MSC response to physical stimuli. Moreover, this work furthers the dialogue surrounding MSCs' interaction with different environments, the understanding of which will be critical for the development and evaluation of cell-based therapies.

THE INFLUENCE OF VIMENTIN INTERMEDIATE FILAMENTS ON HUMAN MESENCHYMAL STEM CELL RESPONSE TO PHYSICAL STIMULI

by

Poonam Sharma

Dissertation submitted to the Faculty of the Graduate School of the
University of Maryland, College Park, in partial fulfillment
of the requirements for the degree of
Doctor of Philosophy
2017

Advisory Committee:
Associate Professor Dr. Adam H. Hsieh, Chair
Professor Dr. John P. Fisher
Assistant Professor Dr. Giuliano Scarcelli
Assistant Professor Dr. Kimberly Stroka
Professor Dr. Wenxia Song, Dean's Representative

Acknowledgements

I would like to start by thanking my advisor, Dr. Adam Hsieh for his support and guidance over the course of the last few years. His mentorship has helped me become the researcher that I am today. I would also like to thank my committee members Drs. John P. Fisher, Giuliano Scarcelli, Kimberly Stroka, and Wenxia Song, as well as our collaborator, Dr. Diane Wagner, for all their support towards the completion of this work.

Also, thanks to all of the undergraduate researchers who have helped me over the years, especially Michelle Patkin and Zachary Bolten for their tremendous help in the laboratory. I would also like to especially acknowledge the past and present members of the Orthopaedic Mechanobiology Lab, without whom this work would not have been possible, whether through scientific guidance or emotional support; especially, Lauren Resutek, Dr. Carlos Luna, and Dr. Julianne Twomey. Thank you to the BIOE graduate student village that has stood with me these last few years, with a smiling face, a joke, or a shoulder. Finally, thank you to my parents and my brother for their undying support, my friends for being there and much needed distractions, and Karthik Paco Sangaiah for all of the above. Every one of you made this possible - thank you!

"We have but to toil awhile, endure awhile, believe always, and never turn back."

–William Gilmore Simms

Table of Contents

List of Tables

List of Figures

Chapter 1: Background and Significance

1.1 Mesenchymal Stem Cells (MSCs)

MSCs are a cell population that is increasingly being investigated for therapeutic applications. As strictly defined by the International Society for Cellular Therapy, MSCs are a bone marrow derived stromal cell population that is plastic adherent, positive for the cell surface markers CD105, CD90, CD73, MHC-1, negative for the cell surface markers MHC-II, CD11b, CD14, CD34, CD45, CD31, and can differentiate *in vitro* into osteoblasts, chondrocytes, and adipocytes [1]. However, MSCs in clinical use are generally defined as self-renewing multipotent cells that can differentiate into cells from all skeletal tissues [2]. These cells have also been isolated from a variety of other tissues [1,2]. The desire to use MSCs for therapies can be attributed to the combined advantages of their differentiation potential, immunomodulation properties, paracrine effects, and homing capability [1,3]. Therapeutically, they are thought to only remain transiently in the intended location due to cell death or migration, but influence damaged tissue during this time [4]. MSCs are being investigated for the treatment a variety of diseases, including diseases affecting orthopaedic tissues such as articular cartilage.

1.1.1 Current Research in Treating Cartilage Disease

1.1.1.1 Articular Cartilage Tissue

Articular cartilage is an aneural and avascular tissue with a low resident cell population that is found at the interface of joints. It provides a low friction surface for smooth joint articulation and load bearing [5]. The tissue consists of 70-80% water,

with the remaining solid fraction made up of 50-75% collagen and 15-30% proteoglycans [5]. Cartilage cells, chondrocytes, are responsible for maintenance of the tissue [5] and nutrients and oxygen diffuse to the cells from the synovial fluid in the joint [5,6]. The cells are surrounded immediately by a pericellular matrix (PCM) containing a high concentration of type VI collagen [7]. Surrounding this PCM and making up a large portion of the remaining tissue is type II collagen, which is about half of its dry weight [5]. Other collagen types present in the tissue include types VI, IX, XI [5]. Proteoglycans are large molecules trapped within the tissue's collagen network and are made up of polysaccharide chains or glycosaminoglycans attached to protein cores. Aggrecan, the most predominant, has a hyaluronan protein core with varying main polysaccharide chains, primarily chondroitin or keratin sulfates [5,7]. Negatively charged proteoglycans are responsible for attracting and maintaining fluid within the tissue. This fluid content and its rapid pressurization are responsible for supporting and dissipating compressive loads and allowing frictionless joint movement [5,7]. Other proteoglycans include decorin, biglycan, fibromodulin, perlecan, versican and lumican [5,7].

1.1.1.2 Osteoarthritis

While injuries leading to cartilage defects and trauma can be damaging and have long lasting impacts on subsequent disease progression, osteoarthritis (OA) is a disease of exacerbated dysregulation. The Center for Disease Control and Prevention has reported that 22.7% of adults, and 49.7% of adults over the age of 65, have diagnosed osteoarthritis [8], with symptoms including pain and functional disability [9]. OA is thought to be characterized by an imbalance of catabolic and anabolic regulation,

which is then aggravated by both normal and abnormal loading [5,7,9]. Increases in collagen and aggrecan degradative enzymes, such as matrix metalloproteases (MMPs) and aggrecanases break down the main extracellular matrix (ECM) components [7,9]. As the disease progresses, visible fissures develop in the tissue and it loses proteoglycans until the tissue is eroded [5]. While it is unclear what causes the pathogenesis of OA, these changes to the tissue are manifested by chondrocytes. They lose the ability maintain the tissue in an increasingly adverse environment of abnormal loading and inflammation [7,9]. As the tissue breaks down, the ECM [5] and the PCM [10] become less stiff than normal and even the mechanical properties of OA chondrocytes become impaired [11].

1.1.2 Current Therapeutic Outlook for MSCs

1.1.2.1 Cell Therapy

As of June 2015, there were almost 500 reported clinical trials using MSCs with the greatest number being in the Phase I/II arena [1]. These trials focused on a wide variety of diseases, with bone and cartilage diseases making up the largest percentage, around 19%, of trials [1] (Figure 1.1).

Figure 1.1 MSC Clinical Trials as of 2015 (n=493). 19.1% (n=94) of trials targeting bone and cartilage diseases. Other targeted diseases included Neurological disease (17.8%, n=87), Cardiovascular disease (14.8%, n=73) and Graft vs. Host Disease (GVHD) (7.2%, n=35). Additional targets included lung, kidney, liver, hematological, and Crohn's diseases, diabetes, and others [1].

Currently, many of the MSC therapies under investigation consist of single or multiple intraarticular injections of cells into the joint (Figure 1.2), with the injection either being soon after isolation and concentration of the collected cell population or after a period of *ex vivo* expansion, purification, and characterization of the cells [12]. The injected cell dose in most studies varies from 10 million to 100 million MSCs per dose [12–14]. However, cell death or migration out of the intended location has been observed [4]. For example, cells that remained in a caprine knee joint after injection were found to be localized to the meniscal or synovial membrane surfaces rather than cartilage tissue [12,15] (Figure 1.2). Due to such studies, it has been proposed that MSCs' primary mode of therapeutic action is through coordinating regeneration via trophic or immunomodulatory effects, rather than through direct integration with degenerated or damaged cartilage tissue [12,16].

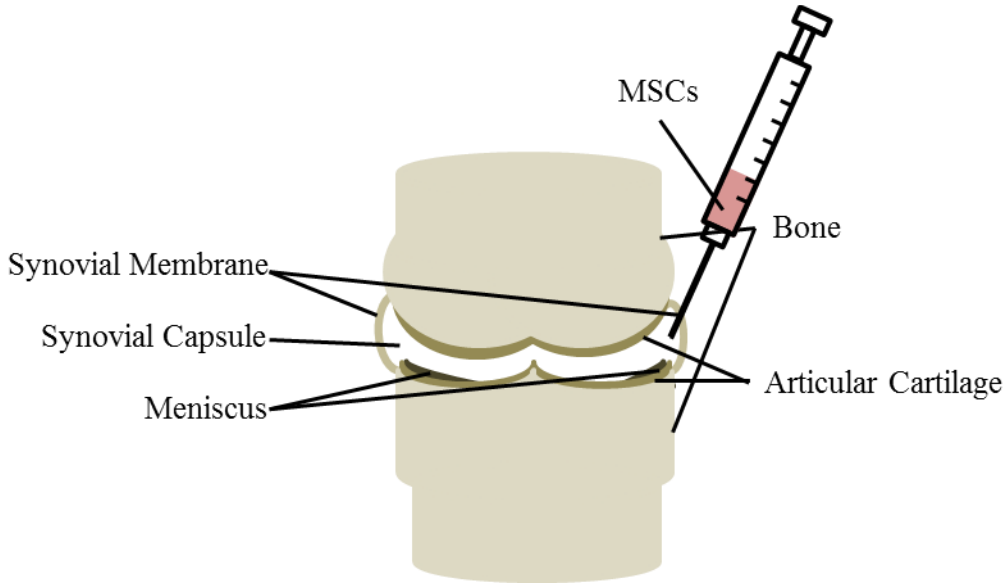

Figure 1.2 Schematic of knee joint and intraarticular injection of MSCs.

As of 2016, there were 58 active clinical trials using MSCs to target OA [4]. Thus far, a few trials focused on OA have shown promising results [1–3]. Direct injection of autologous MSCs into osteoarthritic knee cartilage in pilot studies improved cartilage tissue and quality of life parameters after 6 [13] and 12 months [14]. A 2 year follow-up to the one year study demonstrated consistent results, implying a sustained benefit up to that point [17]. These findings are encouraging. However, distinctive healing and regeneration, in conjunction with already studied quality of life parameters, remain to be achieved and/or measured in many studies. One strategy for improving the therapeutic effect of MSCs is to incorporate a biomaterial cell carrier or scaffold, which would serve potentially limit cell death and lengthen the time that MSCs are present in the desired environment [4,12].

1.1.2.2 Tissue Engineering Strategies and Goals

Tissue engineering strategies combine the use of biomaterials and/or stimulatory factors with cells for the treatment and regeneration of tissues. While biomaterial only strategies have historically been used in the treatment of cartilage, tissue engineering strategies using MSCs for clinical cartilage repair are still very much in their infancy. Use of chondrocytes, both in isolation and in conjunction with biomaterials has been more widely investigated and used clinically thus far [4]. In fact, Carticel is a marketed autologous chondrocyte therapy used in conjunction with porcine derived collagen [4] . Comparatively, there is only one biomaterial-MSC product that is being investigated and is actually on the market in South Korea: Cartistem using MSCs with hyaluronic acid [4,18]. While chondrocytes have been more widely studied than MSCs up until now, their use is limited by a low capacity for stable *ex vivo* expansion, limited cell numbers, and donor site morbidity [4,19,20]. However, biomaterials that are being investigated in conjunction with chondrocytes can also be used with MSCs. A wide variety of biomaterials are being researched, including both natural and synthetic materials to be used as scaffolds or as injectables [4,6]. These include the natural biomaterials fibrin, hyaluronan, agarose, alginate, and collagen as well as synthetic biomaterials such as poly lactic acid and polyethylene glycol [4,6,19]. Incorporation of growth factors into biomaterial scaffolds for MSC therapy could also serve to tune their trophic behavior [12]. While differentiation of MSCs within biomaterial scaffolds is common in academia, further research is needed to better understand the governing cellular mechanisms for success *in vivo*.

1.1.3 Challenges for Stem Cell-based Therapies

As clinical research is still in the early stages, there have been many trial failures, either due to lack of sufficient data or limited clinical benefit [2]. However, there have been promising initial results that warrant further improvement of MSC therapies. There are still many challenges ahead including short residence time [4,21,22] and unknown mechanisms of action for therapeutic and off target effects, especially due to cell source [2,21,23]. Isolated cell populations are heterogeneous [3,21,22], but the development of standards and protocols for isolation may help provide consistent cell populations for evaluation [3]. However, potential cell death, limited therapeutic matrix formation, mineralization present in cartilage tissue, and growth of fibrous tissue instead of healthy cartilage remain as hurdles [4,22]. The combined use of cells with biomaterials introduces additional challenges, including development of scaffold materials, optimization of scaffold mechanical properties, and design of *in vitro* culture strategies. The comparative safety, benefit, ease of use, and cost of autologous and allogeneic MSCs are also still being evaluated [22]. Further, uncertainty regarding appropriate cell dose, underdeveloped manufacturing processes, and high cost need to be resolved [3,17,21,23]. The limited success in the clinic thus far may simply be an indication of the field's age and potential. Better understanding of MSC source, properties, functions, and MSCs' response to their physical environment is needed to design and evaluate these therapies as they are developed and analyzed.

1.2 Behavior of Mesenchymal Stem Cells

1.2.1 Homing and Adhesion

Migration of MSCs to damaged tissue, and subsequent engraftment in the tissue, is an essential component of their therapeutic function and is an established attribute of MSCs [24–26]. MSCs' engraftment in new environments, damaged or physiological, depends on the characteristics of the environment itself, such as the state of the ECM. Adhesion and spreading of MSCs has been shown to be modulated by changes to substrate stiffness [27–29], substrate composition (e.g. ECM protein) [28–32], the density of ECM proteins on substrates [33], cell shape [34,35], and cell size [36], with these all affecting MSC differentiation. Fibronectin and type I collagen are two ECM proteins that have been used in research frequently to promote MSC adhesion to surfaces, as MSCs have shown a high affinity for attachment and spreading on them [31,32]. Further, differences in cell area, especially on substrates of different stiffness', have been associated with changes in MSC function and characteristics as well, such as cellular stiffness, differentiation potential, and branching of neurogenic MSCs [27,34,37,38]. Substrate stiffness itself has also been correlated with changes in cell area and differentiation potential of the cells, specifically soft substrates leading to smaller cells and more adipogenic lineage and stiff substrates leading to larger cells and more osteogenic lineage [27,29,39,40].

1.2.2 Differentiation - Chondrogenesis

Another component of MSC therapeutic function is their demonstrated capacity to undergo differentiation down multiple lineages, including toward osteoblasts,

adipocytes, myoblasts, tenocytes, chondrocytes, as well as a variety of other cell types [1] (Figure 1.2). Chondrogenic differentiation, as with many other lineages, is primarily achieved through the use of growth factors, such as those in the transforming growth factor-β (TGFβ) family, insulin-like growth factor (IGF) family, or some combination of multiple growth factors [6,20]. The TGFβ family, including TGFβ1, 2, and 3 along with several bone morphogenic proteins are well established in their capacity for chondrogenic stimulation [6].

Chondrogenic differentiation of MSCs is generally conducted in pellet cultures or within biomaterials and induced by growth factors of the TGFβ family (Figure 1.3). However, high density monolayer culture is also used to verify chondrogenic potential. MSC chondrogenesis within pellet cultures is used to recapitulate developmental condensation-like differentiation through to terminal hypertrophy [41,42]. However, while MSC pellet cultures are used frequently to examine the progression of *in vivo*-like chondrogenesis, they are impractical for therapeutic use due to their size and hypertrophic differentiation. For regenerative or tissue engineering applications, growth factors and MSCs are combined within biomaterial scaffolds with properties that can be manipulated. These scaffolds can be designed to have an interconnected structure, can be biodegradable, can allow for cell attachment and/or tissue development, and their mechanical properties can be modulated [5]. A wide variety of materials have been used successfully for chondrogenic differentiation of MSCs, including alginate, agarose, gelatin, and fibrin [6,6,20,43–50].

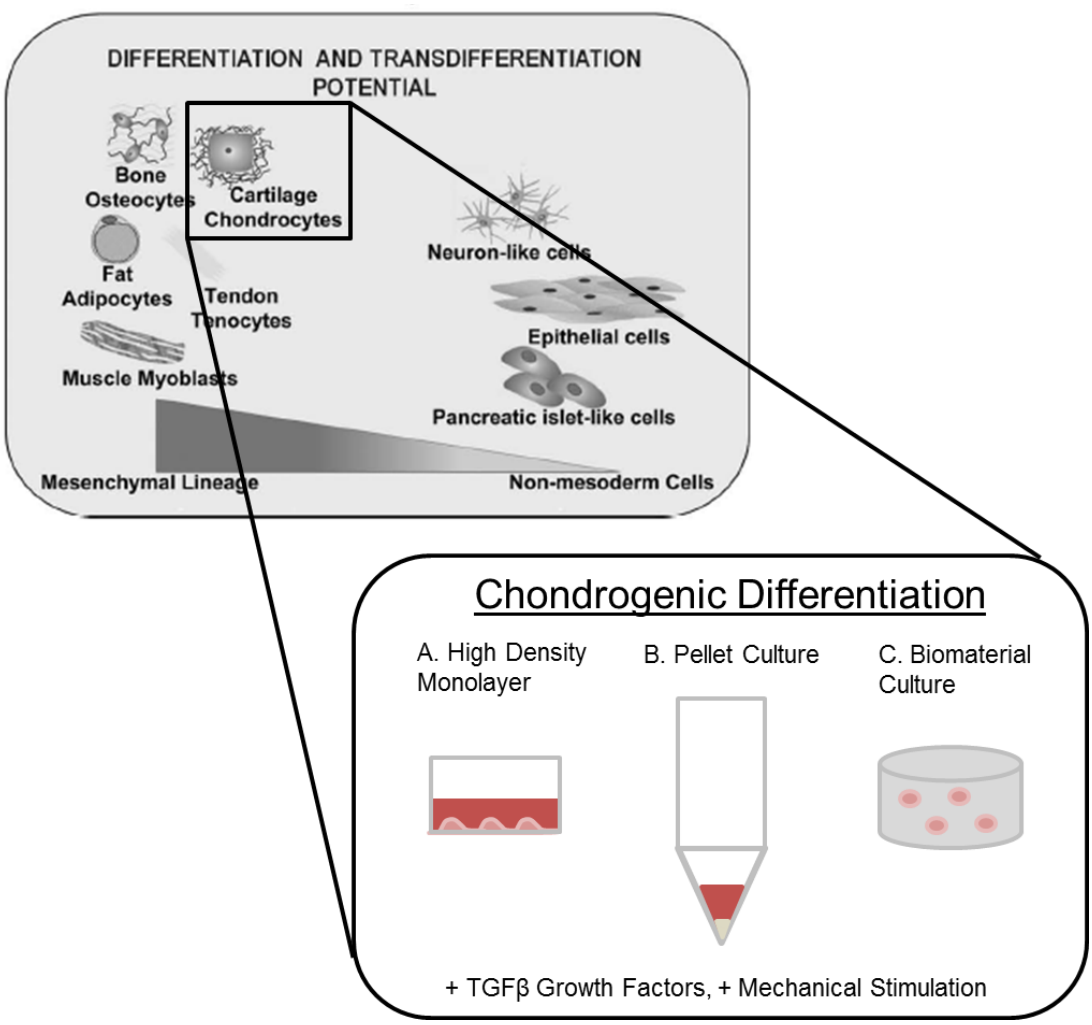

Figure 1.3 Schematic depicting MSC differentiation potential and various chondrogenic differentiation culture environments. Schematic adapted from Squillaro, et al (2016)[1].

1.2.3 Mechanosensing and mechanical properties

MSC mechanical properties and their mechanosensitivity are tied to their capacity to differentiate [51–53]. Differentiation of MSCs down different lineages has been found to cause changes in MSC mechanical properties [52–56]. Changes in surface stiffness from stiff to soft also promote durotaxis prior to differentiation [57]. Further, the physical properties of MSC environments, such as changes in substrate stiffness, have been found to initiate MSC differentiation along different lineages [27]. Mechanical loading

also typically induces differentiation of MSCs [51]. A variety of mechanical stimuli, including dynamic compression, hydrostatic pressure, osmotic pressure and fluid flow, in conjunction with growth factors, have been used to stimulate chondrogenic differentiation and the subsequent extracellular matrix deposition and tuning of tissue/scaffold mechanical properties [51,58]. Loading magnitude, frequency, and duration all affect the outcome of the stimulation, but dynamic compression [43,49,50,58] and hydrostatic pressure [48,58–64] have been used most frequently to successfully promote ECM deposition and increase chondrogenic gene expression. Fluid flow in isolation has typically been shown to promote osteogenesis [65], but can also stimulate fibrocartilage ECM deposition and gene expression [66]. Aside from effects on differentiation, mechanical stimuli, specifically fluid shear stress has been shown to potentially promote increases in proliferation and migration through calcium and mitogen-activated protein kinase signaling pathways [65,67–69]. From a therapeutic perspective, mechanical loading of MSCs has also been shown to promote the secretion of various growth factors [70] and MSC spreading on endothelial cell layers [71].

1.3 Vimentin intermediate filaments

One tool that MSCs use to sense and respond to their physical environment is the cytoskeleton, which in MSCs primarily consists of actin microfilaments, microtubules, and vimentin intermediate filaments. Together with other proteins, the cytoskeleton serves to structurally support cells, allow for cell movement and division, assist in mechanosensing, and additionally support the trafficking of intracellular molecules [52,72]. Actin microfilaments have a well-established role in cell shape changes, migration, and adhesion [52,72]. Further, the disruption of actin and the

negative modulation of the RhoA/Rho-associated kinase (ROCK) pathway both promote chondrogenesis [52,73,74]. MSC mechanical properties also appear to be dependent on actin microfilaments [52,56,75,76]. Comparatively, microtubules are involved in cell division, organelle and protein transport, as well as cell migration [72], but appear to have limited involvement in chondrogenesis or MSC mechanical properties [52].

While actin and microtubules are well studied components of the cytoskeleton, the role of vimentin intermediate filaments (IFs) in MSC response to external stimuli still requires further clarification. Vimentin is a 57kDa type III intermediate filament primarily expressed in cells of the mesenchymal lineage [77,78]. Structurally, vimentin is made up of a central alpha helical rod with head and tail domains [79]. Together these monomers form coiled-coil dimers and then organize into staggered antiparallel tetramers (Figure 1.4). Groups of tetramers form unit-length filaments that join to form mature vimentin filaments that are involved in cellular function. Vimentin IFs connect the cell membrane with the nucleus, promoting transduction of information from the cell surface to the nucleus [80].

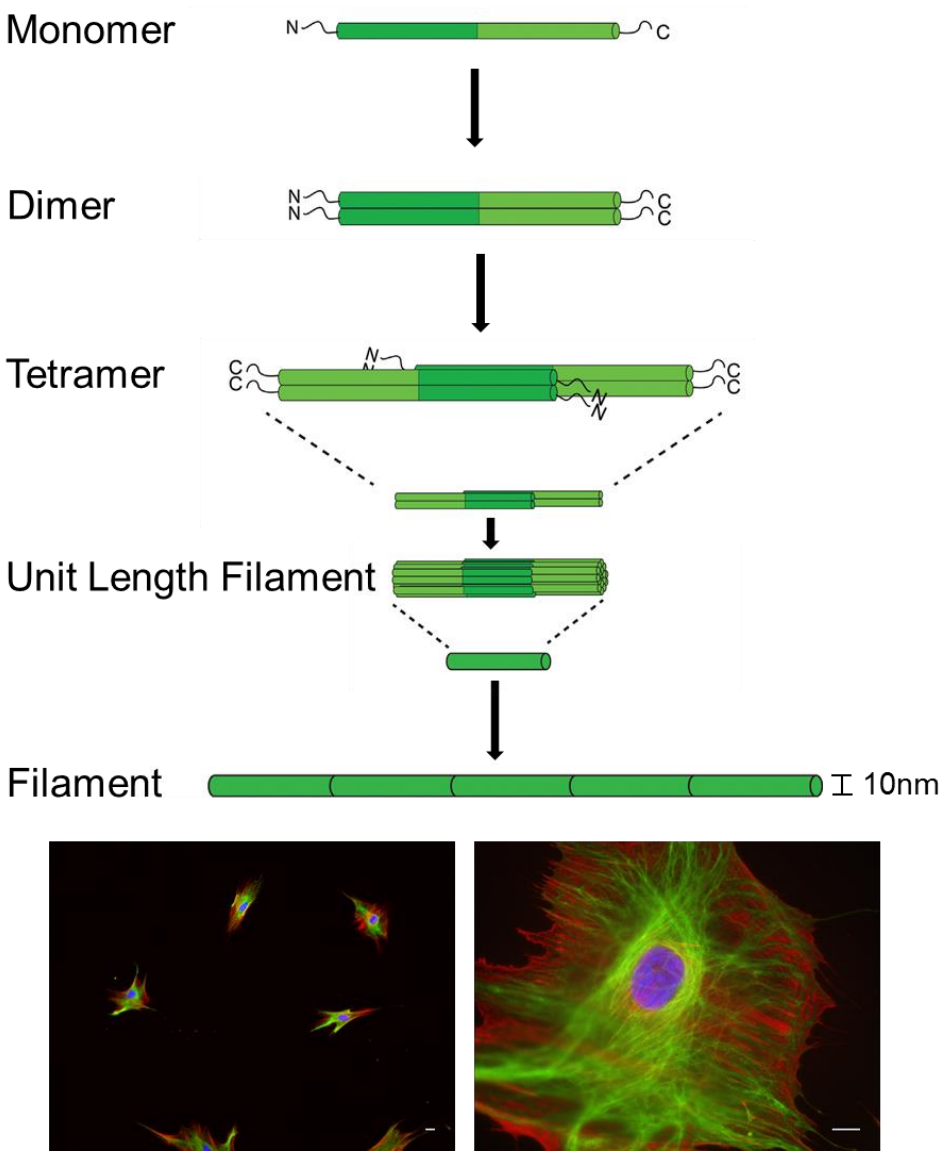

Figure 1.4 Vimentin intermediate filament formation and vimentin in mesenchymal stem cells imaged at low and high magnifications. Scale bars 20µm and 10µm, respectively. Vimentin = green, F-actin (phalloidin) = red, nucleus (DAPI) = blue. Schematic adapted from Robert, *et al* (2016) [81].

1.3.1 Vimentin Involvement in Disease

Early research suggested that vimentin was not an essential protein; vimentin null mice appeared to survive normally without any obvious defects [82]. However, later research found that a lack of vimentin in mice led to impaired wound healing and resistance to renal pathologies [83,84]. Similarly, cerebellar defects, impaired equilibrium, altered action coordination, and impaired steroid production were observed [85,86]. Further, vimentin appears to play a role in a variety of diseases. Upregulation of vimentin is established as a key marker in the epithelial to mesenchymal transition of tumor cells, leading to poor prognosis and metastasis [78,87,88]. Mutations in vimentin appear to be linked to cataract formation [89] and antibodies against vimentin with altered post-translation modifications are measured to detect early rheumatoid arthritis [90]. Interestingly, in giant axonal neuropathy, vimentin present in non-neural tissues has been found to be disrupted [80,91]. Vimentin has also been found to be disrupted or dispersed in osteoarthritic chondrocytes [92,93]. Damaged osteoarthritic chondrocytes were less stiff, and therefore their stiffness was less affected by vimentin disruption, compared to healthy chondrocytes, in which vimentin disruption led to a decrease in stiffness [11]. In contrast, another study found that vimentin disruption caused a decrease in stiffness and viscoelastic parameters in both healthy and osteoarthritic chondrocytes [94]. Notably, vimentin has also been found to be downregulated in MSCs isolated from osteoarthritic patients [95]. Taken together, altered or absent vimentin is not as benign as originally observed and bears further study. Beyond involvement in disease, it has also been found to be involved in

a variety of cellular properties and functions including mechanical properties, cellular spreading, and chondrogenesis.

1.3.2 Vimentin in Cellular Mechanosensitivity and Mechanical Properties

Vimentin filaments are thought to maintain cellular integrity due to their intrinsic mechanical properties. They have actually been found to have a strain dependent response to load; at low strain vimentin networks remain less rigid, but then harden at high strains and resist breakage [96,97]. Their properties make vimentin filaments a part of the cellular machinery that is involved in maintaining or adapting cellular mechanical properties in response to manipulation or loads. Correspondingly, vimentin has been tied to the ability of cells to transduce the effects of fluid shear stresses [98] and are physically displaced within endothelial cells in response to fluid shear *in vitro* [99]. Similarly, they have been shown to be involved in the dilatory response to fluid shear flow in harvested arteries [100]. There is evidence that vimentin responds to various mechanical loads through reorganization. This has been observed with changing environmental stiffness [101], hydrostatic pressure loading [101], swelling pressure [102], compressive load [102], and single impact loads [103]. There is still growing evidence as to how vimentin participates in mechanotransduction, but research indicates that vimentin's interaction with focal adhesions and integrins may play a role [104–110].

Vimentin has also been found to be critically involved in the mechanical properties of cells [97]. Well spread vimentin-null fibroblasts were found to have decreased cytoplasmic stiffness, but not cortical stiffness [111]. In other studies, vimentin-null

fibroblasts, endothelial cells, and cancer cells were found in general to have decreased cellular stiffness [38,88,112,113]. Similarly, vimentin-deficient fibroblasts exhibited impaired stiffening capacity, cellular mechanical stability at high strain, and decreased contractility[112,113], but the effect on contractility may be substrate and cell density specific [38]. Comparatively, increases in vimentin lead to increases in cellular stiffness [114,115]. While these measurements were taken in cells that were spread on a substrate, suspended or semi-suspended cells demonstrated similar decreases in cellular mechanical properties in response to vimentin disruption. Vimentin network collapse due to pharmacological drug treatment led to a decrease in cellular stiffness in lymphocytes [116] and natural killer cells [117]. Similarly, disruption of vimentin in chondrocytes or chondrocyte-like cells yielded a decrease in elastic moduli and viscoelasticity parameters [11,94,118]. In contrast, other studies found that disruption of vimentin decreased compressibility of chondrocytes [119].

1.3.3 Vimentin in Cellular Spreading and Adhesion

Vimentin IFs have also been found to be involved in cellular adhesion and spreading in a variety of cell types. Vimentin deficiency been linked to slower adhesion by cancer cells [87,120], decreased adhesion strength when subjected to fluid flow [105], and altered adhesion structure formation (i.e. focal adhesions). Vimentin filament co-localization with vinculin-positive focal adhesions has been long established [121] and vimentin deficiency has been linked to smaller and fewer vinculin-positive focal adhesions in cancer cells [88]. Comparatively, in vimentin-null fibroblasts, focal adhesions were found to be irregular and did not organize into distinct and separate contacts as assessed through vinculin and talin visualization [113]. Vimentin IFs have

also been shown to physically interact with a variety of integrin subunits including αVβ3, α2β1, α6β4, α5β1, as well as β3 and β1 integrin subunits [104–110]. Vimentin deficiency yielded smaller αVβ3 integrin-positive focal adhesions in endothelial cells [105] and it was also shown to affect the expression of β1 integrin subunits. A decrease in vimentin has led to decreases in β1 integrin subunit protein levels as well as cell surface β1 integrin subunits [88,107]. Comparatively, overexpression of vimentin has been observed to lead to an increase in β1 integrin subunit levels [88]. It has been suggested that these interactions between vimentin, focal adhesions, and integrin subunits may be tied to cytoskeletal linker proteins such as plectin and filamin A, which are known to interact with vimentin [107–109,122].

1.3.4 Chondrogenesis

Vimentin has also been implicated in maintenance of chondrocyte phenotype or early stage chondrogenesis of progenitor cells. However, studies evaluating vimentin-null mice did not assess deleterious effects of vimentin-deficiency on articular cartilage development [82–84]. Studies disrupting vimentin or decreasing vimentin found decreased chondrogenic gene expression in chondrocytes and in chondrogenic MSCs [123,124]. Disruption of vimentin in chondrocytes resulted in decreased aggrecan and collagen gene expression, sulfated glycosaminoglycan (sGAG) and collagen degradation, and collagen synthesis [123]. A decrease of vimentin in progenitor cells similarly caused decreased aggrecan and type II collagen gene expression as well as sGAG and type II collagen deposition [124]. However, these studies were conducted in the early stages of *in vitro* culture and it is not yet clear whether vimentin influences chondrogenesis over longer culture times. Studies have also suggested that vimentin

is involved in sensing hydrostatic pressure loading used for the stimulation of chondrogenic differentiation. The change from punctuated vimentin organization to diffuse organization was found to be associated with hydrostatic pressure stimulation of chondrogenesis [101]. Thus, it appears the vimentin may have some influence on the progression and stimulation of chondrogenesis.

1.4 Methods for Manipulating Vimentin

Studies evaluating vimentin use a variety of techniques to manipulate vimentin networks for study. Vimentin-null mice and the isolation of then vimentin-null cells has been used [38,111,113,125]. However, simpler and more cost-effective techniques are also commonly implemented in research to approximate the effect of complete ablation of vimentin expression such as the use of pharmacological disrupters [11,94,116–118,126], introduction of oncogenes [127] and mutated proteins [128], and RNA interference [98,105,124].

1.4.1 Disruption of the Vimentin network

Manipulation of the cytoskeleton is often achieved by using chemical disruptors. Specifically for vimentin, the most commonly used chemical disruptor is acrylamide [11,94,112,118,119,123,126,129,130], however withaferin A [117] and calyculin A [116] have also been used to similar effect. Withaferin A causes disruption and aggregation of vimentin while Calyculin A targets vimentin phosphatases inducing disruption of the vimentin network [97]. Calyculin A however exhibits off target effects due to its impact on other cellular phosphatases [97]. Acrylamide treatment has been seen to cause a perinuclear collapse and aggregation of vimentin [112,123,126,129,130] as well as diffuse vimentin

staining throughout the cell [94]. Perinuclear collapse of the vimentin network has also been induced by the overexpression of the oncogene simian virus 40 large T antigen [127], and microinjection of vimentin mimetic/dominant-negative mutant peptides [131,132]. Aggregation and elimination of vimentin has similarly been observed through overexpression of gigaxonin [91]. Interestingly, treatment with platelet derived growth factor was also found to cause reorganization of vimentin filaments [133].

While acrylamide is the most widely used disruptor, in MSCs, we've observed off target effects on actin (Figure 1.5). This has also been seen in some other cell types, with the theory being that a minor disruption of vimentin yields an indirect effect on actin organization [118,119]. After treatment with a variety of acrylamide concentrations (0.4mM, 2mM, 4mM, 15mM, and 40mM) and treatment durations (3hr, 4hr, and 9hr), vimentin network disruption was not observed in isolation from cytoplasmic collapse (Figure 1.5). Unfortunately, whenever cytoplasmic collapse was observed, F-actin organization was also completely disrupted (Figure1.5). As actin has been well established as being involved in cellular mechanical properties and behaviors such as cellular spreading and adhesion, using acrylamide to attempt to interrogate the role of vimentin in these processes was not practical.

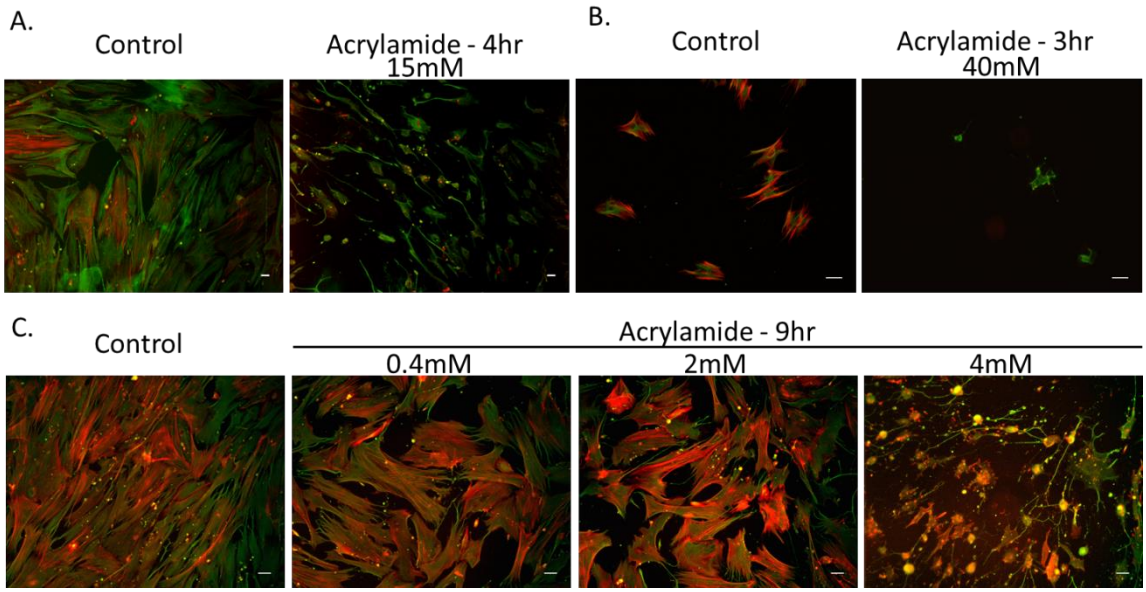

Figure 1.5 Acrylamide disruption of vimentin in hMSCs. Vimentin=green, F-actin (Phalloidin)=red A. Disruption of vimentin in hMSCs (Lonza) using 15mM acrylamide for 4 hours. Scale Bar: 25µm. B. Disruption of vimentin in hMSCs (RoosterBio) using 40mM acrylamide for 3 hours. Lower cell density and shorter culture time used in B in comparison to A and C. Scale Bar: 50µm. C. Concentration dependency of acrylamide-based disruption of vimentin in hMSC (Lonza) after 9 hours. Scale Bar: 40µm. Disruption of actin seen as punctuated spots of staining instead of visible fibers.

1.4.2 RNA Interference

An alternative method for manipulating vimentin, which was used in this body of work, is RNA interference (RNAi). This is a commonly used technique to manipulate gene expression products and knock down the expression of a gene of interest. While it has been investigated for use in therapeutics, it is also being used extensively in the research sector. This technique uses an inherent cellular pathway and machinery that cells use to respond to the presence of foreign double-stranded RNA, as shown in Figure 1.6 [134]. In short, complementary double stranded short hairpin RNA (shRNA)

is introduced into cells and this is then cut by a ribonuclease, Dicer, into small interfering RNA (siRNA). siRNA can be directly introduced into cells, bypassing this step. Next, a protein complex, RISC, binds to these siRNA and separates the two strands. One strand is degraded and the other strand is used as a template to bind and degrade any sequences that are complementary to it. The shRNA can be designed to have strands that are complementary to the mRNA of the gene of interest. The RISC complex uses the siRNA template strand to find and bind to the mRNA of the gene of interest, in this case, vimentin, and then degrades it. Once the mRNA is degraded, the RISC complex bound to the siRNA template strand remains and continues to find and bind to more mRNA, thereby decreasing the vimentin available in the cell. This knockdown effect, however, is diluted by continued cell division. Regardless, siRNA has been used successfully to decrease vimentin expression in a number of cell types for the short term [98,105,124].

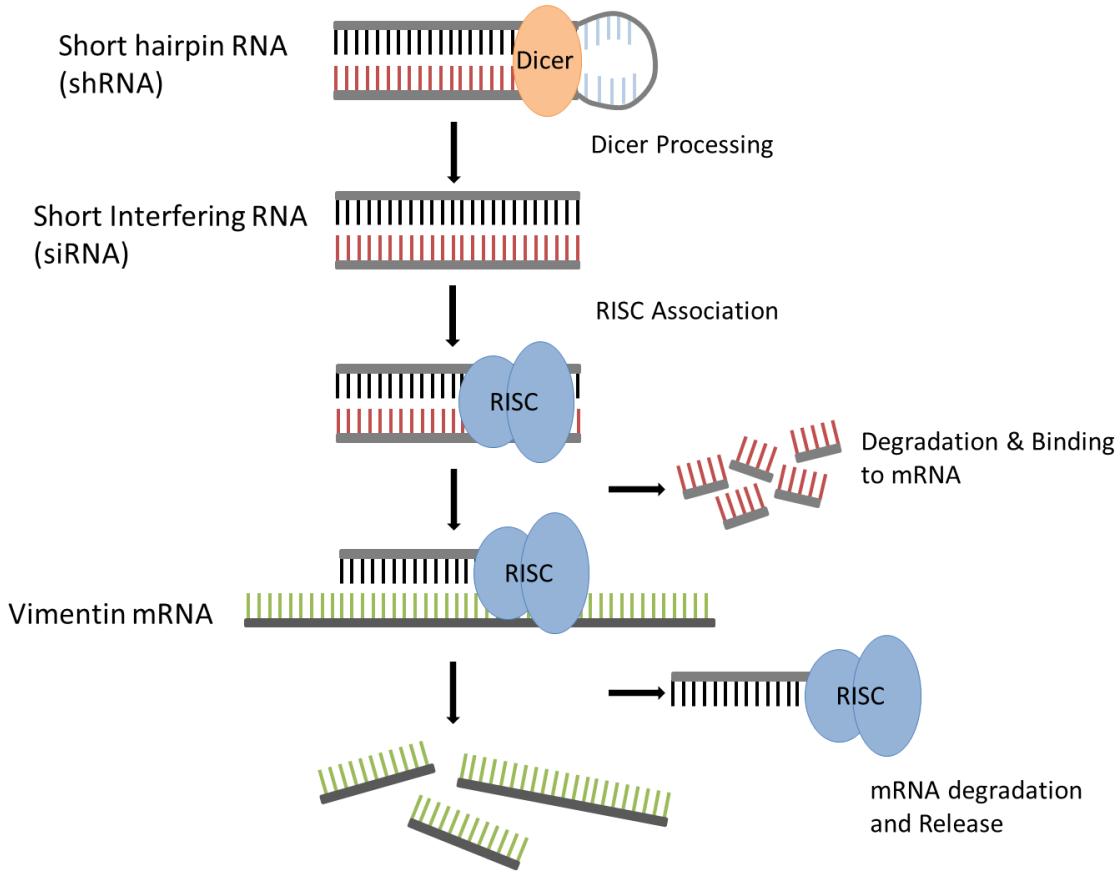

Figure 1.6 Schematic of shRNA-based RNAi

However, to increase the knockdown effect duration, alternative shRNA delivery methods must be used, such as inducing the cells to express these shRNAs intracellularly long term. Viral delivery can be used to achieve this. Essentially, oligonucleotides containing the shRNA sequence are cloned into a viral vector. There are a variety of viral vectors that have been used with RNAi including adenovirus, adeno-associated virus, retrovirus, and a subset of retrovirus called lentivirus [134]. However, only retroviruses and lentiviruses incorporate their DNA into the host genome, which allows for extended expression of the shRNA sequence. Further, lentiviruses can transduce both dividing and non-dividing cells increasing their utility

for research purposes. Lentiviruses can also be made replication incompetent, improving the safety of the virus for use.

To increase the versatility of this technique, the shRNA viral vector can be further manipulated. In the case of this body of work, the viral vector chosen included the capacity to turn the shRNA expression on and off. The promoter for the shRNA expression is blocked by a repressor protein until doxycycline binds to it. In the presence of doxycycline, the promoter region is free to proceed with the transcription of the shRNA and the subsequent knockdown of vimentin. This system provides the ability to manipulate the timing of shRNA expression.

1.5 Significance and Specific Aims

MSCs demonstrate potential for use in cell therapies and in tissue engineering. Understanding of how MSCs sense and respond to their environment, whether it is responding to external load, sensing of extracellular matrix proteins, or differentiation cues, will help to clarify how therapeutic MSCs will react to different physical stimuli. Their ability to interact with and respond to their environment is tied to the cytoskeleton, of which vimentin's contribution to MSC behavior is still being explored. Vimentin has been found to influence cellular mechanical properties, mechanosensitivity, and cellular adhesion. Further, as aberrant vimentin expression or organization has been found in osteoarthritic chondrocytes, MSCs from osteoarthritis patients, and in cancer cells, there is a clear need to understand how vimentin is influences cellular behavior. Specifically, as MSCs from osteoarthritic patients have been found to have altered expression of vimentin, the use of autologous MSCs from

this patient population for a therapeutic purpose could be influenced by changes in vimentin expression, motivating a need for a better understanding of vimentin's role in MSC behavior. The global hypothesis of this set of studies is that vimentin intermediate filaments contribute significantly to how MSCs respond to different physical and micro-environments. To test this hypothesis, vimentin expression was decreased using lentiviral shRNA targeting vimentin in MSCs and these cells were then used to examine cellular response to varying physical stimuli through the following aims:

1.5.1 Aim 1: Determine if vimentin contributes to mesenchymal stem cell deformability.

The first objective of this project was to determine the relationship between the vimentin intermediate filament network and the deformability of the MSCs in response to the compression of their external environment. Further, it was to evaluate whether other cytoskeletal proteins play a compensatory role in this response. Our hypothesis was that decreasing the vimentin levels in MSCs would lead to an increase in deformability.

1.5.2 Aim 2: Evaluate vimentin's influence on mesenchymal stem cell spreading in response to different microenvironmental conditions.

The second objective was to determine if vimentin intermediate filaments are involved MSC spreading and if their influence is dependent on environmental cues, such as different substrate protein coating, substrate stiffness, and low fluid shear stress. Further, it was to determine if adhesion proteins were affected by vimentin

deficiency. We hypothesized that a decrease in vimentin would lead to altered cell spreading due to interactions with focal adhesions in different microenvironments.

1.5.3 Aim 3: Determine if an initially intact vimentin network is required for chondrogenic differentiation

As vimentin is thought to be involved in short term chondrogenesis and chondrocyte phenotype maintenance, this final objective was to determine if vimentin intermediate filaments are involved in long term *in vitro* chondrogenesis up to 14 and 21 days in two different culture environments: pellet cultures and agarose hydrogel cultures. Our hypothesis was that the chondrogenesis of MSCs with an initially decreased vimentin level would ultimately lead decreased chondrogenic extracellular matrix deposition.

Chapter 2: Deformability of Human Mesenchymal Stem Cells Is Dependent on Vimentin Intermediate Filaments[1]

2.1 Introduction

Mesenchymal stem cells (MSCs) have recently shown promise as a therapeutic cell source for the treatment of many diseases, including osteoarthritis [13,135]. However, osteoarthritic cartilage presents a challenging environment for therapeutic MSCs, injected systemically or implanted within a biomaterial scaffold, due to the abnormal biochemical and mechanical environment [136,137]. One characteristic of this mechanical environment is regular compression that deforms the tissue and chondrocytes, eliciting extracellular matrix protein expression [50,138–142]. Response to mechanical stresses is partially governed by cellular mechanical properties. Changes in MSC mechanical properties have been found to be related to both their physical environment and differentiation potential [52–55]. Mechanical properties and mechanotransduction are in part regulated by the cytoskeleton, consisting primarily of actin microfilaments, microtubules, and vimentin intermediate filaments (IFs) for cells of mesenchymal lineage [55,56,75,76,94,112,113,118,119]. While their role in the pathogenesis of OA is still unknown, vimentin IFs have recently been found to be disrupted or dispersed in osteoarthritic chondrocytes [92,93]. Notably, vimentin has also been shown to be downregulated in MSCs of osteoarthritic patients [95], which raises

[1] This work has been published in the Annals of Biomedical Engineering and is reproduced here with permission from the publisher.
Sharma, P., Bolten, Z.T., Wagner, D.R., Hsieh, A.H. Deformability of Human Mesenchymal Stem Cells Is Dependent on Vimentin Intermediate Filaments. Ann Biomed Eng (2017) 45: 1365.

questions about the potential efficacy of autologous stem cell therapies for treatment of OA.

The role of vimentin is still being examined using a variety of techniques to decrease, disrupt, or collapse vimentin IFs, but it is clear that they are involved in modulating the mechanical properties of cells. In fibroblasts, mutations resulting in vimentin deficiency have been linked to not only impaired migration, but also reduction of mechanical stability and stiffness of the cytoplasm [111,112]. Further, in these cells, decreases in vimentin led to compromised ability for fibroblasts to contract collagen gels, which is critical for wound healing [113].

Perinuclear collapse of vimentin networks in fibroblasts has also been induced using proteins, such as the oncogene simian virus 40 large T antigen [127] or one variant of mutated desmin [128]. Oncogene expression-dependent collapse of the vimentin network in fibroblasts caused an increase in cellular stiffness, which supports vimentin IFs association with tumor invasion and tumor cell stiffness [127]. IF collapse caused by mutated desmin revealed a complex distribution of cellular stiffness with increased cellular stiffness in regions of the collapsed vimentin and a decrease in stiffness in the remaining vimentin-deficient cytoplasm [128].

Collapse of the vimentin network has also been induced by pharmacological inhibitors such as withaferin A [117], calyculin A [116], and acrylamide [11,94,118,126]. Non-adherent cell populations or cells suspended in hydrogels have revealed decreases in

cellular mechanical properties with the use of pharmacological inhibitors. Specifically, in chondrocytes and chondrocyte-like cells, disruption of vimentin networks using acrylamide resulted in decreased elastic moduli and viscoelasticity, as measured by atomic force microscopy and micropipette aspiration, as well as a decrease in deformability [11,94,118,126]. Likewise, in T lymphocytes and natural killer cells, disruption of vimentin IFs caused a decrease in cellular stiffness [116,117].

Much of the research investigating how vimentin intermediate filaments contribute to cell mechanics and function has been conducted in fibroblasts by introducing the expression of abnormal proteins or pharmacological inhibitors, which may have off target effects that can influence the measurement of cellular stiffness. However, whether vimentin IFs similarly affect the biophysical properties of MSCs has not been established and an improved understanding of how IFs are involved in mechanosensing and mechanical properties of MSCs will be valuable for interpreting outcomes from stem cell therapies. In this study, we examine the relationship between MSCs' capacity to deform under external compression and the involvement of vimentin IFs using shRNA mediated RNA interference (RNAi). The aim is to investigate the effect of a decreased vimentin IF network on MSC deformability independent of effects from cell-substrate adhesion and long culture times. Our results suggest that a decrease in vimentin IFs paradoxically reduces the deformability of MSCs, potentially due to changes in the manner by which actin microfilaments and microtubules organize and function to resist loads.

2.2 Materials and Methods

2.2.1 hMSC cell culture

For initial lentiviral construct screening experiments, hMSCs from Lonza (Walkersville, MD) were expanded per manufacturer's instructions and used at passage 5 (P.5). For subsequent experiments, population doubling level (PDL) 9 bone marrow derived human mesenchymal stem cells (hMSCs) (RoosterBio; Frederick, MD) were expanded using RoosterBio Enriched Basal media supplemented with GTX Booster (RoosterBio) per manufacturer instructions and used at PDL 13-18 hMSCs (approximately 4-5 passages). All subsequent subculture for lentiviral transduction and experimentation was completed using hMSC growth media: high glucose DMEM containing 4mM L-Glutamine (Gibco) supplemented with 10% fetal bovine serum (FBS) (Gibco), 100 U/mL Penicillin Streptomycin (Gibco), 1% MEM non-essential amino acids (Gibco), and 4 mM L-Glutamine (Gibco). Complete media exchange was completed every 2-3 days and the cells were maintained at 5% CO_2 and at 37^{o}C.

2.2.2 Lentivirus design and generation

52 nt shRNA sense-loop-antisense sequences were designed and selected from human vimentin [Gen Bank: NM_003380] mRNA using the shRNA Designer through Biosettia, Inc. Single strand oligonucleotides were annealed and these double stranded oligos were then ligated into an inducible lentiviral RNAi vector conveying resistance to blasticidin and a TetO -H1 promoter following manufacturer instructions. This inducible system only allows shRNA transcription to take place in

the presence of tetracycline antibiotics, specifically doxycycline. The pLV-RNAi kit and pLV-Pack Packaging mix (Biosettia) were used to generate the shRNA constructs and package into replication-deficient lentivirus using HEK 293FT cells and Lipofectamine 2000. Two sequences were evaluated, listed in Table 2.1, and a control shRNA lentiviral vector targeting the LacZ gene was used (Biosettia). Virus-containing supernatants were collected 72hr post transfection and stored at -80^{o}C until use.

Table 2.1 shRNA sequences screened for effective vimentin knockdown in hMSCs. Grey indicates overhang or loop shRNA

Sequence Name	Sequence
shVim1	5'-AAAAGGCAGAAGAATGGTACAAATTGGATCCAATTTGTACCATTCTTCTGCC-3'
shVim2	5'-AAAAGGAATAAGCTCTAGTTCTTTTGGATCCAAAAGAACTAGAGCTTATTCC-3'
Neg. Control (LacZ)	5'-GCAGTTATCTGGAAGATCAGGTTGGATCCAACCTGATCTTCCAGATAACTGC-3'

4.2.3 shRNA transduction

We performed hMSC transduction with the shVim-vector for 24hrs at a multiplicity of infection (MOI) of 15. Cells transduced with a shLacZ-vector and non-transduced cells were used as controls. Transduction was completed in the presence of 6µg/ml hexadimethrine bromide (Polybrene) (Sigma) to assist with transduction efficiency. Titered viral concentrations for an MOI of 15 were determined through a Quanti-IT PicoGreen Assay (Invitrogen). Two days post-infection, pure populations were selected using 12µg/ml Blasticidin for 4 days. Both shVim-hMSCs and shLacZ-hMSCs were cultured in the presence of 1µg/ml doxycycline to induce RNAi. Cells

were cultured for 7, 14, or 21 days on tissue culture plastic before being harvested to be assayed.

2.2.4 Western blotting

To quantify levels of vimentin protein translation, cells were transduced and induction carried out for 7, 14, and 21 days. Cells were harvested and resuspended in a lysis buffer (50mM HEPES, 150mM sodium chloride, 1% Triton X-100, 1mM EDTA, 10mM Na-pyrophosphate, 10% glycerin) supplemented with a 1:100 concentration of protease inhibitor cocktail (Fisher Scientific). Protein concentrations were determined using a modified Lowry assay with a Folin-phenol color reaction detected by a ND-1000 spectophotometer (Nanodrop). After sample removal, the supernatant was mixed at a concentration of 1:1 with a loading buffer (13% (v/v) Tris-HCl, 20% (v/v) glycerol, 4.6% (w/v) SDS, 0.02% (w/v) bromophenol blue, 200 mM dithiothreitol). Samples and a human vimentin protein positive control were subjected to SDS-PAGE using pre-cast Criterion Tris-HCl gels (BioRad). 293FT HEK cell lysate was used as a protein positive control for β-actin. Approximately 9µg of protein from each sample was loaded into the Criterion Tris-HCl gels. After SDS-PAGE, proteins were electrophoretically transferred to a polyvinylidene fluoride membrane and detected using a rabbit IgG anti-human vimentin primary antibody (ThermoFisher) and Vectastain ABC-AmP for chromogenic detection. Detection of β-actin using a mouse IgG anti-human β-actin primary antibody was used as a loading control. Semi-quantitative analysis was completed using ImageJ (NIH) to determine band intensities and protein expression levels were determined relative to non-

infected cells. For semi-quantitative analysis of vimentin protein expression levels, the top band of the cluster was used, as it aligns with the positive protein control.

2.2.5 Immunofluorescence imaging

To visualize decrease in translated vimentin protein in 2D cultures, vimentin RNAi was induced for 7 and 14 days. Sham control (shLacZ) samples were performed in parallel. As an additional control, non-transduced cells were subjected to the RNAi-inducing agent (1µg/ml doxycycline) for 14 days to determine its potential effects on cytoskeletal organization. Cells were fixed with 4% paraformaldehyde and permeabilized using 0.1% Triton X-100. Cells were labelled with either rabbit IgG anti-human vimentin primary antibody (ThermoFisher) or mouse IgG anti-human tubulin primary antibody (Santa Cruz) and visualized with biotinylated (anti-rabbit IgG or anti-mouse IgG) secondary antibodies (Vector) and fluorescein-labelled streptavidin (Vector). F-actin filaments were then stained with Alexafluor 594 phalloidin (Invitrogen), and the nucleus labelled with DAPI (Invitrogen). Fluorescence images were taken at 100x magnification with an Olympus IX81 microscope.

To visualize the cytoskeleton in agarose gels, vimentin RNAi was induced for 14 days before being harvested. Sham control (shLacZ) samples were performed in parallel. Cells were then resuspended in 4% (w/v) agarose and pipetted into a 6mm x 3mm diameter mold, followed by overnight fixation in 4% paraformaldehyde. These were infiltrated with 30% sucrose, embedded in Tissue-Tek O.C.T compound (Sakura), and then stored at -80^{o}C until sectioning. Frozen sections (20µm) were

created using an HM550 series cryostat (Richard Allen Scientific). These sections were labelled with either rabbit IgG anti-human vimentin primary antibody (ThermoFisher) or rabbit IgG anti-human tubulin primary antibody (Abcam) and visualized with biotinylated anti-rabbit IgG secondary antibodies (Vector) and fluorescein-labelled streptavidin (Vector). In additional sections, F-actin filaments were stained with Alexafluor 488 Phalloidin (Invitrogen) and the nucleus stained using Slow Fade Gold anti-fade reagent with DAPI (Invitrogen). Confocal fluorescence images were taken at 600x magnification with a Nipkow (spinning) disk-equipped Olympus IX81 microscope. Confocal Z-stacks (1 μm slices) of the entire cells were taken and projected into a single image for analysis. Fluorescence intensity of labelled proteins was quantified using Image J (NIH) [143]. Cells were manually traced and corrected total cell fluorescence intensity measurements per cell area were calculated using the following equation: corrected total cellular fluorescence (CTCF) = (Integrated Density – (Area of selected cell x mean fluorescence of background reading)) / Cell Area (pixels). Data are shown as mean CTCF + s.e.m.

2.2.6 Cell deformation

To measure cell deformation, after 14 days of inducing vimentin (and LacZ) RNAi cells were incubated with Cell Tracker Green CMFDA (Invitrogen) to stain the cell cytoplasm. Subsequently, 300-400k cells were resuspended in 2% (w/v) or 4% (w/v) agarose and pipetted into a 6mm x 6mm x 10mm mold. After gels solidified, they were placed into a custom microscope-mounted micrometer-controlled deformation device [126]. This process took at least two hours from time of trypsinization. Samples

were then subjected to 0, 10, and 20% uniaxial bulk compressive strain. Fluorescence images of cells were generated at 400x magnification and cell diameters in the loading direction and perpendicular to the loading direction were measured using ImageJ (NIH). Analysis was performed similar to a previously study [126]. Aspect ratios (ARs) were calculated as cell diameter in the loading direction/ cell diameter perpendicular to load, and the deformed population ARs were then normalized to the undeformed population ARs. Data are shown as mean normalized aspect ratio ± standard deviation.

2.2.7 Cytoskeletal disruption

To determine the effect of microfilament and microtubule disruption on the shVim-hMSC and shLacZ-hMSC deformability, after 14-15 days of RNAi induction cells were incubated with CMFDA live cell tracker (Invitrogen). Afterward 300-400k cells were resuspended in 4% (w/v) agarose and pipetted into a 6mm x 6mm x 10mm mold. Following encapsulation and prior to deformation, cell-agarose constructs were incubated with either 20μM colchicine or 9.85μM cytochalasin D for 3hr in 37°C at 5% CO_2 to disrupt microtubules or actin microfilaments, respectively [126]. Agarose blocks were subjected to strain and the images analyzed, as described above. Data are shown as mean aspect ratio + standard deviation.

2.2.8 Statistical Analysis

Statistical analyses for all studies were performed using non-parametric Kruskal-Wallis tests followed by a Mann-Whitney post-hoc for pairwise analysis using the statistical software SPSS. Statistical significance was set to $\alpha = 0.05$.

2.3 Results

2.3.1 Inducible lentiviral shRNA mediated knockdown of vimentin expression in hMSCs

Initially, two shRNA vectors (Table 2.1), designed using different locations within the gene, were assessed for effectiveness in decreasing vimentin expression over 14 days in the presence of 1 μg/ml doxycycline, the highest recommended dose. Because shVim1 yielded greater RNAi than shVim2 (Figure 2.1A), it was used for all subsequent experiments and is henceforth referred to as shVim. Cultures of shVim-transduced hMSCs exhibited approximately a 30% decrease in vimentin expression after 14 days of induction, as determined by Western blot in the initial screen and in experiments to further characterize the vimentin knockdown by shVim (Figure 2.1A, 2.1B). A decrease in vimentin protein was visible as seen by immunofluorescence in cells seeded on tissue culture plastic and in agarose hydrogels (Figure 2.1C, 2.1D, Figure 2.2). Visually, we confirmed that 1 μg/ml doxycycline had negligible effect on the organization of vimentin, tubulin, and F-actin in 2-D culture (Figure 2.1E). Based on these results, it was determined that inducing RNAi for at least 14 days sufficiently knocked down vimentin protein levels, and this minimum induction period was used for all subsequent experiments.

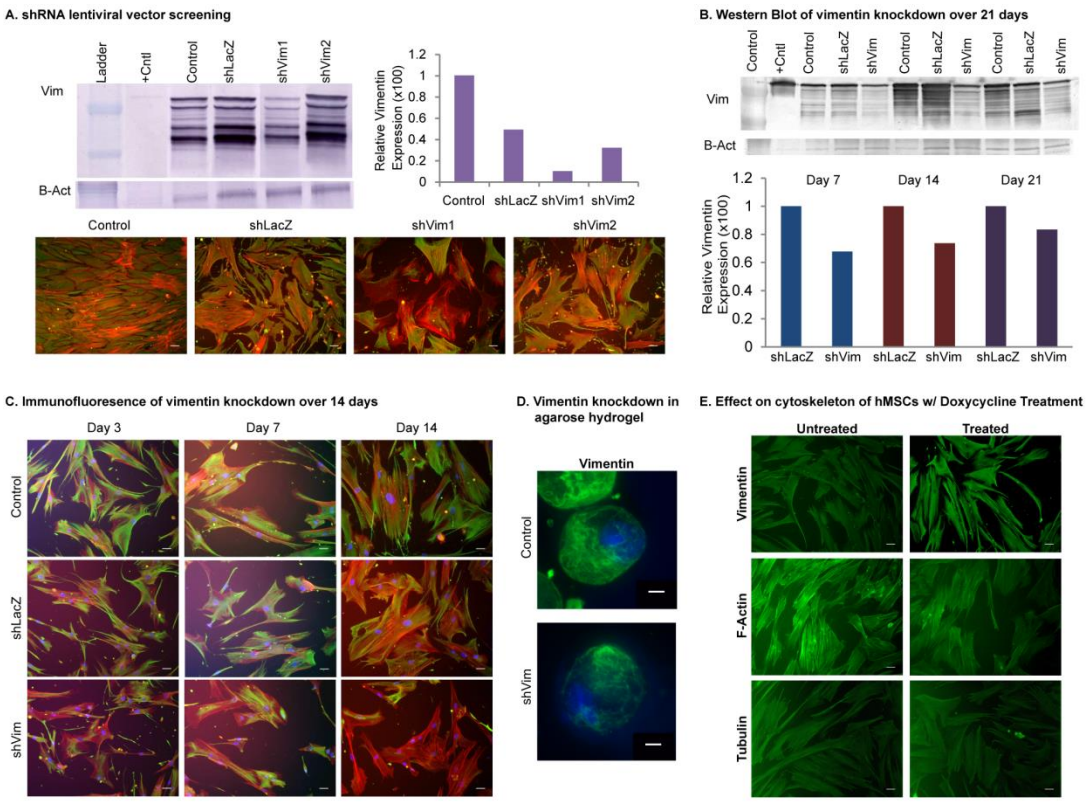

Figure 2.1 Characterization of vimentin knockdown in hMSCs. a. Two lentiviral vectors were screened using western blots and immunostaining on Day 14. In Western blots, '+Cntl' is a purified vimentin protein positive control for Vim and a 293FT HEK cell lysate for B-Act. Scale bar: 50µm. b. Characterization of knockdown by Western blot on days 7, 14, and 21 of shRNA induction. '+Cntl' is purified vimentin protein for Vim and 293FT HEK cell lysate for B-Act. c. Observation of vimentin knockdown by immunostaining on days 3, 7, and 14 of shRNA induction; vimentin (green), F-actin (red), nucleus (blue). Scale bar: 50µm. d. Observation of vimentin knockdown in agarose hydrogel; vimentin (green), nucleus (blue). Scale bar: 50µm. e. Effect of 1µg/ml doxycycline treatment on cytoskeletal proteins of control, non-transduced, hMSCs. Scale bar: 50µm.

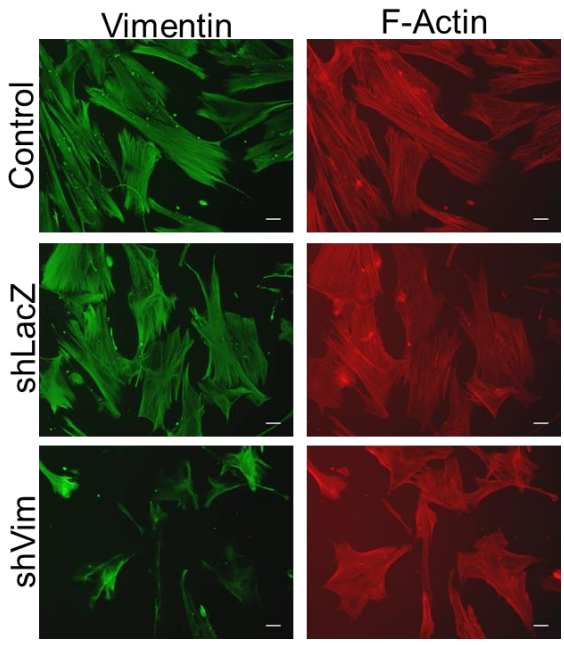

Figure 2.2 Characterization of vimentin knockdown at day 14. Representative fluorescence images of non-transduced, shLacZ-hMSCs, and shVim-hMSCs each labelled by immunostaining for vimentin (green) or phalloidin staining for F-actin (red). Scale Bar: 50μm.

2.3.2. Vimentin knockdown reduces hMSC deformability

Knockdown of vimentin expression over 14 days resulted in decreased deformability of cells compared to both non-transduced hMSCs and shLacZ hMSCs in 4% agarose hydrogels. Compression of shVim-hMSCs yielded significantly higher normalized aspect ratios (Figure 2.2A), or smaller deformations, compared to non-transduced hMSCs at 10% ($p=0.003$) and 20% ($p<0.0005$) strain (Figure 2.2B), as well as compared to shLacZ-hMSCs at 20% strain ($p<0.0005$). We found no significant difference between shLacZ-hMSCs and non-transduced hMSCs, indicating that lentiviral transduction did not significantly affect cellular deformability (10%, $p=0.528$; 20%, $p=0.913$; Figure 2.2B). Interestingly, no significant difference was

observed between any of the groups during deformation within the 2% agarose gels (10%, p=0.182; 20% p=0.093; Figure 2.2C). Further, it was found that doxycycline treatment itself did not convey any resistance to the hMSCs (Figure 2.2D). After 14 days of 1 µg/ml doxycycline treatment, no significant difference in deformation was observed between untreated and treated hMSCs in 4% agarose gels in any strain group (10%, p=0.929; 20%, p=0.383).

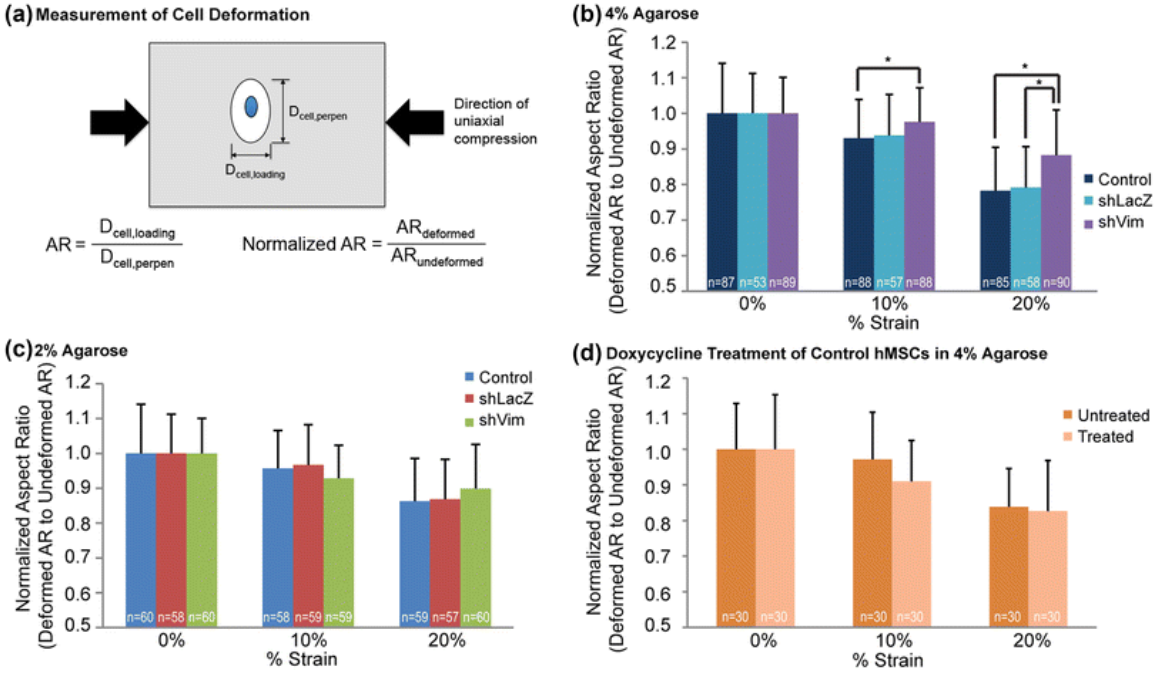

Figure 2.3 Cell Deformation of Vimentin-deficient hMSCs. Normalized aspect ratios of cells subjected to 0%, 10%, or 20% strain. a. Depiction of deformation and calculations. b. Deformation of control, non-transduced, hMSCs, shLacZ-hMSCs, shVim-hMSCs in 4% agarose hydrogels. c. Deformation of control, non-transduced, hMSCs, shLacZ-hMSCs, shVim-hMSCs in 2% agarose hydrogels. d. Deformation of control, non-transduced, hMSCs with or without treatment with 1µg/ml doxycycline for 14 days. All data are expressed as mean aspect ratio ± SD. Asterisks represent statistically significant differences ($p < 0.05$).

2.3.3. Functional role of actin filaments, but not microtubules, is altered by vimentin knockdown

To determine whether the reduced deformability of shVim-hMSCs was caused by changes in the actin or microtubule network, we exposed transduced cells seeded in 4% agarose to either cytochalasin D or colchicine, respectively. The non-transduced hMSCs sample group was not included in this experiment, because these cells were found to have no significant difference in deformability compared with shLacZ-hMSCs (Figure 2.2). Comparisons in this experiment focused only on the effect of vimentin knockdown to the sham (shLacZ) control. After disruption of the microtubule network, shVim-hMSCs remained significantly less deformable at both 10% (p=0.007) and 20% (p=0.001) strain compared to shLacZ-hMSCs (Figure 2.3A). In contrast, disrupting the actin microfilament network resulted in comparable cell deformations between shVim-hMSCs and shLacZ-hMSCs (Figure 2.3B). Normalized aspect ratios were still slightly higher for shVim-hMSCs compared to shLacZ-hMSCs, but no longer significant at both 10% (p=0.164) or 20% strain (p=0.215).

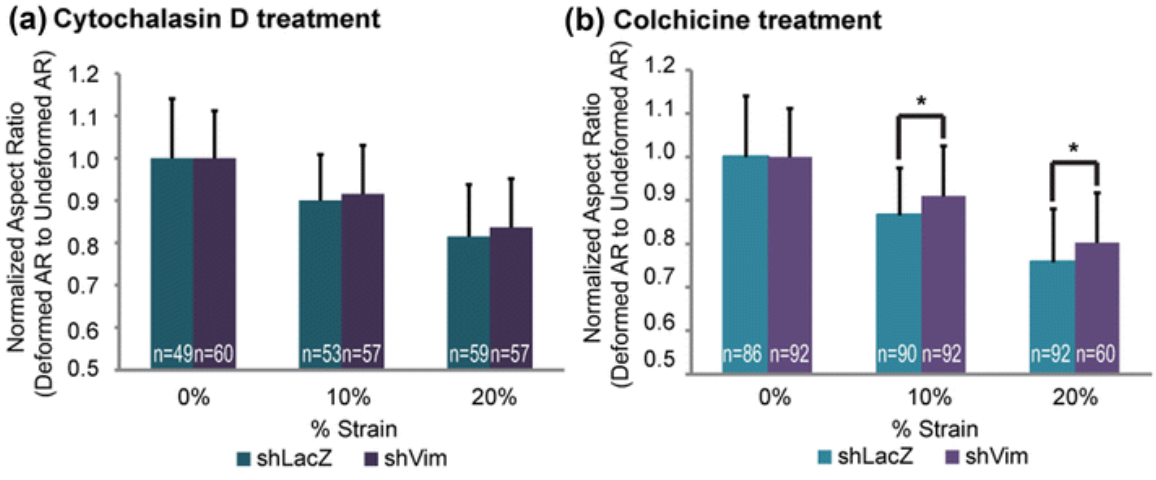

Figure 2.4 Effect of Cytoskeletal Disruption on Cell Deformation. Normalized aspect ratios of shVim-hMSCs and shLacZ-hMSCs subjected to 0%, 10%, or 20% strain after chemical disruption of actin microfilaments or tubulin microtubules. a. Deformation of shLacZ-hMSCs and shVim-hMSCs after actin microfilament disruption b. Deformation of shLacZ-hMSCs and shVim-hMSCs after microtubule disruption All data are expressed as mean aspect ratio ± SD. Asterisks represent statistically significant differences ($p < 0.05$).

2.3.4. Cytoskeletal organization and quantity in agarose embedded hMSCs

To further investigate the involvement of the actin or tubulin networks in the deformation of shRNA transduced cell populations, cytoskeletal protein content was semi-quantitatively determined from fluorescence microscopy of non-deformed cells. It was found that shVim-hMSCs and shLacZ-hMSCs did not have statistically significant differences in fluorescence intensities of F-actin staining ($p=0.267$) (Figure 2.4). However, the microtubule network fluorescence intensity was significantly lower in the shVim-hMSCs compared to the shLacZ-hMSCs ($p=0.01$) (Figure 2.4).

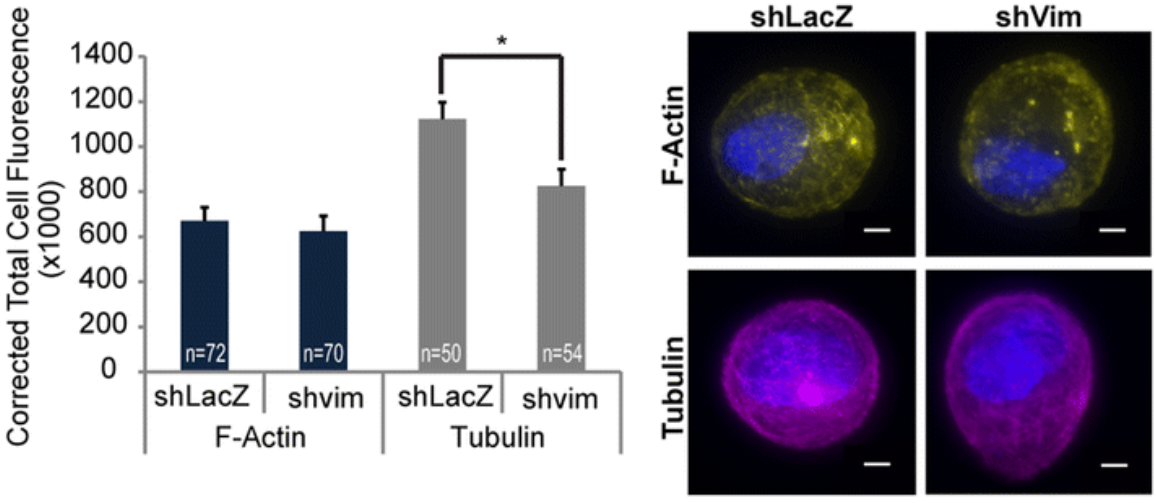

Figure 2.5 F-actin microfilament and Tubulin microtubule fluorescence intensity in shVim-hMSCs and shLacZ-hMSCs. Fluorescent intensity measurements of shLacZ-hMSCs and shVim-hMSCs stained for F-Actin and tubulin. All data are expressed as CTCF ± s.e.m. Asterisks represent statistically significant differences ($p < 0.05$). Scale bar: 50μm.

2.4 Discussion

Recently, studies have found vimentin IFs to be disrupted in chondrocytes and even in MSCs harvested from osteoarthritic bone marrow [92,93,95]. Because mechanical loading is a strong regulator of cell behavior, we investigated how an altered vimentin network affects deformation of hMSCs during loading of agarose constructs. As a major component of the cytoskeleton, vimentin IFs are involved in the cellular response to mechanical loading and in modulating cellular mechanical properties. However, extracellular matrix and substrate stiffness also introduce changes in cell shape and cytoskeletal tension via adhesion complexes [52]. Thus, the mechanical behavior of a cell is highly complex and context-dependent.

In this study, we focused on the deformation of MSCs in an experimental system that minimizes the ability for cells to interact physically with their surrounding microenvironment. As MSCs are not habitually unattached to extracellular matrix, this study provides a snapshot of the intrinsic deformability of undifferentiated MSCs. To prevent cell-matrix interactions, which would confound measurements of intrinsic deformability, we examined deformation of cells embedded in agarose hydrogels without allowing for extended culture time, as previously described [126].

Contrary to expectations, our experiments showed that in 4% agarose hydrogels MSCs with decreased vimentin expression are more resistant to deformation compared to control cells. In an attempt to elucidate the mechanism behind this phenomenon, we additionally disrupted either actin microfilaments or microtubules. Although cells were generally more deformable with either treatment, only disruption of actin microfilaments eliminated the difference in deformability between shLacZ and shVim cells. That vimentin-deficient MSCs maintained a significantly greater resistance to deformation with microtubule disruption suggests a less prominent role for microtubules. Semi-quantitative measurement of the fluorescence intensity of immunostaining for F-actin and tubulin yielded further insight. Since actin fluorescence was unchanged, microfilament organization rather than quantity may be involved in the decreased deformability. The lower fluorescence intensity of the tubulin in shVim-hMSCs implies that the decrease in microtubules and organization of the actin microfilaments may work cooperatively to enhance resistance to cell deformation.

One obvious limitation of our RNAi approach is that vimentin IF expression is not completely ablated, unlike in fibroblasts isolated from vimentin null mice [112,113]. On the other hand, our approach precludes any compensatory mechanisms that cells may develop physiologically in a knockout animal. Because vimentin continued to be expressed, albeit at a decreased level, we did not observe a complete collapse in the IF network with vimentin-silencing, as has been reported with acrylamide treatment

[94,118]. It is possible that the remaining vimentin network consists primarily of larger filaments, rather than the more diverse network of larger and smaller filaments that might support that strain normally. While large filaments were not observed in the immunostaining, Western blots did show a decrease in the smaller fragments in the knockdown cells compared to the control cells (Figure 2.1B).

The increased resistance to deformation that we observed in the MSCs with decreased vimentin appears to contradict much of the literature in this area. Whole cell deformation experiments using chondrocytes and immune cells with chemically disrupted vimentin networks have resulted in mechanically less stiff and more deformable cells [11,94,116–118], though it is questionable how specific these treatments are for a given cytoskeletal target. Likewise in anchored vimentin-deficient fibroblasts, torsional loads applied via cell adhesions resulted in decreased stiffening or cytoplasmic rupture, suggesting that without vimentin, cells are mechanically unstable and unable to stiffen in response to load [112,113]. It is not clear at this time how much our unexpected findings might be explained by the lack of cell-matrix attachment and the 3D hydrogel microenvironment of our experimental system.

Other studies, however, observed trends that are consistent with our results. One study reported a decrease in compressibility of acrylamide-treated chondrocytes [119]. The authors postulated that vimentin IFs act as tensional elements preventing elongation orthogonal to the direction of compression, while microtubules prevent the compression of cells along the loading axis. Our data suggest that the actin

microfilaments may play a more significant role in the resistance to deformation in the presence of a diminished vimentin network. Interestingly, dose-dependency of acrylamide treatment can also affect mechanical properties, implying a nonlinear relationship between the organization of vimentin and any change in cellular mechanical properties [94]. Disruption of vimentin in chondrocytes using acrylamide was found to affect mechanical properties measured by micropipette aspiration only at high concentrations [94]. Further, we have shown previously that chondrogenic hMSCs treated with this same high concentration of acrylamide trended toward increased deformability, but without statistically significant results [126]. In this study, we did not observe a complete collapse of the vimentin network, and this could be why we see a dissimilar response to deformation in vimentin-deficient MSCs.

One critical parameter of this study is the choice of culture duration in the agarose hydrogel. Without significant culture time, cells would not be able to develop adhesion moieties that could subvert the deformation results. It has been observed that cytoskeletal proteins will undergo reorganization over chondrocyte culture time in agarose hydrogels over the timescale of days [144], implying that the cytoskeletal organization is dynamic over time. Here, we allowed a brief recovery after transfer to 3D culture in an attempt to capture an environment that simulates how vimentin may be involved in mechanosensing when hMSCs are first placed into a carrier biomaterial for therapy just prior to implantation. However, observations of cellular deformability at different stages in culture could provide more information about cell deformability and how microtubules and actin microfilaments reorganize to

compensate for a less robust vimentin network over time. Further, longer culture periods would allow insight into changes in cellular phenotype due to 3-D culture, and changes in cellular behavior with the deposition of extracellular matrix.

The mechanical loads experienced by hMSCs in our experimental system are analogous to inclusions that deform within a loaded bulk porous material, which compounds the complexity of factors – beyond those associated with the cytoskeleton – that contribute to the cell deformation results. On a superficial level, the measurements that were made using 2% and 4% agarose can provide some insight into the balance of stiffness between cells and their surrounding material. In 2% agarose, cells deformed less across all groups than in 4% agarose, whose modulus is roughly five times that of 2% [145]. It is possible that, due to the lower modulus of 2% agarose, cells were not subjected to sufficiently high compressive loads to resolve differences between shVim- and shLacZ-hMSC deformabilities. Delving deeper, some studies have shown differences in cytoskeletal organization with different agarose concentrations [101]. Further, the non-linear mechanics of the cells might be distinct between shVim- and shLacZ-hMSCs, where deformation may be similar under low load, but distinct at high load. Our previous work on chondrogenic hMSCs deficient in type VI collagen [146] is one example of such behavior.

Some important aspects of cell deformation that we were not able to explore in this study include potential anisotropy of cell deformation, which would require more time consuming confocal imaging and 3D strain analysis of cells, as well as the

possibility of discontinuities at the cell-gel interface due to differential stiffnesses that could interfere with analysis of cellular deformation. A more rigorous mechanical analysis of how cell deformability is governed in this complex system is certainly warranted. In this particular study, we chose a more straightforward approach to characterizing cell deformation in order to collect sufficient data for statistical comparisons between treatment groups.

While deformability measured by whole cell compression in 3D and stiffness measurements of anchored cells on a planar substrate yield different mechanical property relationships, it may be possible to relate the two sets of characteristics with further investigation. It has been speculated that the reduced mechanical stability observed in vimentin negative fibroblasts may not necessarily be directly correlated with cellular flexibility, implying that their ability to withstand large deformations, e.g. migration through small pores, could be impaired [113]. We have also observed impaired chemotactic migration in the vimentin knockdown MSCs and further found that robust vimentin networks may be required for migration through small pores (*unpublished data*). Further analysis of this phenomenon may shed light on the relationship between our observed deformation behavior in unanchored cells and cells experiencing mechanical stimuli due to adhesion and cytoskeletal remodeling during migration.

One variable of this study that has not been systematically studied in stem cells is MOI used for lentiviral transduction and its potential effects on cellular physiology.

In order for us to achieve the desired knockdown of a gene as robustly expressed as vimentin, a relatively high MOI was required. Our previous studies using lentivirus-mediated RNAi in hMSCs had shown no detrimental effects on differentiation [146], but those prior experiments had used lower MOI. Though we did not observe any overt differences in morphology in any cells used for this present study, it is possible that other aspects of stem cell function may have been affected, independent from decreased vimentin. There has been some anecdotal evidence that MOI-dependent effects may be important.

This study reveals a unique relationship between vimentin IFs and MSCs' capacity to deform due to external whole cell compression. Our observations suggest that deformability of MSCs is dependent on the robustness of the vimentin IF network in unanchored cells. Varying expression and organization of vimentin in healthy and diseased cells may affect the mechanical properties, and consequently the mechanotransduction, of these cells. Literature suggests that vimentin disruption or absence is present in osteoarthritic chondrocytes and even mesenchymal stem cells from osteoarthritic patients, but it is not yet clear if this change is a symptom of the developing disease environment or an early actor in disease progression. In addition to examining vimentin's role in the intrinsic properties of MSCs in agarose hydrogels, this study sheds initial light onto changes to mechanical properties that may occur to hMSCs due to an abrogated vimentin network that may be relevant in a cell therapy environment. Our observations introduce another variable and piece of information in understanding how IFs are involved in cellular mechanical properties.

2.5 Conclusion

The objective of this first Aim was to determine whether vimentin IFs are involved in the capacity for MSCs to deform, and we found that they are, if in an unexpected way. As mentioned above, deformation of chondrocytes within the load bearing environment of articular cartilage occurs as a result of the regular tissue compression and such compression can have functional outcomes such as changes in extracellular matrix protein expression [50,138–142]. Thus, it is valuable to understand how MSCs entering such as environment may be affected by the compression, and how vimentin may contribute. The findings in this Aim suggest that the effect of decreasing the amount of vimentin in hMSCs is not completely separate from the remainder of the cytoskeleton, which can compensate for the vimentin deficiency when subjected to compression caused by the deformation of the environment. Further, cell-ECM interactions are likely to affect deformability of MSCs, perhaps differently if the vimentin networks are decreased. Thus, we decided to move our focus away from examining cell deformability and instead evaluated the role of vimentin in MSC spreading in response to different microenvironments, such as surfaces coated with different ECM proteins, in the second Aim.

Chapter 3: Vimentin Intermediate filaments influence Mesenchymal Stem Cell Spreading on Fibronectin

3.1 Introduction

Mesenchymal stem cells (MSCs), increasingly being investigated for therapeutic use, respond to a variety of extracellular cues. External stimuli can include extracellular matrix (ECM) proteins available for adhesion [32], environmental stiffness [27], mechanical loads [51,58], and other biochemical and physical cues. Understanding the mechanisms that drive cellular response to the environment can motivate further development of MSC-based therapies. Cells transduce external stimuli using a variety of mechanisms, including through cytoskeletal proteins, of which vimentin intermediate filaments (IFs) have recently gained notice for their involvement in sensing the extracellular environment. However, this role for vimentin IFs in the MSC response to different microenvironments remains to be clarified.

A variety of environmental characteristics can modulate the spreading and adhesion of MSCs. These include changes to substrate composition (e.g. extracellular matrix (ECM) protein/binding moieties) [28–32], the density of ECM proteins on substrates [33], and substrate stiffness [27–29], with all of these cues also tuning MSC differentiation toward different lineages. Of the variety of ECM proteins that MSCs bind to, fibronectin and type I collagen are used frequently to promote MSC adhesion to surfaces due to MSCs' high affinity for binding to these proteins compared to other ECM molecules like laminin [28,29,31,32]. Differences in cell spreading and area,

especially on different stiffness environments, have been shown to correspond with changes in MSC function and characteristics as well, such as cellular stiffness and differentiation potential [34,37]. Vimentin IFs potentially influence cellular spreading to these proteins through interactions with cell adhesion structures, specifically focal adhesions [88,105,113,114,121]. They have also been found to directly interact with integrins including αVβ3, α2β1, α6β4, α5β1, as well as β3 and β1 integrin subunits [104–110].

In addition to the composition of the ECM environment, mechanical stimuli, such as variations in substrate stiffness and mechanical loading affect MSC behavior and function. For example, such stimuli have been shown to initiate or promote MSC differentiation along different lineages [27–29,51,58]. Softer substrate stiffness, where cells are typically smaller, is correlated with adipogenic or neural differentiation, while stiffer substrate stiffness, where cells are typically more spread, is more associated with osteogenic or myogenic differentiation [27,29,39,40]. A variety of mechanical loading regimens have been used to promote MSC differentiation including fluid flow, which typically promotes osteogenesis [51,147]. However, perfusion bioreactors have had success with chondrogenesis [58,148]. Aside from effects on differentiation, fluid shear stress has been shown to promote proliferation, migration, and activation of calcium and mitogen-activated protein kinase (MAPK) signaling pathways in MSCs [65,67–69]. Further, low shear stresses have been found to promote fibrocartilaginous ECM deposition and gene expression [66] and MSC spreading on endothelial cell layers [71]. Vimentin IFs may be involved in how MSCs respond to such physical stimuli as they have been found to be a mechanosensitive cellular element. Not only is vimentin

solubility affected by changes in substrate stiffness [149], but it has also been found to be involved in cellular spreading in a substrate specific manner [38]. Further, vimentin IFs reorganize in response to mechanical loading in chondrogenic MSCs and chondrocytes [101–103] and also appears to be involved in the mechanotransduction of fluid shear stress in endothelial cells [98,99].

Altogether, while vimentin has been implicated in a variety of cellular response mechanisms in different cell populations, understanding of their influence on MSC behavior specifically is still lacking. In this study, we focused on vimentin IF's influence on MSC spreading in response to different microenvironments, specifically ECM proteins, substrate stiffness, and low fluid shear stress. Vimentin appears to be involved in MSC spreading on fibronectin-coated stiff substrates. The observed behavior is potentially due to vimentin's interaction with focal adhesion structures in MSCs when spreading on fibronectin. Further, vimentin may play a mechanoprotective role in resisting cell area changes in response to fluid shear stress. Altogether, vimentin appears to influence MSC spreading response to a variety of microenvironments.

3.2 Materials and Methods

3.2.1 hMSC Cell Culture

Population doubling level (PDL) 9 bone marrow derived human mesenchymal stem cells (hMSCs) (RoosterBio; Frederick, MD) were expanded using RoosterBio Enriched Basal media containing GTX Booster (RoosterBio) per manufacturer

instructions. All subsequent subculture for lentiviral transduction and experimentation was completed using hMSC growth media: high glucose DMEM containing 4 mM L-Glutamine (Gibco) supplemented with 10% fetal bovine serum (FBS) (Gibco), 100 U/mL Penicillin-Streptomycin (Gibco), and 1% MEM non-essential amino acids (Gibco). All experimentation with hMSCs cultured in growth media was completed with PDL 13–18 hMSCs (approximately 4–5 passages). Complete media exchange was completed every 2–3 days and the cells were maintained at 5% CO_2 and at 37°C.

3.2.2 shRNA Transduction

hMSC transduction was performed with either the shVim lentiviral vector (5'-AAAAGGCAGAAGAATGGTACAAATTGGATCCATTTGTACCATTCTTCTGCC-3') or the control, shLacZ lentiviral vector (5'-GCAGTTATCTGGAAGATCAGGTTGGATCCAACCTGATCTTCCAGATAACTGC-3'), for 24hr at a multiplicity of infection (MOI) of 15, as previously described [150]. Transduction was completed with 6 µg/ml hexadimethrine bromide (Polybrene) (Sigma) supplemented in the media to assist with transduction efficiency. Titered viral concentrations for an MOI of 15 were determined through a Quanti-IT PicoGreen Assay (Invitrogen). Two days after infection, pure populations were selected using 12µg/ml Blasticidin for 4 days. Both shVim-hMSCs and shLacZ-hMSCs were cultured in the presence of 1µg/ml doxycycline to induce RNAi for 14 days on tissue culture plastic before being harvested to be assayed in all of the following experiments. All subsequent culture of the shLacZ- and shVim-hMSCs was also conducted in the presence of 1µg/mL doxycycline.

3.2.3 Cellular Spreading

To determine the effect of substrate protein on cellular spreading, 25mm diameter glass coverslips were corona-treated for approximately 20s to make the surface more hydrophilic (Electro-Technic Products). After UV sterilization, coverslips were coated with 10µg/ml human fibronectin (FN), 50µg/ml FN, 10µg/ml Type I rat tail collagen (COL I), or 50µg/ml COL I overnight at 4°C. shLacZ- and shVim-hMSCs were then seeded onto the coverslips and allowed to spread for approximately 2hrs or 24hrs. At these times, cells were fixed with 4% paraformaldehyde and stored in phosphate buffered saline (PBS) at 4°C until imaging.

To determine the effect of surface stiffness on cellular spreading, 25mm diameter glass coverslips were amine-activated using 3-aminopropyltrimethoxysilane. 5kPa (8% Acrylamide, 0.07% N,N'-Methylene bisacrylamide) and 13kPa (8% Acrylamide, 0.2% N,N'-Methylene bisacrylamide) polyacrylamide gels were formed onto these coverslips [151]. These gels were then activated with Sulfo-SANPAH and coated with 10µg/ml FN overnight at 4°C. shLacZ- and shVim-hMSCs were seeded onto the gels and allowed to spread for 24hr. Cells were then fixed with 4% paraformaldehyde and stored in PBS at 4°C until imaging.

To determine the effect of fluid shear stress on cellular spreading, after 14-19 days of shRNA induction, shLacZ- and shVim-hMSCs were seeded into Ibidi µ-Slide I 0.2 chamber slides that had been coated with 10µg/ml FN for 1hr at room temperature and allowed to spread overnight. Reciprocal fluid shear at 1dyne/cm^2 was then

applied for 4hr with 30min periods of alternating flow direction. After 4hr, cells were fixed with 4% paraformaldehyde and stored in PBS at 4°C until imaging.

For all samples, phase contrast images were taken at ×100 magnification with an Olympus IX81 microscope and ImageJ was used to determine the cellular areas and/or cell circularity.

3.2.4 Gene Expression

Gene expression was assessed using quantitative reverse transcription polymerase chain reaction (qRT-PCR) as previously described [146]. On day 14 of shRNA induction, cells cultured on tissue culture polystyrene were resuspended in TRIzol and RNA was isolated per manufacturer's instructions through chloroform separation and isopropanol precipitation. Total RNA was then reverse transcribed. Gene expression was analyzed using qRT-PCR (MyiQ System, BioRad, CA) with primers designed for human genes (Table 3.1). Expression levels for *ITGAV*, *ITGA2*, *ITGB1*, and *ITGB3* and the housekeeping gene *18S* were determined using the ΔΔCt method. Cycle threshold (Ct) values were averaged and the ΔCt was calculated by subtracting the average *18S* Ct values from the average Ct values for the genes of interest. ΔΔCt values for genes of interest were calculated by subtracting the shLacZ-hMSC ΔCt values from the shVim-hMSC ΔCt values. Relative gene expression levels (fold difference) were calculated using the exponential relationship of $2^{-\Delta\Delta Ct}$. Data are shown as average values of the range of calculated fold differences ($2^{-\Delta\Delta Ct+SD}$ and $2^{-\Delta\Delta Ct-SD}$) ± range.

Table 3.1 Sequences of primers used for qRT-PCR

Gene	Forward and Reverse Sequences	GenBank accession no.
18S	5'- AAACGGCTACCACATCCAAG -3' 5'- CCTCCAATGGATCCTCGTTA -3'	NR_003286
ITGA2	5'- AGTGGCTTTCCTGAGAACCG -3' 5'- GATCAAGCCGAGGCTCATGT -3'	NM_002203.3
ITGAV	5'- TTTCGGATCAAGTGGCAGAA -3' 5'- TCCTTGCTGCTCTTGGAACTC -3'	NM_002210.4
ITGB1	5'- ATCTGCGAGTGTGGTGTCTG -3' 5'- AAGGCTCTGCACTGAACACA -3'	NM_002211.3
ITGB3	5'- TGCGAGTGTGACGACTTCTC -3' 5'- GTCCAGTCGGAGTCACACAG -3'	NM_000212.2

3.2.5 Western Blotting

On day 14 of induction, cells cultured on tissue culture polystyrene were harvested and resuspended in a lysis buffer (50 mM HEPES, 150 mM sodium chloride, 1% Triton X-100, 1 mM EDTA, 10 mM Na-pyrophosphate, 10% glycerin) containing a 1:100 concentration of a protease inhibitor cocktail (Fisher Scientific). Protein concentrations were determined through a modified Lowry assay with a Folin-phenol color reaction detected by an ND-1000 spectophotometer (Nanodrop). The protein solution was mixed at a concentration of 1:1 with a loading buffer [13% (v/v) Tris–HCl, 20% (v/v) glycerol, 4.6% (w/v) SDS, 0.02% (w/v) bromophenol blue, 200 mM dithiothreitol]. Samples were subjected to SDS-PAGE using pre-cast Criterion Tris–HCl gels (BioRad). Approximately 3 µg of protein from each sample was loaded into gels. After SDS-PAGE, proteins were transferred electrophoretically to a polyvinylidene fluoride membrane and the vinculin content labelled using a mouse IgG anti-human vinculin primary antibody (ThermoFisher). Vinculin content was visualized using a Vectastain ABC-AmP kit for chromogenic detection. GAPDH visualization using a rabbit IgG anti-human GAPDH primary antibody was used as a

loading control. Semi-quantitative analysis was completed using ImageJ (NIH) to determine band intensities.

3.2.6 Immunofluorescence and focal adhesion analysis

To visualize changes to focal adhesions, 25mm diameter glass coverslips were corona-treated for approximately 20s to make the surface more hydrophilic. After UV sterilization, coverslips were coated with 10µg/ml human fibronectin (FN) overnight at 4^{o}C. shLacZ- and shVim-hMSCs were then seeded onto the coverslips and allowed to spread for 24hrs. Cells were fixed with 4% paraformaldehyde and stored in phosphate buffered saline (PBS) at 4^{o}C until staining. Cells were then permeabilized using 0.1% Triton X-100 and blocked with 1.5% normal goat serum. Cells were labelled with a mouse IgG anti-human vinculin primary antibody (Thermo Fisher) and visualized with biotinylated AlexaFluor594-tagged anti-mouse IgG secondary antibody (Invitrogen). The nucleus was stained with DAPI (Invitrogen). Fluorescence images were taken at ×600 magnification with an Olympus IX81 microscope. The areas of focal adhesions in cells were determined using ImageJ's particle analyzer feature.

3.2.7 Statistical Analysis

Statistical differences in cellular spreading and focal adhesion areas were analyzed by first comparing among the groups using the non-parametric Kruskal-Wallis test. Pair-wise analyses were conducted using Mann-Whitney test; Cell area, $\alpha = 0.01$; Focal adhesion area, $\alpha = 0.05$. Differences in gene expression and western blotting, were determined using the Student's T-test, $\alpha = 0.05$.

3.3 Results

3.3.1 Vimentin influences cell spreading on fibronectin coated surfaces

To evaluate the role of vimentin in sensing different extracellular matrices, hMSCs were seeded onto glass coverslips coated with low and high concentrations of FN or COL I and allowed to attach for either 2hr or 24hr. After 2hr, shVim-hMSC areas were significantly smaller on FN regardless of concentration, while shLacZ-hMSC areas were not (Figure 3.1). No significant differences between shLacZ- and shVim-hMSC areas were found on COL I regardless of concentration. After 2hr of spreading time, no significant differences in the circularity of shLacZ– or shVim-hMSCs were measured when spread on any of the surfaces. However, both shLacZ- and shVim-hMSCs were the least rounded on the higher concentration of COL I. Interestingly, with both cell populations, an increase in COL I concentration resulted in a decrease in circularity, whereas an increase in FN concentration resulted in an increase in circularity. Both cell populations were more rounded on the higher concentration of FN than COL I, but behaved similarly on the lower concentrations of the two proteins.

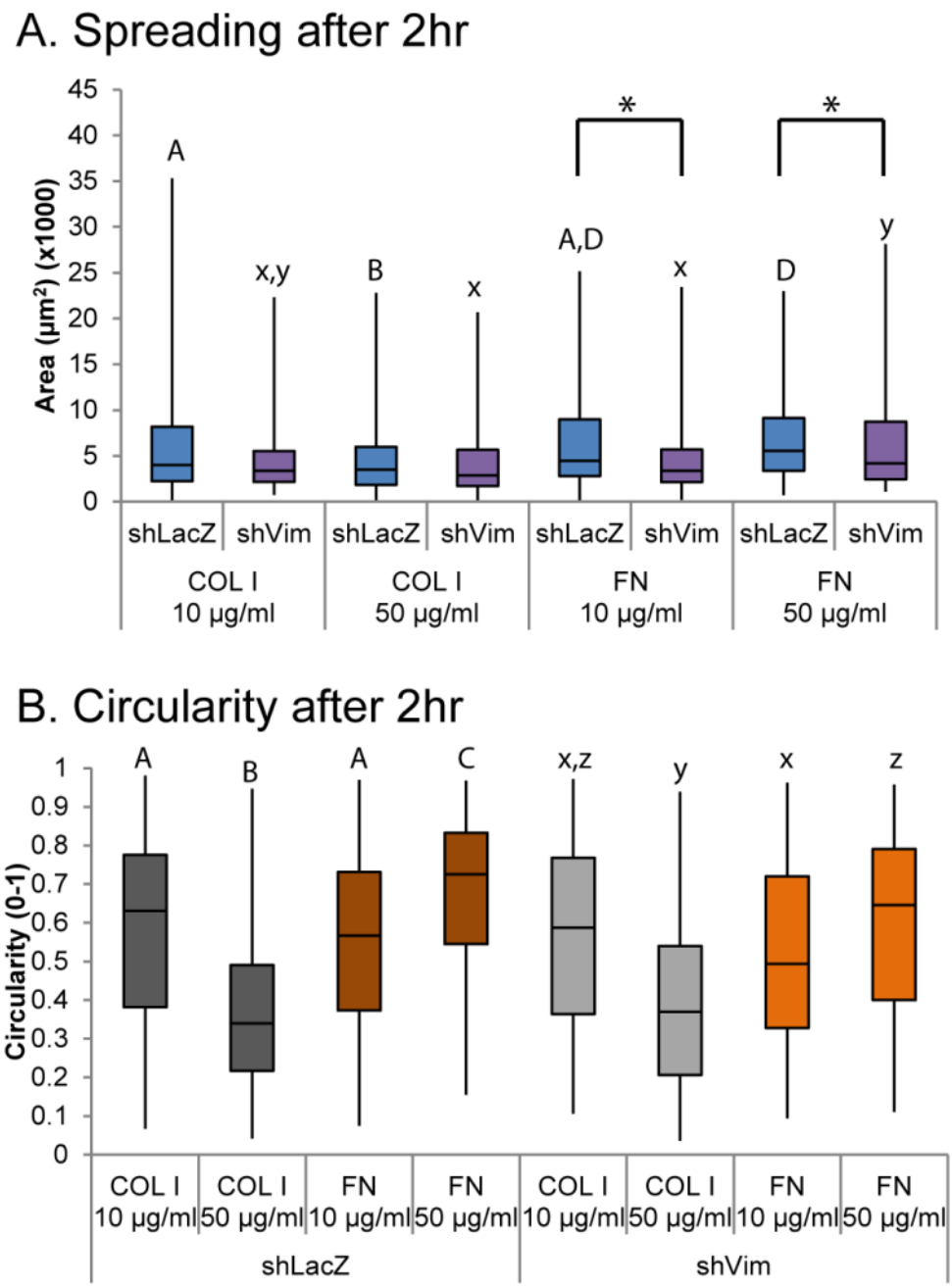

Figure 3.1 shLacZ- and shVim-hMSCs spreading and circularity after 2hrs. A. Area measurement of cells seeded on type I collagen and fibronectin. *p<0.01 between shLacZ- and shVim-hMSCs seeded on the same surface. A,B,D p<0.01 between shLacZ-hMSCs seeded on different surfaces. x,y,z, p<0.01 between shVim-hMSCs seeded on different surfaces. n=140-280 cells. B. Measurement of circularity of cells seeded on type

I collagen and fibronectin. A,B,C p<0.01 between shLacZ-hMSCs seeded on different surfaces. x,y,z p<0.01 between shVim-hMSCs seeded on different surfaces. n=140-280 cells.

After 24hrs, shVim-hMSC areas were also significantly smaller than shLacZ-hMSCs on FN regardless of concentration (Figure 3.2). However, compared to the cell spreading measured at 2hr, shVim-hMSCs were smaller than the shLacZ-hMSCs on the higher concentration of COL I as well. No differences were observed on the lower concentration of COL I. Both shLacZ- and shVim-hMSCs also has larger cell areas with increasing FN concentration, but not on COL I. Circularity was not measured as the cells were highly spread by this point. As the spreading was similarly affected on the FN coated surfaces at both 2hr and 24hr, we chose to focus on the relationship between FN, vimentin, and MSC spreading.

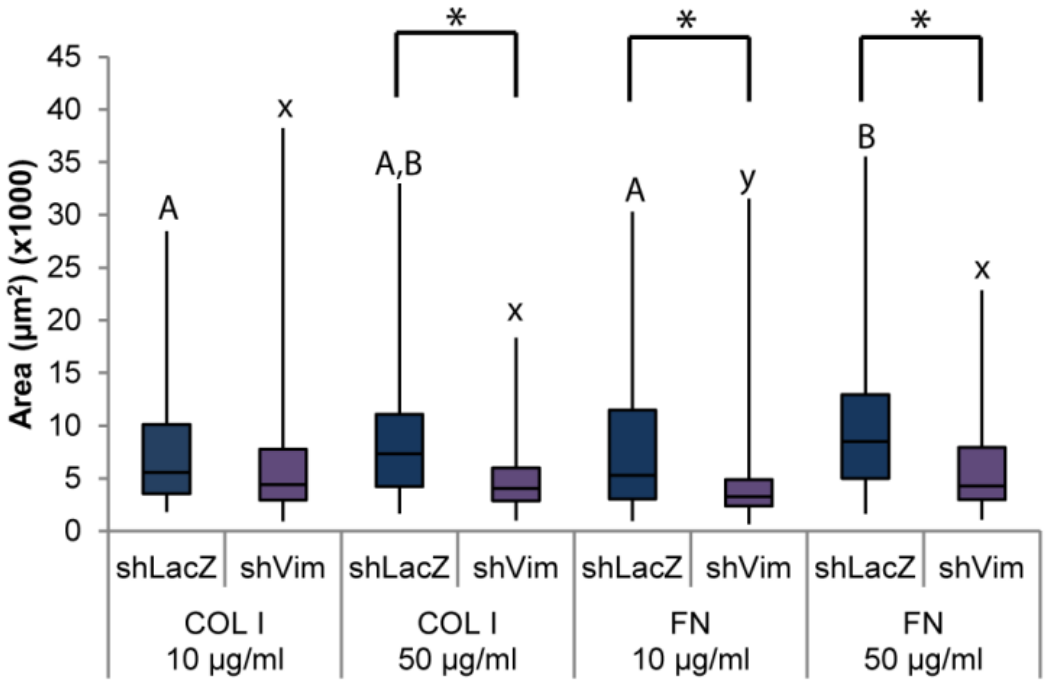

Figure 3.2 Cell spreading of shLacZ- and shVim-hMSCs after 24hrs. Area measurement of cells seeded on type I collagen and fibronectin. *p<0.01 between shLacZ- and shVim-hMSCs seeded on the same surface. A,B p<0.01 between shLacZ-hMSCs seeded on different surfaces. x,y p<0.01 between shVim-hMSCs seeded on different surfaces. n=70-155 cells.

3.3.2 Vimentin may preferentially influence cell spreading on fibronectin-coated stiff substrates

Next, we examined how this relationship between vimentin and MSC spreading on fibronectin coated substrate is affected by substrate stiffness. Both shLacZ- and shVim-hMSCs had larger areas on 13kPa stiffness polyacrylamide gels compared to the 5kPa stiffness gels (Figure 3.3)**.** shVim-hMSCs were significantly smaller on the 13kPa gels compared to the shLacZ-hMSCs (Figure3.3). However, the cell areas were not different between the two cell populations on the 5kPa gels (Figure 3.3).

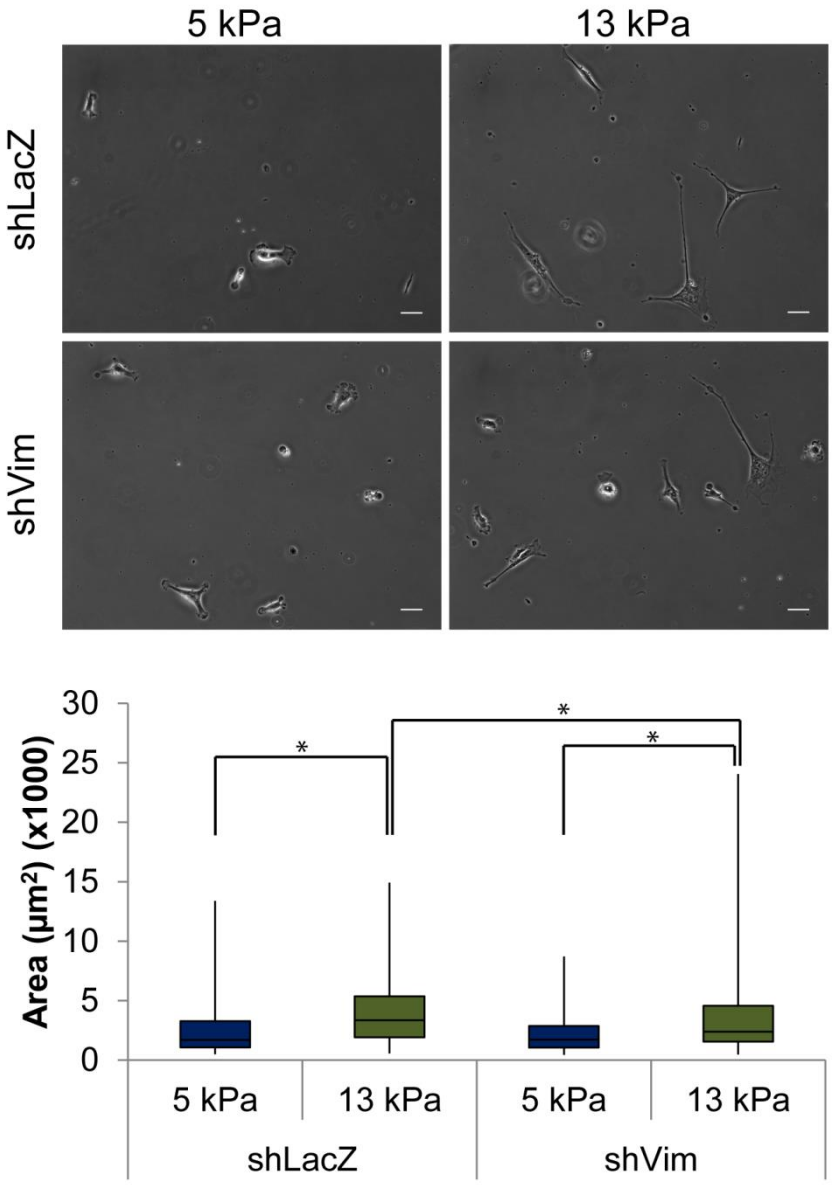

Figure 3.3 Effect of varying substrate stiffness on cell spreading of shLacZ- and shVim-hMSCs. Top: Representative images of cells visualized using phase contrast microscopy. Scale bar 50µm. Bottom: Cell area measurement of shLacZ- and shVim-hMSCs seeded on fibronectin (10µg/ml) coated substrates of varying (5kPa vs. 13kPa) stiffness. *p<0.01, n=185-230 cells.

3.3.3 Vimentin may provide resistance to cell area changes in response to fluid shear stress

Next, we examined the effect of low fluid shear stress on MSCs spreading on fibronectin. shLacZ-hMSCs subjected to fluid shear did not have different cell areas from those subjected to static conditions. Comparatively, shVim-hMSCs subjected to fluid shear stress were significantly smaller than those subjected to static conditions (Figure 3.4). shVim-hMSCs were also smaller than the shLacZ-hMSCs when comparing populations that were subjected to fluid shear stress (Figure 3.4).

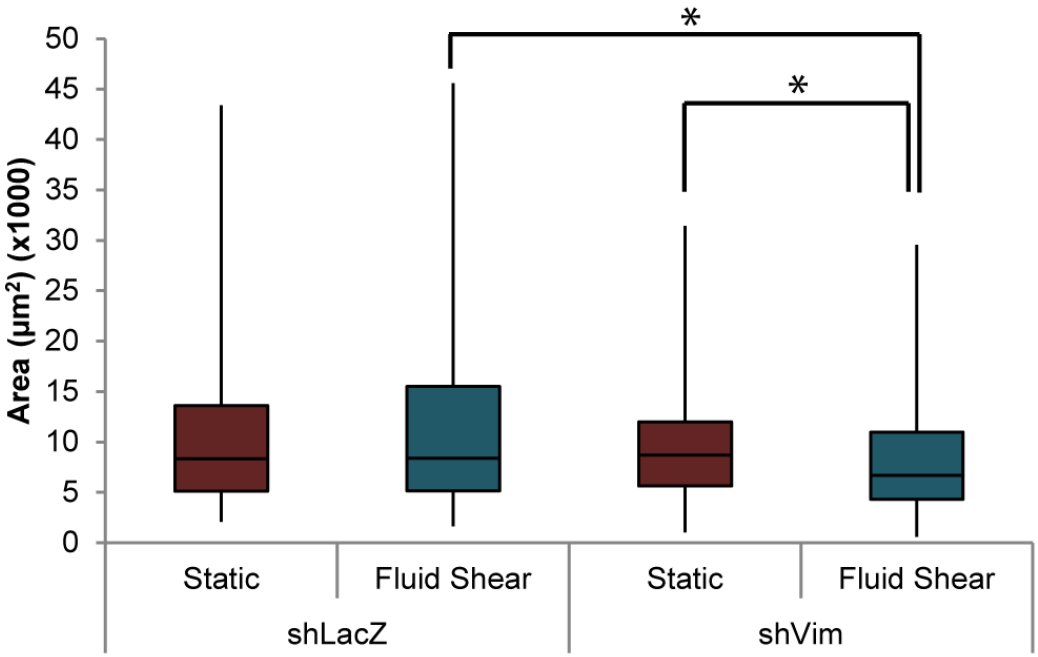

Figure 3.4 Cell spreading of shLacZ- and shVim-hMSCs in response to fluid shear stress. shLacZ- and shVim-hMSCs were seeded in 10ug/ml fibronectin-coated Ibidi µ-Slide I 0.2 chamber slides subjected to reciprocal fluid flow for 4 hours at 1dyne/cm^2 fluid shear stress with change in direction every 30min. *p<0.01, n=125-280 cells.

3.3.4 Vimentin deficiency does not impact hMSC integrin gene expression and vinculin quantity

To examine the relationship between vimentin deficiency and cell spreading related molecules, integrin subunit gene expression of cells cultured on tissue culture polystyrene was assessed, but no significant differences were observed in the gene expression of αV, β3, α2, or β1 integrin subunits between shLacZ- and shVim-hMSCs (Figure 3.5A). As gene expression of these adhesion proteins appeared to be unaffected by vimentin deficiency, the quantity of the focal adhesion protein vinculin in cells cultured on tissue culture polystyrene was analyzed through western blotting, but again no significant differences in vinculin levels were observed between shLacZ- and shVim-hMSCs (Figure 3.5B).

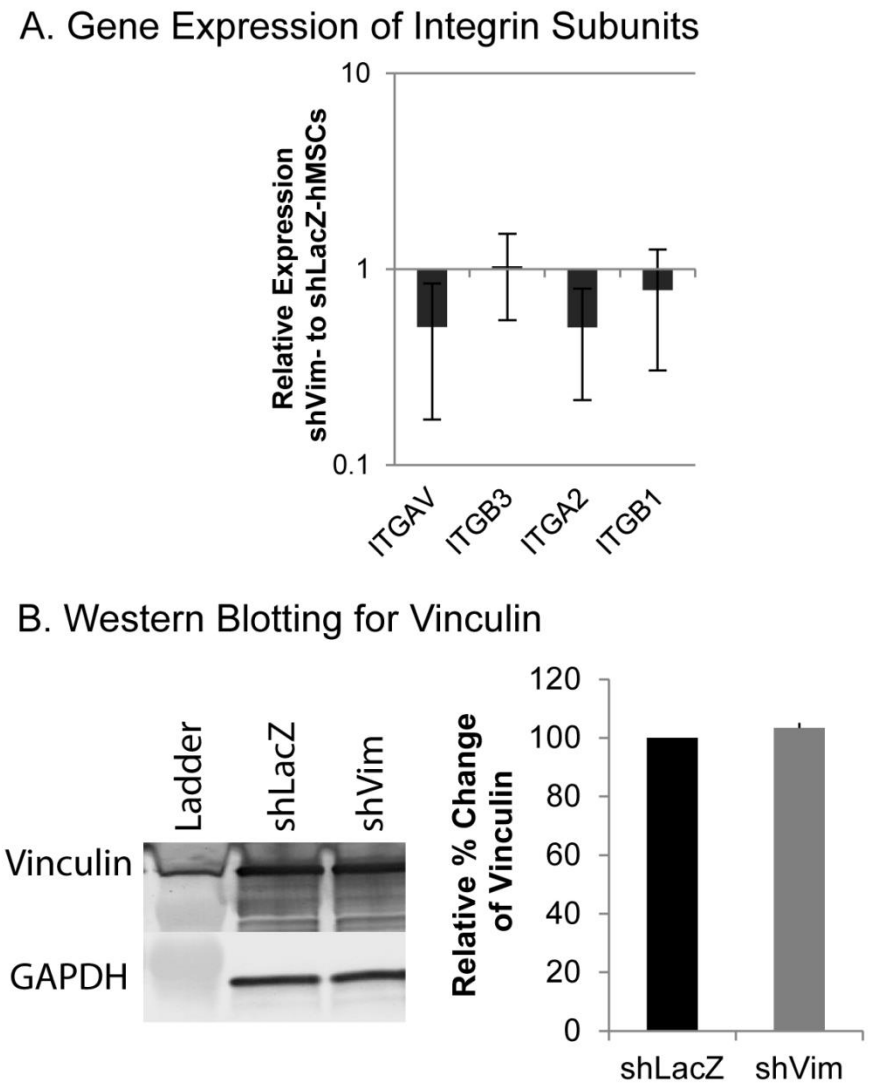

Figure 3.5 Gene expression and western blotting of shLacZ- and shVim-hMSCs cultured on tissue culture polystyrene. A. Relative gene expression levels (fold difference) were calculated using the exponential relationship of $2^{-\Delta\Delta Ct}$. Data are shown as average values of the range of calculated fold differences ($2^{-\Delta\Delta Ct+SD}$ and $2^{-\Delta\Delta Ct-SD}$) ± range and shVim-hMSC gene expression relative to shLacZ-hMSC gene expression. $p<0.05$, n=3. B. Vinculin protein levels as measured by western blotting. Relative percent change of vinculin expression of the shVim-hMSCs relative to the shLacZ-hMSCs, both normalized to the GAPDH expression, mean. $p<0.05$, n=3.

3.3.5 Vimentin deficiency limits focal adhesion size in MSCs spread on fibronectin

Based on the gene expression and western blotting results, a more direct effect of vimentin deficiency on adhesion structures when the cells were spread on fibronectin was analyzed. Specifically, the size of focal adhesions in cells seeded on fibronectin-coated cover glass was assessed. Focal adhesions measured through quantitation of vinculin fluorescence intensity were found to be smaller in shVim-hMSCs compared to shLacZ-hMSCs (Figure 3.6).

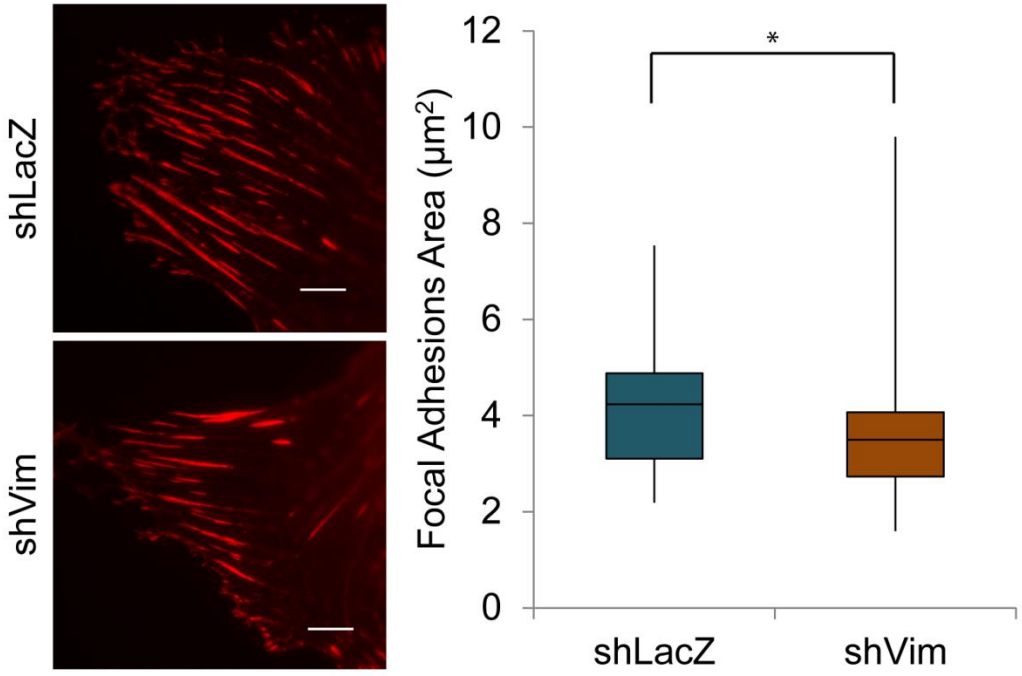

Figure 3.6 Vinculin focal adhesion areas. Areas of focal adhesions were quantified by ImageJ measurements of vinculin immunostaining fluorescence intensity in selected areas of shLacZ- and shVim-hMSCs seeded on fibronectin-coated glass coverslips. $p<0.05$, n=60 cells. Representative images shown on the left. Scale bar: 50μm.

3.4 Discussion

The extracellular environment has been shown to strongly influence MSC behavior. The mechanisms by which MSCs respond to external cues are complex and use a variety of cellular systems, including the cytoskeleton, working together to respond to changes in the environment. Vimentin IFs are increasingly being shown to be involved with basic cellular structures and functions such as cell spreading [38] and focal adhesions [105,113]. Therefore, in this study, we chose to explore the influence of vimentin IFs on cellular spreading in response to different microenvironmental cues.

Initially, cell spreading on substrates coated with type I collagen and fibronectin was analyzed. Vimentin appears to be necessary for unimpaired hMSC spreading on fibronectin from an early stage of spreading onward (Figure 3.1, 3.2), as the vimentin-deficient cells were smaller than control cells on fibronectin, but not on type I collagen, except at the highest concentration of collagen at 24hr. Further, this study suggests that the vimentin-dependent spreading response to fibronectin may be specific to stiff environments, rather than soft (Figure 3.3), as a difference in cell area was only apparent on the stiff polyacrylamide gels and not the soft gels. Previously, the influence of vimentin on cell spreading has primarily been assessed in vimentin-null mouse embryonic fibroblasts (mEFs) and the opposite has been observed [38]. Not only were vimentin-null mEFs found to spread faster on both fibronectin and collagen compared to control cells, but were also smaller on softer fibronectin-coated polyacrylamide gels compared to stiff gels. These discrepancies are likely due to the differences in cell types or the effect of vimentin-knockdown compared to ablation.

In addition to ECM proteins and environmental stiffness, MSCs are also responsive to fluid shear stresses [51,66,71,147]. Thus, the relationship between vimentin, hMSC spreading, and low fluid shear stress was analyzed. Specifically, the shear stress of 1dyne/cm^2 was assessed, as this low level of shear stress has been shown to promote MSC fibro-cartilaginous ECM deposition, especially type II collagen, and chondrogenic gene expression when flow was applied perpendicular to the orientation of the cells[66]. Further, 1dyne/cm^2 is in the physiological range of leukocyte recruitment in low shear areas of arterial circulation and postcapillary venules [71], which can be potentially applied to MSCs traversing the same areas. In fact, 1dyne/cm^2 has been shown to promote MSC spreading on tumor necrosis factor α-activated endothelial cell layers in the presence of the chemokine CXCL9 [71].

Our results suggest that vimentin may be necessary to resist cell area changes in response to this low fluid shear stress, as the control cells did not exhibit any area changes between fluid shear and static conditions, while the vimentin-deficient cells were smaller in response to fluid flow compared to their static controls (Figure 3.4). This is supported by previous work where vimentin, along with α-actinin and filamin A, content increased in osteoblasts in response to fluid flow, exhibiting a proposed mechanoprotective role [152]. Interestingly, higher shear stresses have resulted in the inability for vimentin-deficient endothelial cells to remain attached and these cells have also been found to have impaired focal adhesion formation [105]. It is possible that vimentin-deficient hMSCs would behave similarly when exposed to higher shear

stresses. Previous research also suggests that our results may be explained by impaired recruitment of integrin subunits. β1 integrin subunit recruitment to focal contacts has been observed in osteoblasts stimulated by fluid shear stress [153]. However, vimentin-deficient cells have been found to have fewer β1 integrins at the cell surface as well as lower β1 integrin protein levels [88,107]. This lack of β1 integrins could potentially impair normal mechanotransduction of fluid shear stress. While changes to cell area were the main focus of this study, future analysis of integrin subunit recruitment to cell surface and signaling through proteins such as IL-1β or those in the MAPK family [69] would serve to enhance understanding of how vimentin transduces the effects of this low shear stress.

As spreading of hMSCs on fibronectin, on stiffer surfaces, and in response to fluid shear stress appears to be influenced by vimentin IFs, the effect of vimentin deficiency on adhesion proteins was examined. However, decreasing vimentin levels in hMSCs did not yield any effect at the transcriptional or translational level on the integrin subunit gene expression and vinculin protein levels that were examined in vimentin-deficient and control cells cultured on tissue culture polystyrene (Figure 3.5). Contrary to our gene expression and western blotting findings, in cancer cells, complete vimentin knockdown has been found to result in decreased protein levels of vinculin, β1 integrin, and the cytoskeletal linker filamin A [88]. However, as vimentin deficiency in hMSCs led to a decrease in vinculin-positive focal adhesion size (Figure 3.6), it is possible that vimentin primarily influences MSC behavior at a localized, physical level, rather than impacting transcription or translation.

Previous work has found similar results, with vimentin expression inhibition leading to smaller vinculin-positive [88] and αVβ3-positive [105] focal adhesions. Vimentin has also been found to interact with αV, β3, and α2 integrin subunits as well as with α2β1 integrins in endothelial cells and with αVβ3 integrins associated with vinculin-positive focal contacts [104,106]. In fact, it was observed that vimentin filaments were unable to interact with focal adhesion kinase-positive focal adhesions in the absence of β3 integrins [109]. Vimentin has also been found to interact with β1 integrins, in conjunction with focal adhesion protein talin, to modulate binding of Chinese hamster ovary (CHO) cells to fibronectin [154]. Further, knockdown of vimentin in human embryonic kidney (HEK) cells resulted in not only fewer β1 cell surface integrins, but also impaired cell spreading on collagen as measured by a decreased number of cellular extensions rather than the cell size as measured here [107].

αVβ3 integrins are known to bind to fibronectin and β1 integrin subunits are part of integrins that bind to both collagen and fibronectin [155]. These binding partners coupled with the previous research suggest that vimentin's influence on cellular spreading on fibronectin observed here may also involve vimentin-integrin interactions. Interestingly, previous work has shown that hMSCs internalize activated β1 integrins from the cell surface on collagen-coated soft (0.1-1kPa) substrates compared to stiff (50-100kPa) substrates [156]. This internalization may occur on both fibronectin and collagen as β1 integrin subunits are part of integrins that bind to both [155]. If so, this internalization may indicate a mechanism to explain our findings that on

a soft substrate vimentin-deficiency did not significantly alter cell spreading, implying that vimentin does not play a strong role in cell spreading on soft surfaces. Especially as vimentin appears to interact with β1 integrin subunits [88,107,154]. It also implies a relationship between β1 integrin subunits and vimentin-dependent spreading on stiff substrates and potentially specifically on fibronectin.

Cytoskeletal linkers such as filamin A and plectin have both been associated with vimentin IFs and focal adhesions. Filamin A not only associates with vimentin during cell spreading, but also binds to vimentin directly and serves to regulate β1 dependent adhesion to collagen in conjunction with vimentin [107]. Similarly, recruitment of vimentin IFs to focal adhesions has been shown to involve plectin isoforms [109,122]. A better understanding of vimentin's interactions with different focal adhesion proteins, integrins, and cytoskeletal linkers will help expand understanding of how vimentin influences cellular spreading.

This study is primarily limited by the use of a RNA interference system to decrease the quantity of vimentin rather than ablate it completely, as has been previously used in vimentin-deficient mice [113]. The use of an RNAi system, however, prevents any unforeseen compensation that might occur in knockout conditions. As demonstrated by the discrepancy in the gene expression and western blotting data with literature, more complete knockdown of vimentin may change the effects that we have observed. Alternatively, the culture of these cells on fibronectin or collagen could also affect our gene expression and western blotting observations. Similarly, the use

of a high multiplicity of infection and doxycycline for shRNA induction may affect our findings. Another interesting observation was that the control cells and vimentin-deficient cells did not exhibit differences in cell area in the static controls during the fluid shear study, as was expected based on spreading on the fibronectin-coated glass coverslips and the polyacrylamide gels. This is attributed to the fibronectin adsorption time: overnight at 4°C for the coverslips and gels and 1hr at room temperature for the microfluidics chambers. We presume differences in adsorption time affected fibronectin deposition, either by configuration or quantity.

This study reveals a new relationship between MSC spreading, fibronectin, and vimentin IFs. Our observations suggest that a complete vimentin IF network is needed for unimpaired spreading of MSCs on fibronectin in stiff environments. Further, vimentin may be needed for resisting cell area changes in response to low fluid shear stresses. It appears that these changes in cell spreading may be tied to how an intact vimentin network affects focal adhesions and their formation, potentially with a dependence on integrins. These interactions clearly suggest that continued research into the role of vimentin intermediate filaments within MSCs will be necessary to better understand MSC behavior in differing microenvironments.

3.5 Conclusion

The objective of this second Aim was to examine if vimentin IFs influence cellular spreading in a variety of microenvironments, and they do appear to, based on our findings. MSC area has been correlated with functional changes, such as changes to

cell stiffness and differentiation potential [34,37]. Understanding how vimentin influences cell area can help to clarify how it might be involved in the MSC functional response to their physical environment. Our findings appear to show that vimentin is involved in changes to MSC in multiple microenvironments with different cues such as varying stiffness or low fluid shear stress. Different microenvironmental cues appear to affect the level of vimentin's involvement in cell area, i.e. soft vs. stiff environments. While our data suggests that vimentin is involved in resisting low fluid shear stress, higher fluid shear stress responses may be less dependent on vimentin. Altogether this suggests a complex cellular response mechanism that also involves other cytoskeletal proteins working in concert with vimentin. However, it does appear that vimentin's involvement may require interaction with adhesive structures as both our findings and literature suggests. It is likely that vimentin intermediate filaments work in support of actin microfilaments in regulating cell area in different environments. Further, vimentin may have more influence on particular adhesive structures than others, either directly or indirectly through supporting proteins. In the next area of this work, we sought to determine how the influence of vimentin on individual cells might affect MSC differentiation and subsequent extracellular matrix deposition in a cell population study, using two different culture environments with different capacities for cellular adhesion.

Chapter 4: Vimentin intermediate filaments may have a limited influence on chondrogenesis over extended culture periods[2]

4.1 Introduction

Mesenchymal stem cells are increasingly being investigated for the treatment of orthopaedic diseases such as osteoarthritis [13]. Tissue engineering strategies combine cells and biomaterials, and research suggests that pre-conditioning (e.g. mechanical stimulation) of biomaterial constructs can help improve mechanical properties and extracellular matrix (ECM) deposition [43,47,49]. Understanding the effects of chondrogenic culture environment itself on these properties prior to pre-conditioning can help improve understanding of the effects such treatments.

The matrix environment surrounding chondrocytes and chondrogenically committed MSCs is immediately comprised of a pericellular matrix (PCM) surrounded by an ECM. The PCM consists primarily of type VI collagen and hyaluronan [7] while the surrounding ECM is made up of a variety of collagens and proteoglycans, including type II collagen and aggrecan, but not type VI collagen [5,7]. Research in MSC chondrogenic differentiation is often conducted using pellet cultures to recapitulate and better understand condensation-like cartilage formation with MSCs undergoing terminal differentiation [41,42,157]. In early chondrogenesis and endochondral ossification, cell-to-cell contacts through N-cadherin and neural cell adhesion molecule (N-CAM) are prominent [158] and their loss is concomitant with a

[2]To be submitted for publication: Sharma, P., Wagner, D.R., Hsieh, A.H. Vimentin intermediate filaments may have a limited influence on chondrogenesis over extended culture periods. *In preparation*

commitment to the chondrogenic lineage [158,159]. Comparatively, biomaterials, including hydrogels such as agarose or alginate, are frequently used for evaluating MSC chondrogenesis for tissue engineering cartilage. While cells within these materials often lack the cell-to-cell contacts present in the pellet cultures [157,160], such culture systems are often used because they are permissive for studying chondrogenesis [48,49,157,161,162] and the effects of mechanical loading on cell growth, ECM deposition, and mechanical properties [48,49,101,162,163].

Regardless of culture conditions, MSCs sense and respond to their environment using the cytoskeleton, consisting of actin microfilaments, tubulin microtubules, and vimentin intermediate filaments (IFs). While the role of microtubules in chondrogenesis appears to be limited or not well studied [52], the influence of actin microfilaments has been evaluated. Both disruption of actin and negatively modulating the RhoA/ROCK pathway promote chondrogenesis [52,73,74]. The effect of vimentin IF deficiency on cartilage development has not been specifically investigated, but vimentin-null mice appear to exhibit normal skeletal development [82], albeit with impaired wound healing [83], altered physical coordination potentially due to cerebral defects [85], and reduced response to renal injury [84]. Additionally, disruption or decrease of vimentin in chondrocytes or progenitor cells negatively influenced chondrogenic gene expression and extracellular matrix deposition, synthesis and degradation [123,124]. Further, an increase in vimentin has been observed in MSCs undergoing chondrogenesis [124,164] and changes in the scaffold environment have been shown to cause variations in vimentin [101,165]. There is also evidence for vimentin's

involvement in disease, as dysregulated expression or organization of vimentin is apparent in osteoarthritic chondrocytes [92,93] and in MSCs isolated from bone marrow from osteoarthritis patients [95].

As vimentin IFs are known to have some influence in early chondrogenesis and exhibit abnormalities in degeneration, we sought to evaluate its influence on the capacity for MSCs to undergo chondrogenic differentiation in two different culture environments: agarose hydrogel cultures and pellet cultures. After determining that vimentin may be slightly involved in the deposition of an organized ECM, we next examined the expression of genes related to matrix degradation, cellular adhesion to the surrounding matrix, and chondrogenesis. While a decrease in vimentin at the beginning of chondrogenesis did not affect gene expression compared directly to the control cell population, variations appeared when examining the behavior of MSCs over culture time and when comparing culture conditions.

4.2 Materials and Methods

4.2.1 hMSC Cell Culture

Population doubling level (PDL) 9 bone marrow derived human mesenchymal stem cells (hMSCs) (RoosterBio; Frederick, MD) were expanded using RoosterBio Enriched Basal media with the GTX Booster (RoosterBio) per manufacturer instructions. All subsequent subculture for lentiviral transduction and experimentation was completed using hMSC growth media: high glucose Dulbecco Modified Eagle Medium (DMEM (containing 4mM L-Glutamine (Gibco) supplemented with 10% fetal bovine serum (FBS) (Gibco), 100 U/mL Penicillin-Streptomycin (Gibco), and

1% Minimal Essential Medium non-essential amino acids (Gibco). hMSCs were used for transduction and experimentation at PDL 13–18 (approximately 4–5 passages). Complete media exchange was completed every 2–3 days and cells were maintained at 5% CO_2 and at 37°C.

4.2.2 shRNA Transduction

hMSC transduction with the vimentin targeting lentiviral vector (shVim) (5'-AAAAGGCAGAAGAATGGTACAAATTGGATCCATTTGTACCATTCTTCTGCC-3') or the control vector targeting LacZ (shLacZ) (5'-GCAGTTATCTGGAAGATCAGGTTGGATCCAACCTGATCTTCCAGATAACTGC-3') was completed for 24 h at a multiplicity of infection (MOI) of 15, as previously described [150]. Transduction efficiency was assisted by the presence of 6 µg/ml hexadimethrine bromide (Polybrene) (Sigma). Titered viral concentrations were determined through a Quanti-IT PicoGreen Assay (Invitrogen). Two days post-infection, pure populations were selected using 12µg/ml Blasticidin for 4 days. Both shVim-hMSCs and shLacZ-hMSCs were cultured in the presence of 1µg/ml doxycycline to induce RNAi. All subsequent cultures of shVim-hMSCs and shLacZ-hMSCs were conducted in the presence of 1µg/mL doxycycline. Cells were cultured for 14 days on tissue culture plastic before being harvested to undergo differentiation.

4.2.3 Chondrogenic Differentiation

After 14 days of shRNA induction, shVim- and shLacZ-hMSCs were seeded in two different configurations for chondrogenic differentiation. To form pellet cultures,

$0.250x10^6$ cells were centrifuged and resuspended in incomplete chondrogenic media (high glucose DMEM with 4mM L-glutamine supplemented with 10% FBS, 50µg/mL L-ascorbic acid, 40µg/mL L-proline, 1mg/mL insulin, 0.55mg/mL transferrin, 0.5µg/mL sodium selenite, 50mg/mL bovine serum albumin, 470µg/mL linoleic acid, 100 U/ml penicillin/streptomycin) before being centrifuged again. Complete media (incomplete media with 10ng/mL $TGFB_3$) supplemented with 1µg/ml doxycycline was added to the pelleted cells and they were cultured for 14 and 21 days. To form agarose cultures, cells were resuspended in 4% (w/v) agarose at a cell density of $1x10^6$ cells/ml and pipetted into an Ø6mm x 3mm mold to form agarose discs. Discs were cultured in complete chondrogenic media supplemented with 1µg/ml doxycycline for 14 and 21 days.

4.2.4 Histology and Immunohistochemistry

Chondrogenic agarose discs were sliced in half and then chondrogenic pellets and half agarose discs were fixed with 4% paraformaldehyde. Pellets were then infiltrated with 30% sucrose, embedded in Tissue-Tek O.C.T compound (Sakura), and stored −80 °C until cryosectioning (8µm) using an HM550 series cryostat (Richard Allen Scientific). Agarose samples were dehydrated using sequential ethanol washes and xylene before being embedded in paraffin. 5µm paraffin sections were created using a HM355S microtome (Microm). Paraffin sections were warmed for 2hr and then rehydrated with xylene and sequential ethanol washes. Some sections (OCT or paraffin) were histologically stained for visualizing sGAGs with 0.1% Safranin-O. Additional sections were used for immunohistochemical detection of type II collagen, type VI collagen, or aggrecan. These sections were blocked with 0.3% hydrogen

peroxide and then with 1% bovine serum albumin (BSA). Sections were labeled with either rabbit IgG anti-human type II collagen primary antibody, rabbit IgG anti-human type VI collagen (Col6a1) primary antibody, or mouse IgG anti-human aggrecan primary antibody. For visualization, biotinylated secondary antibodies were used with a horseradish peroxidase-conjugated streptavidin (Vectastain ABC; Vector Laboratories), followed by a 3, 3 –diaminobenzidine substrate color reaction. All sections were then dehydrated through sequential ethanol washes. Chondrogenic pellets were mounted with Cytoseal XYL and agarose culture sections were mounted with Permount. All histology and immunohistochemistry samples were imaged using bright field microscopy at × 100 magnifications with an Olympus IX81 microscope and a Qcolor3 camera. Sections of the images are presented in Figures 4.1 and 4.2.

4.2.5 Gene expression

Gene expression was assessed using quantitative reverse transcription polymerase chain reaction (qRT-PCR). To isolate RNA, after 14 and 21 days of chondrogenesis, chondrogenic pellets and agarose discs were homogenized in TRIzol (Ambion/ThermoFisher). For the chondrogenic pellets, RNA was isolated per manufacturer's instructions. Briefly, RNA was isolated using chloroform phase separation and isopropanol precipitation. For the agarose discs, RNA was isolated by modifying a previously presented method for RNA isolation from agarose [166]. Ethanol (100%) was added to create the final ratio of 2:1 Trizol:100% ethanol. That solution was then was used to isolate RNA using the RNeasy Micro kit (Qiagen). Total RNA was then reverse transcribed, amplified, and analyzed using qRT-PCR (MyiQ System, BioRad, CA) with primers designed for human genes (Table 4.1).

Specifically, the expression of transcription factor sex determining region Y-box 9 (*SOX9),* type VI collagen (*COL6A1*), matrix metalloprotease 13 (*MMP13*), aggrecanases "A disintegrin and metalloproteinase with thrombospondin motifs" 4 and 5 (*ADAMTS4 and ADAMTS5*), N-cadherin (*CDH2*), αV (*ITGAV*) integrin subunit, and β1 (*ITGB1*) integrin subunit and the housekeeping gene *18S* were analyzed using the ΔΔCt method.

Table 4.1 Sequences of primers used for qRT-PCR

Gene	Forward and Reverse Sequences	GenBank accession no.
18SR5	5'- AAACGGCTACCACATCCAAG -3' 5'- CCTCCAATGGATCCTCGTTA -3'	NR_003286
SOX9	5'- AGTACCCGCACTTGCACAAC -3' 5'- CGTTCTTCACCGACTTCCTC -3'	NM_000346
COL6A1	5'- CTACACCGACTGCGCTATCA -3' 5'- GCCACCGAGAAGACTTTGAC -3'	NM_001848
MMP13	5'- AAGGAGCATGGCGACTTCTA -3' 5'- GGTCCTTGGAGTGGTCAAGA -3'	NM_002427.3
ADAMTS4	5'- AGGCACTGGGCTACTAC -3' 5'- GGGATAGTGACCACATTGTT -3'	NM_005099.5
ADAMTS5	5'- TCTAAGCCCTGGTCCAAATG -3' 5'- TCGTGGTAGGTCCAGCAAA -3'	NM_007038.4
CDH2	5'- AGGGGACCTTTTCCTCAAGA -3' 5'- TCAAATGAAACCGGGCTATC -3'	NM_001792.4
ITGAV	5'- TTTCGGATCAAGTGGCAGAA -3' 5'- TCCTTGCTGCTCTTGGAACTC -3'	NM_002210.4
ITGB1	5'- ATCTGCGAGTGTGGTGTCTG -3' 5'- AAGGCTCTGCACTGAACACA -3'	NM_002211.3

Cycle threshold (Ct) values were averaged and the ΔCt was determined by subtracting the average *18S* Ct values from those of the gene of interest. ΔΔCt values for each gene were calculated by subtracting the ΔCt values for the reference sample from the corresponding ΔCt values for the sample of interest at each time point, depending on the relationship being examined. Relative gene expression levels (fold

difference) were calculated using the exponential relationship $2^{-\Delta\Delta Ct}$. Data are shown as average values of the range of calculated fold differences ($2^{-\Delta\Delta Ct+SD}$ and $2^{-\Delta\Delta Ct-SD}$) ± range. Three to five biological replicates were evaluated for each gene.

4.2.6 Statistical Analysis

Statistical differences in gene expression were determined using Student's t-test to compare ΔCt values. Statistical significance was set to $\alpha=0.05$.

4.3 Results and Discussion

In this study, we sought to determine the effects of vimentin knockdown on chondrogenic extracellular matrix deposition and gene expression using two different culture environments: pellets and agarose hydrogels. In short term cultures, vimentin has been found to be involved in chondrogenesis [123,124], however extended culture times have not been evaluated. We sought to address this gap in knowledge by examining its potential involvement in longer chondrogenic culture times, 14 and 21 days, using shRNA lentiviral particles that we previously showed could achieve approximately 30% vimentin knockdown at day 14 of induction [150]. At this point, the cells were placed in the two chondrogenic culture environments and subsequently induced to undergo chondrogenesis for a further 14 and 21 days.

For pellet cultures, immunohistochemical (IHC) and histological staining revealed robust, but varied, matrix deposition by both shLacZ- and shVim-hMSCs (Figure 4.1). Overall, the type II collagen structure appeared to become more densely organized from day 14 to day 21. shLacZ- and shVim-hMSC pellets had similar type

II collagen, type VI collagen and aggrecan organization; however, an apparent decrease in aggrecan intensity was observed from day 14 to 21. Safranin O staining for sulfated glycosaminoglycans (sGAGs) possessed greater definition of structural features in shLacZ-hMSC pellets from day 14 to day 21, while the shVim-hMSC pellets appeared to retain more disordered, amorphous, with possible less intensity, sGAG content at Day 21.

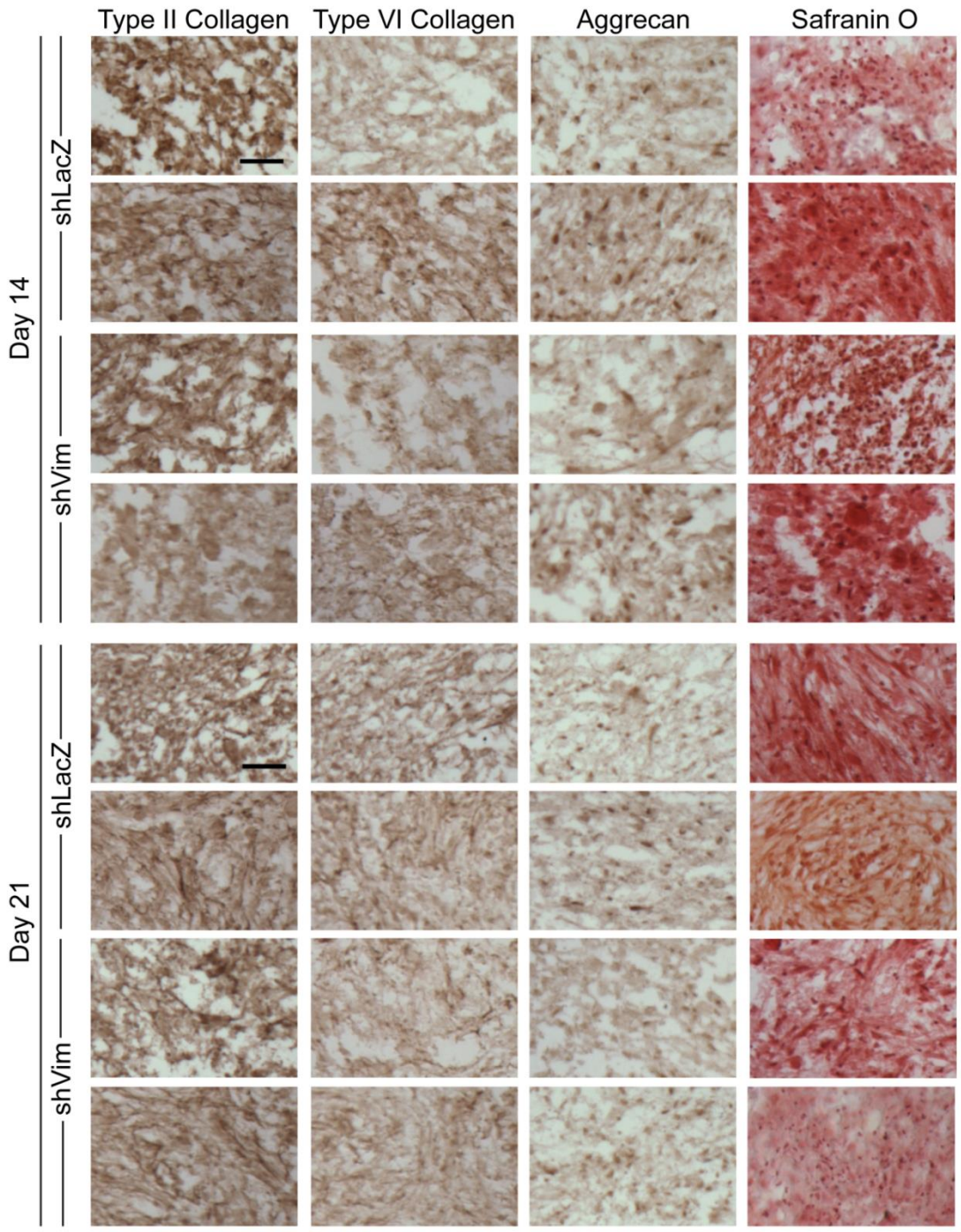

Figure 4.1 IHC and Histology of Pellet Cultures. shLacZ- and shVim-hMSC pellet cultures stained using IHC for type II collagen, type VI collagen, and aggrecan and stained with safranin O for sGAGs on day 14 and day 21 of culture. Scale bar: 50μm.

Comparatively, the agarose hydrogels showed limited ECM deposition (Figure 4.2). Both shlacZ- and shVim-hMSC hydrogels had similar type II collagen staining patterns, with slightly less deposition in the shVim-hMSCs culture. Type VI collagen, aggrecan, and safranin O staining was primarily localized in circular pockets, presumably around individual cells. The low ECM deposition in the agarose hydrogels is likely due to the low cell density [167]. While low cell densities in hydrogels have been successfully used to evaluate chondrogenesis [44,161], higher cell densities typically yield more ECM deposition [49,167,168]. The slight variation in staining in the shVim-hMSC cultures compared to the shLacZ-hMSC cultures suggests that the loss of vimentin could have some effect on ECM deposition or organization.

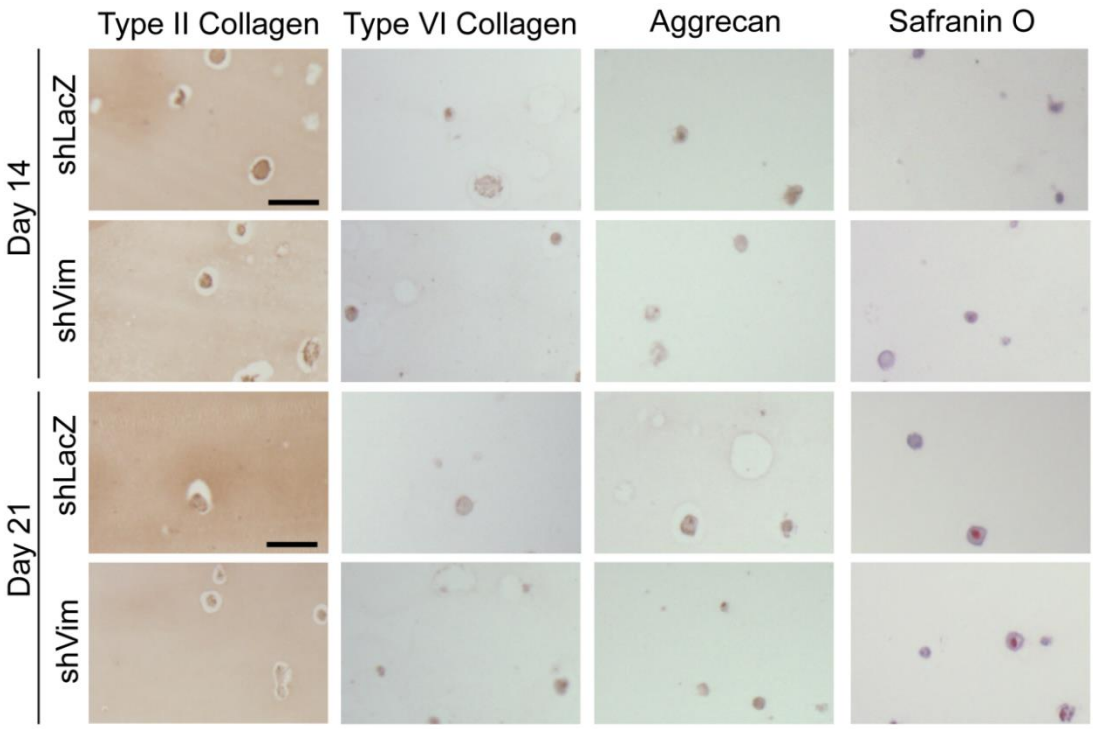

Figure 4.2 IHC and Histology of Agarose Cultures. shLacZ- and shVim-hMSC agarose cultures stained using IHC for type II collagen, type VI collagen, and aggrecan and stained with safranin O for sGAGs on day 14 and day 21 of culture. Scale bar: 50μm.

To further interrogate the potential variation in ECM deposition, gene expression was evaluated. In general, no significant differences were observed in the gene expression between chondrogenic shLacZ- and shVim-hMSCs at Day 14 or Day 21 (Figure 4.3A). These results imply that vimentin's involvement could be in organizing the ECM, rather than upstream at the transcriptional level, during these stages of chondrogenesis. For example, chondrogenesis has previously been shown to be impaired by interfering with arginine-glycine-aspartic acid (RGD)-dependent ECM binding sites, which also caused vimentin reorganization [101]. Similarly, calcium mediated signaling was involved in vimentin reorganization that occurred in response to hydrostatic pressure loading in chondrogenic cultures [101,169]. Part of our previous work evaluated cytoskeletal changes of shVim-hMSCs, where we found that the functional role of actin may be altered with vimentin knockdown. Therefore, it is possible that vimentin has a functional effect on interactions among different cytoskeletal elements in depositing and organizing ECM.

Despite the lack of difference between shLacZ- and shVim-hMSCs, some distinctions in gene expression were observed when comparing the cell populations at day 14 and day 21 (Figure 4.3B) as well as between the two culturing conditions (Figure 4.3C). In pellet cultures, gene expression of *MMP13* increased and *ADAMTS5* decreased from day 14 to day 21, but only in pellet cultures, not agarose hydrogels (Figure 4.3B). Similarly, when evaluating the effects of culture condition at day 21, shLacZ- and shVim-hMSCs both exhibited significantly less degradative enzyme (*MMP13*, *ADAMTS5*, *ADAMTS4*) expression in agarose gels compared to pellet cultures

(Figure 4.3C). As high expression of these enzymes is related to hypertrophy and degeneration [170–172], these results suggest that by day 21 the chondrogenic cells in pellet cultures may have become hypertrophic, as has been previously reported for pellet cultures[41]. Alternatively, the limited ECM deposition in agarose hydrogels compared to pellet cultures may not elicit any remodeling response to hypertrophy. One exception is that in shVim-hMSCs at day 14, we did not observe any difference in expression of *MMP13* and *ADAMTS4* between the agarose and the pellet cultures, suggesting aberrant expression in response to culture environment at this stage of chondrogenesis (Figure 4.3C).

In terms of cell adhesion receptors, we found higher expression of αV integrin in the agarose cultures compared to the pellet cultures (Figure 4.3C). This could be indicative of a bias toward cell-PCM or cell-ECM adhesion in the agarose, whereas in pellet cultures the comparatively high cell density would involve greater cell-to-cell adhesion. In pellet cultures, however, we did not see greater expression of N-cadherin, which is involved in cell-to-cell adhesion. But its expression is typically upregulated during early chondrogenesis and cells might not exhibit elevated expression levels at later stages, especially if cells are hypertrophic [173]. More likely, the expression of αV integrin is related to its specific binding moieties in the PCM and ECM that might be different between the two culture environments. Specifically, αV subunit containing integrins are known to bind to RGD-specific binding sites [174] and they have been found to facilitate chondrocyte binding to cartilage, type II collagen, type VI collagen, and fibronectin [175,176]. When examining the expression of

matrix proteins, we observed lower type VI collagen levels in the shVim-hMSCs in the day 21 agarose hydrogels compared to the pellet culture (Figure 4.3C), suggesting that type VI collagen expression may be negatively affected by vimentin knockdown in a culture condition-dependent manner. Determining differences in the PCM composition or analyzing multiple αV subunit-containing integrins in these environments may help to clarify this result.

A. shVim relative to shLacZ

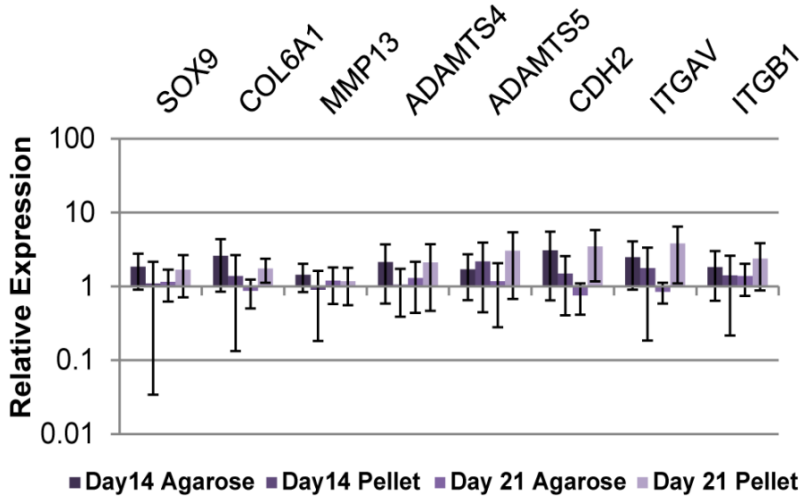

B. Day 21 relative to Day 14

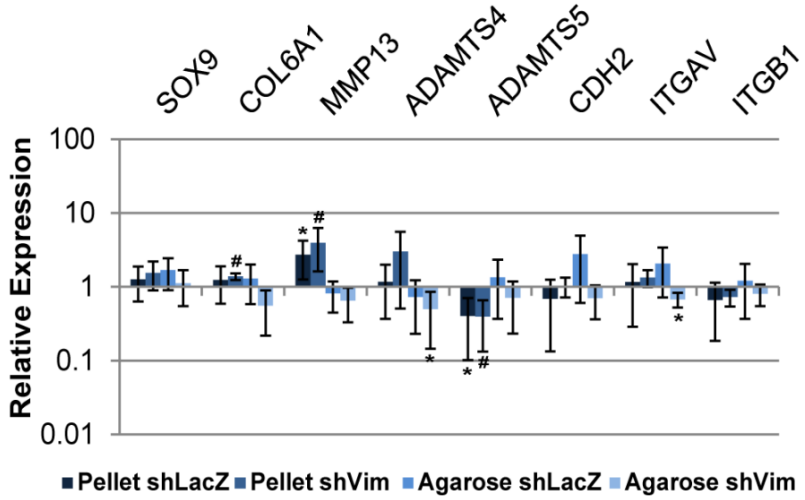

C. Agarose culture relative to Pellet culture

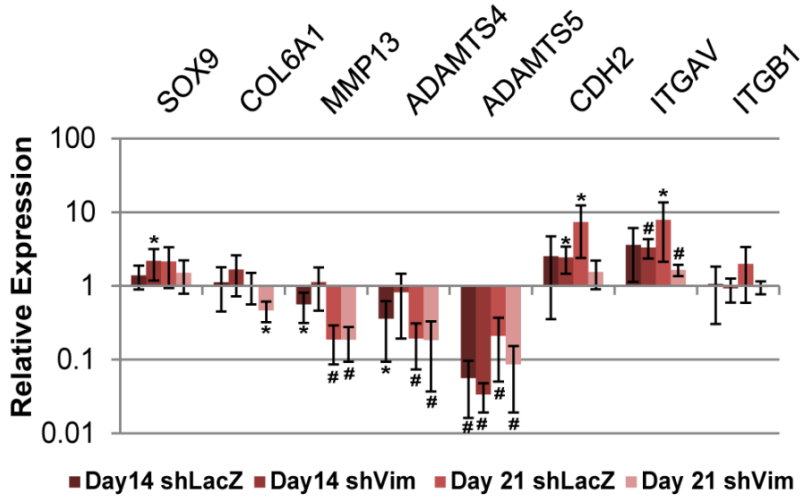

Figure 4.3 Gene expression of Pellet and Agarose Cultures. shLacZ- and shVim-hMSC pellet and agarose culture assayed for gene expression at day 14 and day 21 (n = 3-5). A. shVim-hMSC samples relative to shLacZ-hMSC samples for all both culture conditions and time points. B. Day 21 samples relative to Day 14 samples for both cell populations and culture conditions. C. Agarose culture samples relative to pellet culture samples for both cell populations and time points. *p<0.05, #p<0.01 compared to stated relevant comparison. Data are shown as average values of the range of calculated fold differences ($2^{-\Delta\Delta Ct+SD}$ and $2^{-\Delta\Delta Ct-SD}$) ± range.

This study is primarily limited by the knockdown of vimentin expression rather than the ablation found in cells isolated from vimentin null mice. Thus, it is possible that our observations may be underrepresenting vimentin's involvement in these processes. However, this study better recapitulates a situation in which MSCs from osteoarthritic patients would be isolated for cell therapy, where the MSC function may be impaired [95,177]. Regardless**,** it is possible that over the course of chondrogenesis that the cells were able to overcome the moderate decrease in vimentin. This then focuses our findings specifically on the influence of vimentin decrease at the initiation of chondrogenesis on long term chondrogenic cultures. Further, while we did not observe a deficiency in chondrogenic differentiation, the use of the high MOI for lentiviral transduction and the doxycycline for the shRNA induction could potentially have some, as yet, unidentified effect on MSC differentiation.

This study provides new insight into the involvement of vimentin in the chondrogenesis of MSCs. Namely, vimentin deficiency, at least at the start of chondrogenesis, does not appear to affect gene expression in longer chondrogenic cultures when compared to a control cell population. Variations in ECM deposition, coupled with the gene expression, imply a need for further examination of vimentin's role in interacting with the PCM and whether that interaction truly affects ECM organization and deposition. Differential gene expression of degradative enzymes and the αV integrin subunit in different culture conditions further opens new avenues for this area of research. As MSCs are increasingly being evaluated for cell therapy, understanding how culture environment can affect their behavior and what cellular elements regulate that response will be critical.

4.4 Conclusion

The first two Aims of this work were focused on the effect of physical compression, i.e. cell deformability of MSCs, and then the response to microenvironmental changes, i.e. changes in cell area of MSCs. In contrast, the objective of this final Aim was to determine how vimentin influences the start of chondrogenesis, which ultimately may result in changes in longer *in vitro* culture, and also to determine how that influence would be altered by changes in environmental conditions. With this third aim, we wanted expand our understanding of vimentin's influence from effects on individual cells to its impact on a population of MSCs.

Chapter 5: Conclusions and Future Work

The aim of this work was to examine how mesenchymal stem cells respond to different environments. As MSCs are increasingly being investigated for therapeutic use [1,3], a fundamental understanding of how these cells will behave in different environments is critical for the success and evaluation of MSC therapies. In this work, we focused on the influence of vimentin intermediate filaments on MSC response to varying physical stimuli as vimentin is increasingly gaining notice as being involved in many cell characteristics and functions. Further, its expression has been found to be aberrant in MSCs isolated from osteoarthritic patients, which suggests that understanding vimentin's influence on MSC behavior could impact autologous cell therapies from this patient population. By decreasing vimentin protein levels in MSCs using a lentiviral shRNA-based system, we were able to examine the influence of vimentin on MSC characteristics and behavior in multiple areas (Figure 5.1).

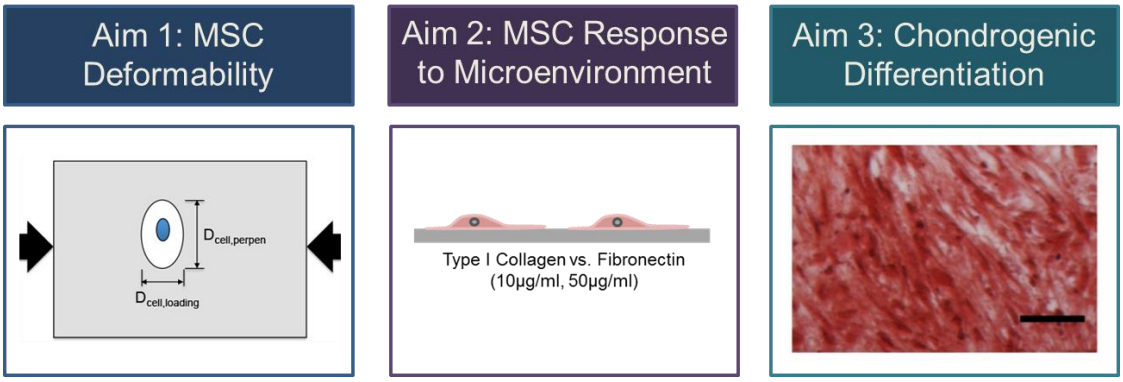

Figure 5.1 The three aims of this dissertation.

Overall, the primary finding from these studies is that vimentin intermediate filaments influence physical changes in MSCs in response to external cues such as mechanical load, different ECM proteins, and environmental stiffness. Vimentin's influence on the regulation of these physical changes in MSCs is likely to be at a localized, direct interaction level, rather than having much control over regulating gene expression and protein translation. While vimentin IFs do not appear to be critical for chondrogenic differentiation, based on these three studies, it is instead likely that they have more of an influence over the mechanical regulation of chondrogenesis. In Chapters 2 and 3, we described how vimentin IFs influenced physical changes, deformability and cell size, in MSCs in response to external stimuli. And in Chapters 3 and 4, we described a potential lack of influence over gene and protein expression.

The objective of the first aim (Chapter 2) was to examine the influence of vimentin intermediate filaments on MSC deformability. MSCs entering a load bearing environment, such as articular cartilage, would be subjected to compression due to tissue deformation caused by normal or abnormal use, and vimentin networks have been shown to influence cellular stiffness and the capacity to resist such compression [11,52,94,112,113,118,139–141]. As mentioned, deformation of cells, such as chondrocytes within this environment are known to be deformed and this compression can result in functional outcomes such as changes in extracellular matrix protein expression [50,138–142]. Thus, it is important to understand how MSCs entering such as environment may be affected by this compression, and vimentin's role in response. In this study, we embedded the cells in agarose hydrogels and subjected them to deformation, finding

that vimentin-deficient hMSCs were actually less deformable than the control cells, supporting that vimentin must have a role in controlling the mechanical properties and physical structure of MSCs. Subsequent disruption of actin and microtubules and quantification of the immunofluorescent intensity of these proteins in vimentin-deficient cells relative to control cells revealed that actin may be compensating for the decrease in vimentin, thereby decreasing the deformability of the cells. These results suggest a complex relationship between cytoskeletal proteins in responding to extracellular compression that needs to be further investigated.

Future work into this area would involve incorporating more realistic cell-ECM adhesions that are absent in the current experiments. Our focus was on the intrinsic cell response, however a more relevant environment would include cell-ECM contacts as these would necessarily complicate cellular deformation in response to external compression of the cellular environment. Based on our findings in Chapter 3, vimentin would also likely play a complex role in influencing cell-ECM contacts dependent on the ECM proteins available for adhesion and this would affect the subsequent deformation of the cells.

The objective of the second aim (Chapter 3) was to determine how vimentin intermediate filaments would influence cellular spreading in various microenvironments, rather than the large physical compression of the agarose gel examined in Aim 1 (Chapter 2). MSC behavior and function are affected by a variety of external stimuli such as different ECM proteins, environmental stiffness, and

mechanical stimuli [27–29,31,32,51,52,58]. Further, the area of MSCs has been associated with functional changes (e.g. cell stiffness, differentiation potential) [34,37]. Clarity of how vimentin influences cell area can lend insight into how IFs are involved in functional changes in response to their physical environment. When we first measured cell spreading on fibronectin- or collagen-coated glass coverslips, the vimentin-deficient cells were found to be smaller than the control cells on fibronectin. Comparatively, this was not the case with the cells on the collagen-coated surfaces, except on the highest concentration at 24hr. Next, we exposed the cells to surfaces of varying stiffness and found that the cell areas were larger on the stiffer substrates in both cell populations. However, while the vimentin-deficient cells were smaller than the control cells on the stiff substrate, no difference was observed on the soft substrate. This suggests that vimentin may only be involved in cellular spreading in stiff environments when adhered to fibronectin. Finally, the cells were exposed to low fluid shear stress and the control cell populations did not respond to the fluid flow by changing cell area. Comparatively, the vimentin-deficient cells were smaller when exposed to fluid flow, suggesting that vimentin may be involved in resisting low fluid shear stress-induced cell area changes. These findings implicate vimentin in the response of MSCs in different microenvironments, specifically a physical change in cell size due to interactions with fibronectin-coated stiff surfaces and in response to low fluid shear stress on a fibronectin-coated surface. Further, instead of affecting expression in MSCs, vimentin IFs appear to affect MSC adhesion structures, which regulate the cell spreading. While gene expression of integrin subunits and the quantity of vinculin protein did not appear to be altered by vimentin deficiency, we

found that when seeded on fibronectin, vimentin-deficient cells had smaller focal adhesion areas. Overall, these studies together indicate a complex role for vimentin in cellular spreading as we've shown that it influences spreading, specifically on fibronectin, in a variety of microenvironments.

There are many directions for future work in this area. First, examining the substrate-stiffness responses using a variety of ECM proteins would expand this work. It would also be valuable to extend the focal adhesion work and delve into the different focal adhesion proteins and integrin subunits that vimentin may interact with to better examine how they affect cell spreading in conjunction with vimentin. Further, cell spreading in 2D environments will necessarily be different than cell spreading in 3D conditions in all types of biomaterial scaffolds. Examining if these findings hold true in three dimensions would be critical for expanding this knowledge to a more *in vivo*-like environment. Finally, our findings with fluid shear stimulation only touch upon how vimentin and cellular response to fluid shear stress may be related. Moving beyond the physical effects to the changes in signaling and relationships with integrin subunits would allow more clarity into this area of research. Ultimately, in practice, this work indicates a need for examining cell behavior in 2D using multiple substrate proteins for cellular adhesion, as this can clearly impact the outcome of research.

The objective of the third aim (Chapter 4) was to move away from analyzing effects of vimentin deficiency on a cell by cell basis, and instead examine the effects on chondrogenesis of the MSC populations. As previous studies had found that vimentin

affects chondrogenic extracellular matrix deposition and chondrocyte phenotype maintenance in short term studies [123,124], we decided to extend this research further and analyze *in vitro* chondrogenesis at 14 and 21 days. In this study, cells with limited vimentin, at least at the start of chondrogenesis, were cultured in two different environments: as pellet cultures and in agarose hydrogels. Ultimately, however, we found that a decrease in vimentin at the start of chondrogenesis had a limited effect on extracellular matrix deposition in both culture environments. In the pellet cultures, histology suggested that the sGAGs may be decreased or less organized in the vimentin-deficient cultures. Comparatively, in the agarose, it seemed that only type II collagen deposition might be decreased with decreased vimentin. However, gene expression for chondrogenic, degradative, and adhesion proteins between the two cell populations did not reveal any differences. By delving further into the gene expression and comparing the culture time and condition, we found, in general, a higher presence of degradative enzymes in the pellet cultures compared to the agarose cultures, suggesting that the MSCs were hypertrophic within the pellet cultures at these time points. However, the higher expression of αV integrin subunits in the agarose culture compared to the pellet culture suggests that pericellular matrix deposition may be different between the two culture conditions possibly due to cell density or cell shape. Ultimately, this work indicates that decreasing the levels of vimentin protein at the start of chondrogenesis may have a limited role in chondrogenesis in later stages of *in vitro* culture.

Future studies in this area could take three directions. First, stepping away from studying the role of vimentin in chondrogenesis, better understanding of the effect of culture condition on the pericellular matrix would clarify and expand our findings. Second, instead of focusing on the inherent role of vimentin in chondrogenesis, examining how vimentin is involved in mechanical stimulation of chondrogenesis could be more valuable as vimentin has been shown to be involved in mechanosensing of hydrostatic pressure-based stimulation of chondrogenesis [101]. We've shown that vimentin is involved in physical changes in MSCs in response to external stimuli in Chapters 2 and 3, and thus coupled with previous literature, it appears that vimentin may have a greater role in the mechanical regulation of chondrogenesis. Third, as vimentin has been found to be disorganized, disrupted, downregulated, or absent in osteoarthritic chondrocytes and even MSCs, the focus could be shifted to vimentin's role in osteoarthritis pathology in chondrocytes and MSCs. Vimentin may have a more clear effect on cellular behavior in an osteoarthritic environment as these cells must respond to deteriorating changes in their physical surroundings.

Altogether these studies clearly indicate a role for vimentin in how MSCs interact with their physical and micro-environments, if not during chondrogenesis. Decreasing the amount of vimentin in MSCs had a limited effect on cells at the transcription or translational level as seen in both Chapters 3 and 4. Coupled with the results from Chapter 2, vimentin appears to instead have a more physical, and likely direct, interaction with the rest of the cytoskeleton or other structures and proteins that

typically allow the cells to interact with the environment in an unimpaired manner. Further, decreasing the quantity of vimentin likely affects the internal mechanical balance of the cell as well as signaling cascades which together may contribute to the observed changes in MSCs' physical response to their environment.

In this work, we did not emphasize the relationship between the three cytoskeletal proteins, in an attempt to isolate the role of vimentin. Functionally, however, it is known that actin microfilaments, microtubules, and vimentin intermediate filaments as well as other supporting proteins are interconnected and do not have an isolated effect on cellular behavior. And thus, the changes in the physical behavior of MSCs are likely caused by alterations of the mechanical equilibrium, the subsequent compensation by the other cytoskeletal proteins, and altered signaling cascades in response to the environment when vimentin is decreased. It is largely accepted that actin microfilaments and vimentin intermediate filament act as tensional elements in the cell, while microtubules serve to resist compression. In the first aim, with a decrease in vimentin, we observed a decrease in deformability. The resistance to compression is likely due to the remaining vimentin network and reorganization and compensation by the remaining cytoskeleton. This decrease in deformability may or may not be present when cell adhesions are introduced, as in Aim 2. This ambiguity is related to how actin microfilaments' role in cellular stiffness changes through the formation of actin stress fibers and increased cellular contractility when the cells are no longer rounded and from adhesions to their environment. Vimentin's related role must also change with cellular spreading and attachment and we observed that

vimentin may specifically be involved in adhesion to fibronectin in stiff environments, likely in support of the actin microfilaments' function. However, it is certainly possible that the decrease in deformability is still present with the addition of cell adhesions, opening up the question of whether vimentin-dependent cellular deformability itself could contribute to the observed changes in adhesions and cell areas**.** The interaction of cellular deformability and cellular adhesion could again play a role in chondrogenesis. While vimentin-deficient cells, at least at the initiation, were used for chondrogenesis, it is not clear if the expression of vimentin over the culture period was recovered. However, this early limited vimentin expression does not appear to impact chondrogenesis in longer term culture. This suggests that chondrogenic induction and the related signaling cascades may occur independent of the effects of the deformability and area changes that might be caused by vimentin deficiency. It is known that a disrupted actin network is often associated with chondrogenic differentiation and microtubules appear to have a limited role in chondrogenesis. Our findings indicate a limited role for vimentin as well. Altogether it appears that vimentin's primarily influence is in affecting MSCs' physical response to different environments, i.e. deformability and maintaining cell area.

These findings also indicate that while vimentin may not be a regulator of chondrogenesis of MSCs, physical responses to external cues such as different ECM proteins and stiffness or mechanical loads are influenced by vimentin IFs. Thus, further studies are needed to determine how this role for vimentin in the MSC response will affect cell signaling in different environments and subsequently MSCs'

trophic and immunomodulatory roles for therapeutic purposes. Similarly, further studies are needed to examine how vimentin's involvement in MSC interaction with different ECM environments can affect mechanical preconditioning of chondrogenic MSCs prior to the implementation as a therapeutic.

One challenge facing allogenic cell therapies is the donor-to-donor variability among isolated cell populations. This is also a challenge in the research sector, where human MSCs from different donors can be purchased. While we did not examine the donor-to-donor variability in expression of vimentin, it is unlikely that there are large variations in its expression in healthy MSC populations as it appears to be a robustly expressed protein. In fact, changes in culture environment and culture time are more likely to impact changes in cytoskeletal structure [144]. However, it is possible that donor variability could impact the chondrogenic potential of the populations of MSCs as well as affecting chondrogenesis-dependent increases in vimentin [124,164]. These variations could potentially impact our findings from Aim 3 (Chapter 4).

This work contributes to the current scientific body of knowledge in a multiple ways. We are the first to show that a lentiviral RNAi platform can be used to elicit a decrease in vimentin in human MSCs. Most of the previously reported studies rely on non-specific chemical disruption of intermediate filaments, which in our experience can have important off-target effects on the actin cytoskeleton. Other studies use short term RNAi interference, rather than relying on a lentiviral approach for an extended effect. Further, we showed that vimentin is involved in the cell deformability of

MSCs in an unexpected way. Specifically, a moderate decrease in vimentin did not increase deformability, as one might expect, but instead decreased deformability. Moreover, our results suggest one potentially novel mechanism of this phenomenon might be a shift in the resistance to deformation from the vimentin network to the actin network, potentially in combination with the remaining vimentin filament network. Most critically, we show for the first time that vimentin is involved in maintaining MSC area in response to different microenvironments, specifically when adhered to fibronectin and on stiff substrates. Practically, this emphasizes the need for evaluating cellular behavior on substrates coated with different ECM proteins as it can clearly affect research outcomes. We further found that vimentin may be involved in resisting call area changes in MSCs in response to low fluid shear stress. Finally, we found that an initial deficiency in vimentin is not sufficient to impact chondrogenesis of MSCs during long term culture regardless of culture condition, which corroborates normal overall joint development that has been observed in vimentin knock-out mice.

MSCs' popularity as a therapeutic cell population has necessitated further study into how these cells behave fundamentally. With an understanding of the factors that affect MSC behavior, researchers will not only be able to better design therapies, but evaluate their success as well. As the cytoskeleton is involved in functional cell behaviors, vimentin intermediate filaments will likely influence cell behavior in many of the latest technologies that are being developed using MSCs, especially as cell microenvironment has such a large influence on behavior. Success of technologies

such as MSC-derived extracellular vesicles and incorporation of MSCs into 3D printed scaffolds will ultimately be affected by MSCs' response to physical stimuli and different microenvironments. The responses to these stimuli will be controlled by a variety of cellular structures, such as focal adhesions and other cytoskeletal elements that vimentin may directly influence as demonstrated by the work in this dissertation; these studies demonstrate that vimentin is involved in the physical MSC response to a variety of microenvironments. Ultimately, these studies serve to extend the discussion regarding how MSCs interact with different environments, the understanding of which will be critical for the development and evaluation of mesenchymal stem cell therapies.

Appendix A: Downregulation of Vimentin Intermediate Filaments Affect Human Mesenchymal Stem Cell Adhesion and Formation of Cellular Projections[3]

This work was collaboratively completed with my contributions being toward the generation of the lentiviruses and the cell culture of the transduced cell populations. Additionally, I was involved in manuscript preparation as I authored most of the introduction, methods, and discussion sections. As this work relates to the findings in Chapter 3, I chose to include it as an Appendix. The manuscript is still currently in preparation.

A.1 Introduction

Mesenchymal stem cells (MSCs) are increasingly being investigated for a variety of therapeutic applications, including musculoskeletal disorders such as osteoarthritis [13] and degenerative disc disease [178]. The use of MSCs as a therapeutic cell source for these conditions, among others, can be attributed to the combined advantages of diverse differentiation potential, immunomodulation properties, paracrine effects, and their homing capability [1]. Migration and adhesion of MSCs to a damaged tissue's extracellular matrix are essential for MSCs to carry out their therapeutic function. Their capacity to migrate to diseased or damaged tissues has been investigated in a number of models [24–26], and further understanding of their homing potential has come

[3] To be submitted for publication: Sharma, P.*, Peesay, T.*. Bolten, Z., Hamilla, S., Wagner, D.R., Hsieh, A. H., Luna, C.L. Downregulation of Vimentin Intermediate Filaments Affect Human Mesenchymal Stem Cell Adhesion and Formation of Cellular Projections. *In preparation*

from studies focusing on MSCs' chemotactic response to chemokines or growth factors [24,26,179,180]. In addition to migration, MSC adhesion and spreading have been found to be particularly important for phenotypic changes. For instance, changes to cell shape [34], size [36], substrate stiffness [27], and composition [30,31] have been shown to be capable of tuning MSC differentiation.

As with most other cell types, migration and adhesion of MSCs are largely governed by the cytoskeleton, which consists of actin microfilaments, microtubules, and intermediate filaments (IFs), primarily vimentin. The roles of actin and microtubules in migration and adhesion, in concert with a complex collection of supporting proteins, have been well described. Actin microfilaments form multiple structures required for migration at the leading edge of the cell. Lamellipodia are made up of branched microfilaments while filopodia are formed from microfilament bundles [181,182]. The development and stability of these structures is mediated by the formation and separation of focal adhesions or integrin clustering at the leading and trailing edges of the cells [182]. It is thought that microtubules help to polarize cells for migration through extension into the lamellopodia and trafficking of vesicles containing adhesion molecules to the leading edge of the cell [182]. Similarly, actin has also been found to be required for the formation of cellular projections for migration while microtubules are needed for cellular cytoplasmic projection elongation [181]. Comparatively, significantly less is known about the related function of vimentin IFs in these processes.

There is increasing evidence that vimentin IFs are involved in cellular adhesion and spreading. Vimentin deficiency results in slower adhesion by cancer cells[87,120]. Further, vimentin IFs are known to interact with, and potentially regulate, focal adhesions [88,105,113,114,120,121] and interact with numerous integrin subunits [104–110]. These interactions with adhesion proteins appear to be associated with the activity of cytoskeletal linkers plectin and filamin A [107–109,122]. However, the relationship between cellular adhesion, spreading, and vimentin IFs in MSCs has not been fully explored.

Vimentin IFs also appear to be involved in cellular migration. While changes in vimentin IFs have been found to correlate with changes in the migration of MSCs [183], vimentin's involvement in migration has been more extensively investigated in cancer cells and fibroblasts. Increased vimentin expression has been designated as a key marker in the epithelial to mesenchymal transition and is associated with increased tumor cell migration, metastasis, and poor prognosis [78,87,88,114]. Down regulation or absence of vimentin in carcinoma cells, fibroblasts, and epithelial has been shown to impair cell migration [87,113,114,132,184,185] and alter the migration of lymphocytes and leukocytes through endothelial cells [186,187]. Vimentin IFs further appear to be involved in modulating cellular structures involved in migration. Long cellular cytoplasmic projections during migration through matrix pores have been found to require vimentin IFs for elongation [181]. Similarly, pseudopodia of leukocytes interacting with their target endothelial cells were shown to require vimentin

reorganization [186]. While it is apparent that vimentin IFs are involved in cellular migration, the mechanism by which they act in MSCs remains to be clarified.

In this study we sought to investigate the role of vimentin IFs in adhesion and protrusion formation during MSC migration. Specifically, we examined the relationship among MSC adhesion, cellular projection formation, and vimentin IFs using lentiviral shRNA-mediated RNA interference (RNAi) to determine the effect of decreased vimentin expression on these behaviors. Our results indicate that vimentin IFs are necessary for the cellular structural integrity required for forming cellular protrusions and normal cell-substrate adhesion.

A.2 Materials and Methods

A.2.1 Human Mesenchymal Stem Cell Culture

Population doubling level (PDL) 9 bone marrow derived human mesenchymal stem cells (hMSCs) (RoosterBio; Frederick, MD) were expanded using RoosterBio Enriched Basal media supplemented with GTX Booster (RoosterBio) per manufacturer instructions. PDL 13-18 hMSCs were used for all experiments. Subsequent subculture for lentiviral transduction and experimentation was completed using hMSC growth media: high glucose DMEM containing 4mM L-Glutamine (Gibco) supplemented with 10% fetal bovine serum (FBS) (Gibco), 100 U/mL Penicillin Streptomycin (Gibco), 1% MEM non-essential amino acids (Gibco), and 4mM L-Glutamine (Gibco). Complete media exchange was completed every 2-3 days and the cells were maintained at 5% CO_2 and at 37^{o}C.

A.2.2 shRNA Lentivirus Generation

shRNA lentivirus was designed and generated as previously described[150]. Briefly, a 52 nucleotide shRNA sense-loop-antisense (5'-AAAAGGCAGAAGAATGGTACAAATTGGATCCAATTTGTACCATTCTTCTG CC-3') sequence was designed and selected from human vimentin [Gen Bank: NM_003380] mRNA using the shRNA Designer through Biosettia, Inc. After annealing, double stranded oligonucleotides were ligated per manufacturer instructions into an inducible lentiviral RNAi vector conveying resistance to blasticidin and containing a TetO-H1 promoter. RNA interference in this inducible system occurs only in the presence of doxycycline. The pLV-RNAi kit and pLV-Pack Packaging mix (Biosettia) were used to generate the shRNA constructs and package into replication-deficient lentivirus using HEK 293FT cells and Lipofectamine 2000. A shRNA lentiviral vector targeting the LacZ gene (5'-GCAGTTATCTGGAAGATCAGGTTGGATCCAACCTGATCTTCCAGATAACT GC-3') was used as a control (Biosettia). Three days post-transfection, virus-containing supernatants were collected and stored at -80^{o}C until use.

A.2.3 shRNA Transduction

hMSCs were transduced with the shVim- or shLacZ- lentiviral particles for 24hrs at an multiplicity of infection (MOI) of 15. The shLacZ-transduced hMSCs served as our non-targeting control for all experiments, as previously described [150]. Transduction was completed in the presence of 6µg/ml hexadimethrine bromide (Polybrene) (Sigma) to assist with transduction efficiency. Titered viral concentrations for an MOI of 15 were determined using a Quanti-IT PicoGreen Assay

(Invitrogen). Two days after transduction, 12µg/ml Blasticidin was used to select for pure populations for 4 days. Subsequently, shVim-hMSCs and shLacZ-hMSCs were cultured in the presence of 1µg/ml doxycycline to induce RNA interference (RNAi). Cells were cultured for 14-18 days on tissue culture polystyrene before being harvested to be assayed. The success of this knockdown in hMSCs has been previously described [150].

A.2.4 GFP-Vimentin Transfection

5 x 10^5 PDL ~15-17 hMSCs (RoosterBio) were transfected with 6µg EGFP-Vimentin-7 DNA plasmid according to the Amaxa™ Optimized Protocol provided by the LONZA Nucleofector Kit for hMSCs (Lonza). EGFP-Vimentin-7 (subsequently GFP-Vimentin) was a gift from Michael Davidson (Addgene plasmid # 56439). On day 3, pure populations were selected using 500µg/mL geneticin for 1 day. On Day 7, cells were harvested to be assayed.

A.2.5 Surface Reflective Interference Contrast Microscopy and Immunofluorescence

Surface reflective interference contrast microscopy (SRIC) was used to detect surface-to-surface interference between light rays reflected from the substrate/medium interface and those from the medium/cell membrane interface. The intensity of the light is a measure of the proximity of the cell membrane to the glass surface, so the membrane closest to the surface appears darker and those further away appear brighter. Therefore, SRIC is an optimal method when evaluating cellular attachment, adhesion, and spreading behavior. Cells were fixed in 4% paraformaldehyde prior to imaging and stained for vimentin. To visualize vimentin,

cells were labelled with a rabbit IgG anti-human vimentin primary antibody (ThermoFisher) followed by a biotinylated (anti-rabbit IgG) secondary antibody (Vector) and fluorescein-labelled streptavidin (Vector). For image capture using SRIC and to visualize vimentin, we used a Nikon Eclipse TE2000-E microscope.

A.2.6 Immunofluorescence for F-Actin and Focal Adhesion Analysis

To visualize vimentin and analyze focal adhesion staining, cells seeded on glass coverslips coated with 100µg/ml human fibronectin for 30min (Corning) were fixed with 4% paraformaldehyde were then permeabilized using 0.1% Triton-X-100. Cells were then labelled with a rabbit IgG anti-human vimentin primary antibody (ThermoFisher) followed by a biotinylated (anti-rabbit IgG) secondary antibody (Vector) and fluorescein-labelled streptavidin (Vector). To dual stain for vimentin and vinculin, after vimentin staining, cells were then labelled with a mouse IgG anti-human vinculin primary antibody followed by an Alexafluor 594-labelled goat anti-mouse IgG secondary antibody. To dual stain for vimentin and F-actin, after vimentin staining, Alexa Fluor 594 Phalloidin was used to label F-actin. DAPI was used to stain cellular nuclei. Fluorescent imaging was completed using a Nikon Eclipse TE2000-E microscope. ImageJ was used for the quantification of the average vinculin adhesion area. All images were converted to binary images to isolate individual vinculin adhesions, and the particle analyzer in ImageJ was used to detect all adhesions greater than 0.5 μm^2 to prevent the quantification of background noise. The average vinculin adhesion area was recorded for each individual cell.

A.2.7 Cytoskeletal Disruption and Visualization

25mm diameter glass coverslips (VWR) or 35mm diameter (14mm diameter glass) glass bottomed dishes (Matek) were sterilized using UV light for 30 min and then coated with 100µg/ml human fibronectin for 30min (Corning). GFP-vimentin hMSCs were seeded onto glass-bottomed dishes while shVim- and shLacZ- hMSCs were seeded onto the glass coverslips. Chemical disruption of actin microfilaments and inhibition of cellular contractility was completed using 0.4µM cytochalasin-D (Sigma) and 50µM blebbistatin treatment, respectively. Chemical treatments were conducted at 37°C and 5% CO_2. After the designated treatment time, the cells were fixed with 4% paraformaldehyde. To visualize vimentin with disrupted cytoskeletal elements in shVim- and shLacZ-hMSCs were then permeabilized using 0.1% Triton-X-100. Subsequently, cells were labelled with a rabbit IgG anti-human vimentin primary antibody (ThermoFisher) followed by a biotinylated (anti-rabbit IgG) secondary antibody (Vector) and fluorescein-labelled streptavidin (Vector). Fluorescent imaging was completed using a Nikon Eclipse TE2000-E microscope.

Chemical disruption of cytoskeletal elements and time lapse microscopy of GFP-vimentin hMSCs was completed after 4 days of nucleofection. After adding the chemicals directly to the cells, fluorescence images were taken every 2 min for 1.5hr using an Olympus IX81 microscope with an environmental chamber to maintain the environment at 5% CO_2 and 37 ^{o}C.

A.2.8 Cellular Cytoplasmic Projection Formation Assay and Analysis

Tissue culture treated polyester transwell inserts with 3.0 µm pores were coated with 100µg/mL fibronectin for 30 min at room temperature. shVim- and shLacZ-hMSCs were seeded onto transwell inserts for 20 min. The bottom chamber was filled growth media containing SDF-1 (ThermoFisher) (200 ng/ml) Cells were incubated at 37°C and 5% CO_2 for 24hr, after which the cells were fixed with 4% paraformaldehyde and permeabilized using 0.1% Triton-X-100. To visualize protrusion formation, cells were then labelled with a rabbit IgG anti-human vimentin primary antibody (ThermoFisher) followed by a biotinylated (anti-rabbit IgG) secondary antibody (Vector) and fluorescein-labelled streptavidin (Vector). Alexafluor 594-labelled Phalloidin was used to stain F-Actin. Fluorescence images were taken of the protrusions using a Nikon Eclipse TE2000-E microscope. 15-30 fields of view were taken for the bottom face of each transwell insert only and the number, length, and average area of protrusions were analyzed on ImageJ or Fiji software.

A.2.9 Statistical Analysis

To determine significant differences in focal adhesion area between shVim- and shLacZ-hMSCs, Student's T-test (α=0.05) was used. To determine significant differences between the average number, length, and area of protrusions on by shVim- and shLacZ-hMSCs, a Student's T-test (α =0.05) was also used.

A.3 Results

A.3.1 Vimentin is involved in cell-substrate contact and might be involved in pseudopodia-substrate interactions in hMSCs

First, we evaluated the relationship between the cell-substrate contact and the vimentin network (Figure A.1). We used surface reflective interference contrast microscopy (SRIC) to evaluate the contacts between the cell membrane and the underlying substrate. In the same cells, we used immunofluorescence of vimentin filaments to analyze the relationship between cell contacts and vimentin expression. Throughout this paper, we used shLacZ-transduced human mesenchymal stem cells as a control, as previously described [150]. We used darker areas in micrographs to characterize cell-substrate adhesion (Figure A.1B, dark color). These dark contrast areas indicate a closer contact distance between the cell membrane and the glass substrate, whereas white/gray areas indicate that the cell membrane and the glass substrate are farther apart.

We observed that for vimentin knockdown cells (shVim-hMSCs), the fluorescence intensity of vimentin was diminished in certain areas of the cell, especially at the edges (Figure A.1D, G). More importantly, the areas that lacked vimentin fluorescence intensity (Figure A.1F, I) also corresponded to darkened areas using the SRIC filter. This effect is due to the enhanced contact between the cell membrane and the substrate, which causes an increased in interference and therefore, darker areas in

the resulting micrograph. These results clearly indicate that the absence of vimentin network is directly correlated to areas of increased cell-substrate contacts.

Our observation of shLacZ-hMSCs indicated that the organization of the vimentin network varied at the cell edge depending on the presence of pseudopodia (cytoplasmic projections). For example, cells with no evident projections at the edge have vimentin filaments that point outwards toward the membrane in addition to the curved filaments oriented in the same direction as the cell membrane (Figure A.1J). When projections were present at the edge, we found more vimentin filaments pointed outwards in the direction of the projection than those oriented along the cell body (Figure A.1K, L). shVim-hMSCs lacked vimentin staining at these surface projections (Figure A.1N, O). We found that vimentin-absent projections had an increased cell-substrate contact, as indicate by the dark contrast areas in shVim-hMSC samples (Figure A.1 Q, R). These results seemed to indicate that the vimentin network plays a key role at modulating cell projections and cell-substrate adhesion at the cell edge.

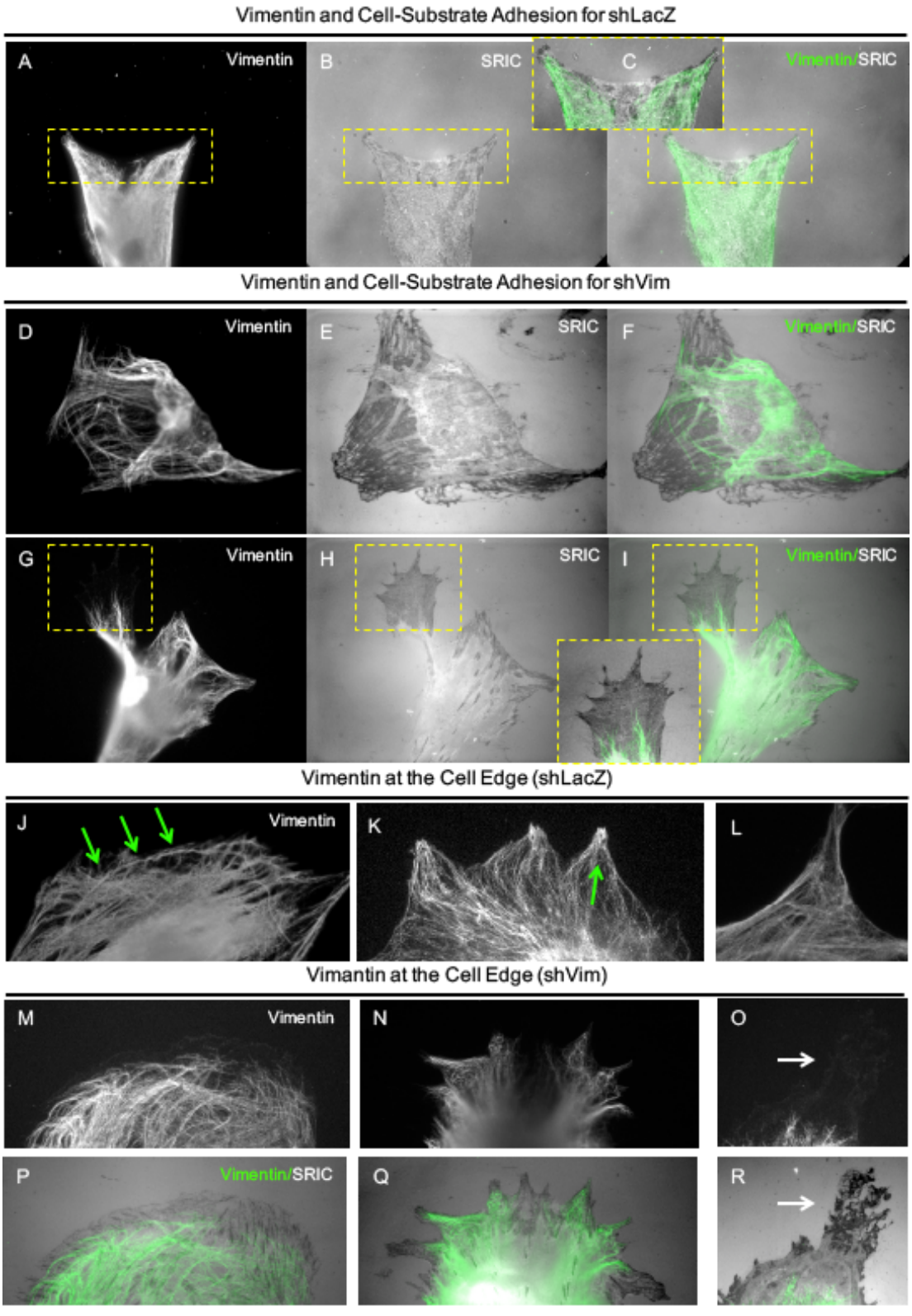
Vimentin and Cell-Substrate Adhesion for shLacZ
A
Vimentin
B
SRIC
C
Vimentin/SRIC
Vimentin and Cell-Substrate Adhesion for shVim
D
Vimentin
E
SRIC
F
Vimentin/SRIC
G
Vimentin
H
SRIC
I
Vimentin/SRIC
Vimentin at the Cell Edge (shLacZ)
J
Vimentin
K
L
Vimantin at the Cell Edge (shVim)
M
Vimentin
N
O
P
Vimentin/SRIC
Q
R

Figure A.1 Vimentin is involved in cell-substrate contact and might be involved in pseudopodia-substrate interactions in hMSCs. (A-C) Vimentin and cell-substrate adhesion in shLacZ cell. (A) Vimentin staining in shLacZ cell. (B) SRIC image in shLacZ cell. (C) Vimentin and SRIC overlay of shLacZ cell. (D-I) Vimentin and cell-substrate adhesion for shVim cells. (D,G) Vimentin staining in shVim cells. (E,H) SRIC image of shVim cells. (F,I) Vimentin and SRIC overlay shVim cells. (I) Zoom panel shows vimentin and SRIC overlay at cellular protrusion in shVim cell. (J-L) Vimentin at the cell edges in shLacZ cells. (M-O) Vimentin staining at the cell edges in shVim cells. (P-R) Vimentin and SRIC overlay. (R) White arrow points to lack of vimentin staining in the cell protrusion.

A.3.2 Increased actin expression and vinculin focal adhesion area play a role in increased cell-substrate contacts in shVim cells

We next focused on the organization of actin microfilaments in shVim- and shLacZ-hMSCs. In shLacZ-hMSCs, both vimentin and actin filaments were observed along the cell edge as well as actin stress fibers (Figure A.2A). When comparing the actin staining with the SRIC images, it appears that the darker areas contain actin. In shVim-hMSCs, the protrusions and edges of the cell were largely absent of vimentin, but appeared to have increased actin filaments, especially compared to the shLacZ-hMSCs (Figure A.2B, C). When we compared the ratio of actin fluorescence between shlacZ and shVim-hMSCs we found that at the cell edges shVim-hMSCs expressed more vimentin (Figure A.2D). The ratio of actin to vimentin was significantly increased in shVim-hMSCs compared to shLacZ-hMSCs (Figure A.2D), due to both

the reduction in vimentin expression and the increase in actin fluorescence intensity at the cell edges.

To gain a better understanding of the relationship between cell-contacts and vimentin, we examined vinculin staining. We noticed that shLacZ-hMSCs appeared to have a smaller focal adhesion area compared to shVim-hMSCs (Figure A.2G, H, I). We calculated the average area of the focal adhesions by taking a binary image of the fluorescent images and using ImageJ throughout the cell (Figure A.2 E, F, G). We found that, indeed, shVim-hMSCs had larger areas of vinculin expression compared to shLacZ-hMSCs (Figure A.2G), with a large variation in the data due to the many different sizes of focal adhesions. In the case of shLacZ-hMSCs, the darkened areas correspond almost precisely to vinculin fluorescence expression (Figure A.2H), indicating that SRIC correctly represents focal adhesions. In the case of shVim-hMSCs, upon looking at co-localized images of vinculin and SRIC, we observed that vinculin staining did not always line up with the darkened cell membrane areas that are closest to the substrate (Figure A.2I). The darkened areas are in fact much larger compared to the vinculin-positive areas. This data seems to indicate that although changes in vinculin may play a role shVim-hMSC adhesion, there are other factors that are involved. Together with our actin images, this data seems to suggest that increased amounts of actin and stress fiber formation at the cell edges, coupled with the increase in vinculin focal adhesion area, may account for the increase in cell-substrate contacts in shVim-hMSCs.

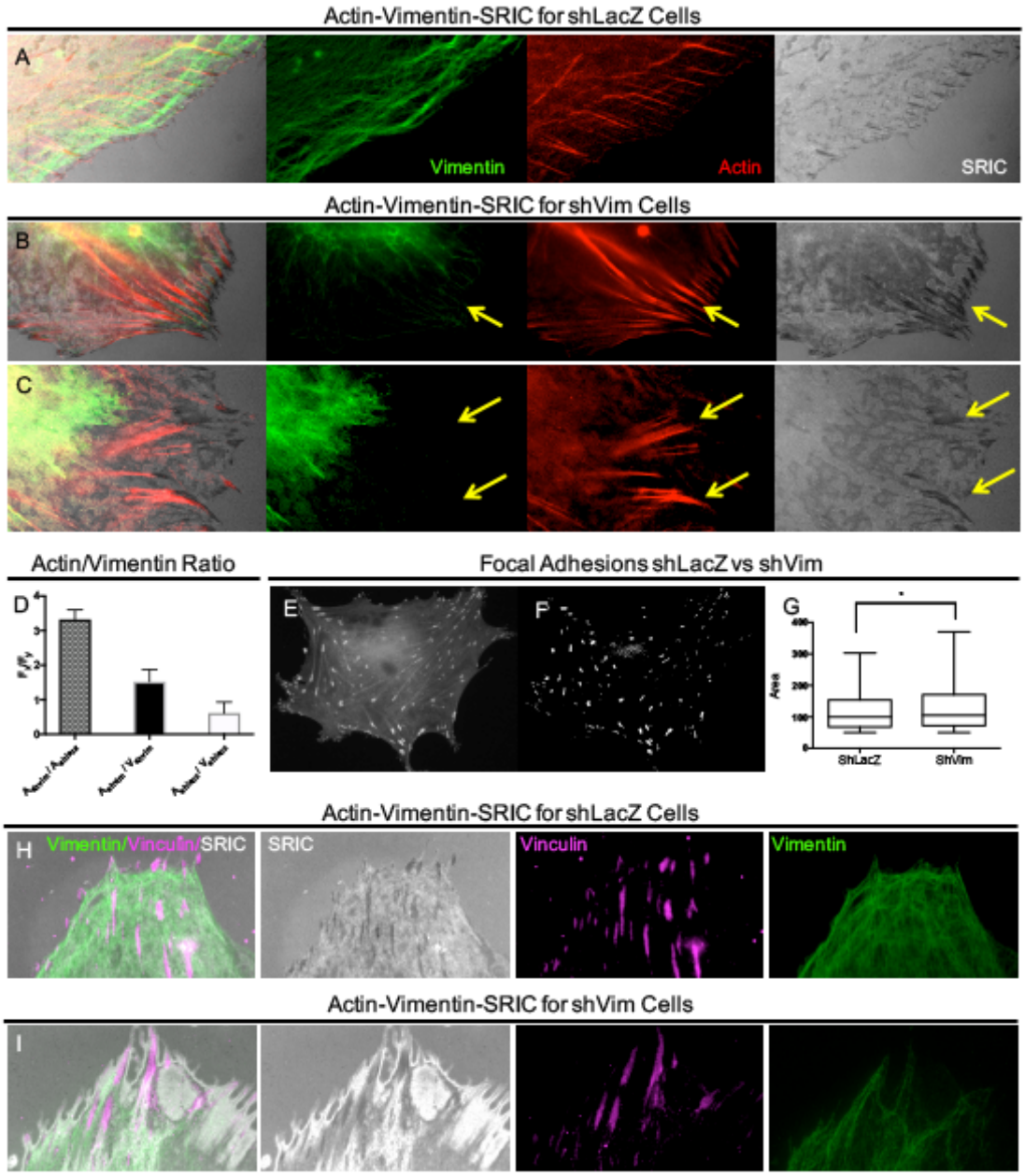

Figure A.2 Increased actin expression and vinculin focal adhesion area play a role in increased cell-substrate contacts in shVim cells. (A) shLacZ cell showing vimentin, actin, and SRIC images. Vimentin is located on the periphery of the cell and actin does not form defined stress fibers. (B-C) shVim cell showing actin, vimentin, and SRIC images. Yellow arrows indicate where vimentin expression does not extend into cellular

projections, but where actin expression is increased with stress fiber formation. (D) Ratio of actin and vimentin fluorescence expression at the cell edge. Ashvim is actin fluorescence in shVim cells, AshlacZ is the actin expression in shLacZ, Vshvim is vimentin expression in shVim and VshlacZ is vimentin expression in shLacZ cells. (E) ShLacZ vinculin immunofluorescence staining. (F) Binary image of shLacZ vinculin. (G) Vinculin adhesions in shLacZ hMSC and shVim hMSC (H) shLacZ cell showing vimentin, vinculin and SRIC. (I) shVim cell showing vimentin, vinculin and SRIC.

A.3.3 Vimentin-rich cell protrusions resist cell retraction

Due to actin's apparent role in the adhesion of shVim-hMSCs to the substrate, we decided to inhibit actin polymerization using cytochalasin D (Figure A.3). In shLacZ-hMSCs, upon treatment of cytochalasin D, the cell body retracted, but did not completely round up (Figure A.3A,B,C,D,E,G). As the cell body retracted, some small cytoplasmic protrusions remained in place (Figure A.3B,D,E,G). Using live-cell imaging of GFP-Vimentin expressing cells, we observed that these cytoplasmic protrusions contained vimentin (Figure A.3 C,D). When we treated shVim-hMSCs with cytochalasin D, the cell bodies retracted into a rounded morphology and no cytoplasmic protrusions were left remaining in place (Figure A.3F,H), compared to the shLacZ-hMSCs where these projections were still observed. These results indicate that vimentin plays a role in the stability of cellular projections.

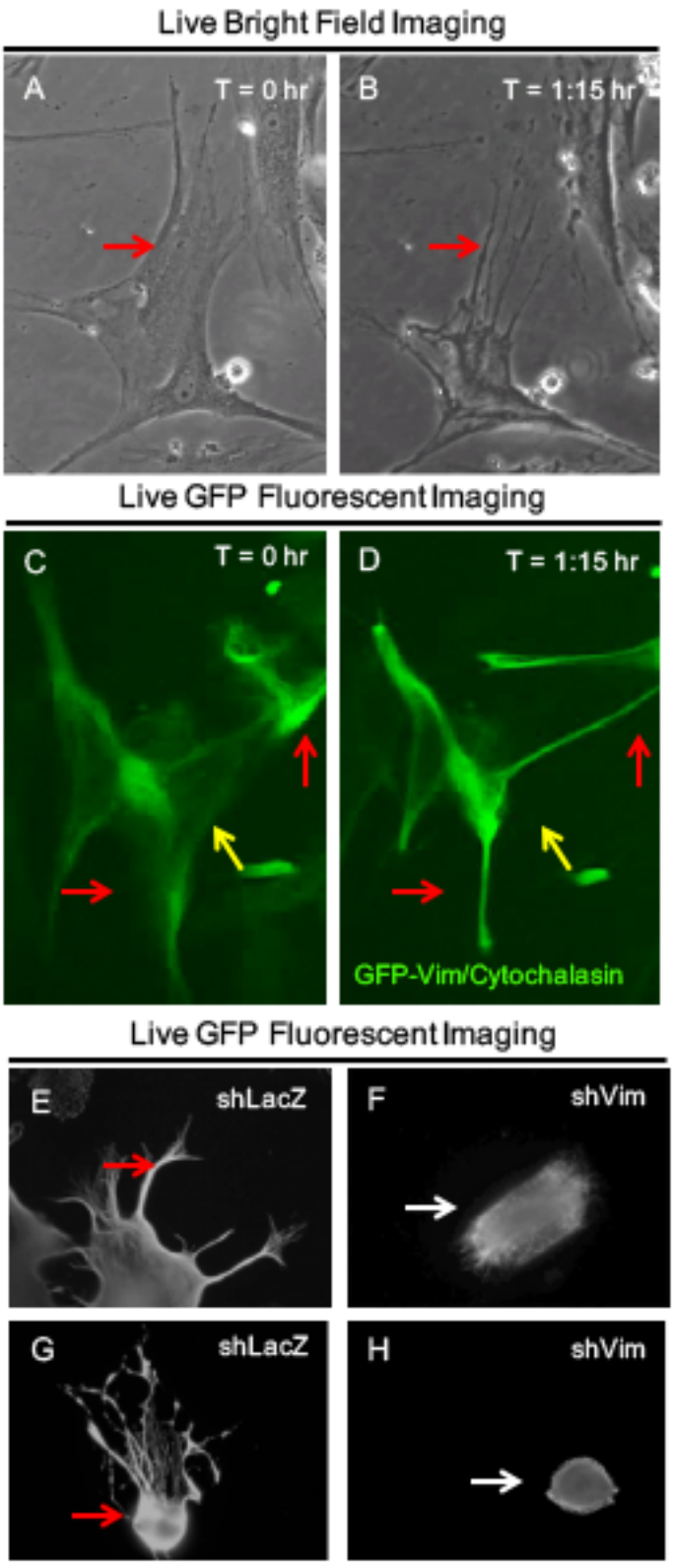
Live Bright Field Imaging
A
T = 0 hr
B
T = 1:15 hr
Live GFP Fluorescent Imaging
C
T = 0 hr
D
T = 1:15 hr
GFP-Vim/Cytochalasin
Live GFP Fluorescent Imaging
E
shLacZ
F
shVim
G
shLacZ
H
shVim

Figure A.3 Vimentin projections resist cell retraction. (A) Live cell imaging of shLacZ cells treated with 0.4µm cytochalasin D at T=0 and T=1:15hr. (B) Live cell imaging of shLacZ GFP-vimentin cells treated with 0.4um cytochalasin D at T=0 and T=1:15hr. (C) Immunofluorescence images of vimentin staining in shLacZ cells and shVim cells untreated (top panel) and cytochalasin (D) (bottom panel).

A.3.4 Vimentin plays a key role in the formation of cell protrusions

Thus far, we observed the role of vimentin in cell adhesion on 2D substrates. Next, we wished to gain a better understanding of the role of vimentin in protrusion formation. To do this, we used a transwell migration assay to evaluate the differences between the control (shLacZ-hMSCs) and vimentin knockdown (shVim-hMSCs) hMSCs (Figure A.4A). SDF-1 was used as a chemoattractant to stimulate migration to the bottom portion of the transwell insert (Figure A.4A). One major difference between shVim- and shLacZ-hMSCs was the lack of protrusions visibly extending from the bottom of the transwell insert in vimentin knockdown cells. In shVim-hMSCs short, actin-rich, cytoplasmic extensions could be observed having migrated shortly beyond the transwell pores (Figure A.4B). shVim-hMSCs did not form the long cellular projections (or protrusions) rich in vimentin that were observed in the shLacZ-hMSCs (Figure A.4C). In shLacZ cells, z-projections revealed that these protrusions extending from the shLacZ-hMSCs contained both actin and vimentin (Figure A.4 D-F). Vimentin appeared to be centrally located within the cells, and was surrounded by cortical actin on the outside. Furthermore, when shLacZ-hMSCs migrated through the transwell to the bottom well, they maintained a similar cytoskeletal organization, with actin mainly being organized on the outer edges of the cell with vimentin more centrally located (Figure A.4G-I)

To quantify the differences in protrusion formation between shLacZ- and shVim-hMSCs, we determined the average number of protrusions per viewing frame (Figure A.4J,K, L). Significantly more shLacZ-hMSCs formed long cellular projections compared to shVim-hMSCs. However, because we knocked down the expression of vimentin rather than ablated it, vimentin positive projections could still be observed in shVim-hMSCs. There was no difference observed in the normalized length of each protrusion (data not shown), demonstrating that vimentin knockdown cells can still grow cell projections if they retain enough vimentin to form vimentin positive protrusions.

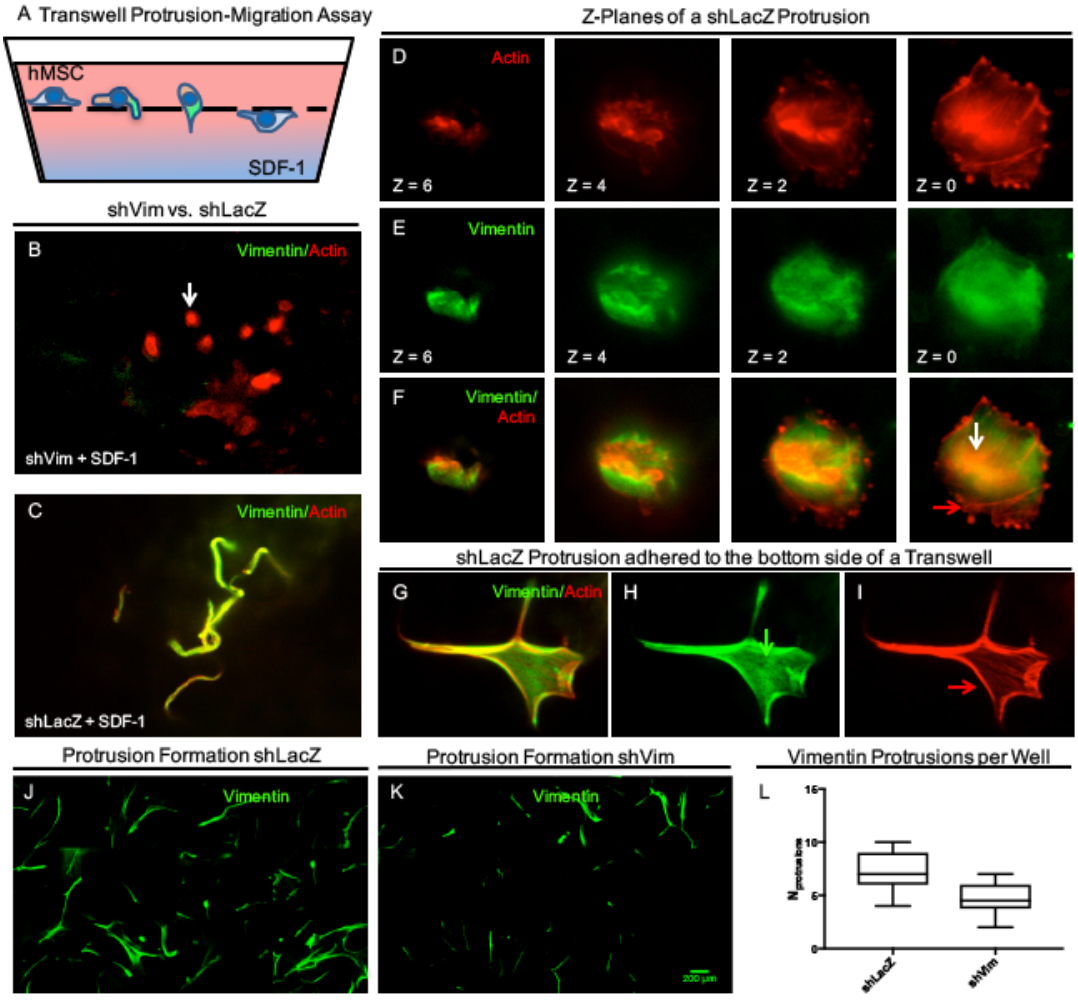

Figure A.4. Vimentin plays a key role in the formation of cell projections (A) Migration of hMSCs were monitored through 3µm transwell pores using fluorescent microscopy.

Transwells were coated in fibronectin and SDF-1 was included in the bottom well to stimulate cell migration through the pores. (B)-C Fluorescent images showing projection formation through transwell pores of shLacZ and shVim cells. (D-F) Z plane projections of shLacZ cells stained with actin and vimentin migrating through transwell pores. (G-I) Vimentin and actin staining of a shLacZ hMSC adhered to the bottom side of a transwell. Green arrow (H) points to vimentin staining in the central area of the cell. Red arrow (I) points to actin stress fibers on the periphery of the cell (J-K) Vimentin staining of shLacZ and shVim transmigrating through transwell pores. This panel depicts vimentin staining of protrusion formation through the pores to the bottom chamber. (L) Quantification of the average number of protrusions of shLacZ-hMSCs vs. shVim-hMSCs.

A.4 Discussion

In this study, we sought to clarify vimentin's role in MSCs by using lentiviral-based RNAi to decrease expression of vimentin IFs in the cells, and then examining the interplay between vimentin networks and MSC adhesion and migration. Our results reveal that intact vimentin networks are needed for retaining organized substrate adhesions. Immunofluorescence shows that the control shLacZ-hMSCs have vimentin IFs present throughout the cell. Further, SRIC micrographs show interspersed adhesion-like areas within the shLacZ-hMSCs. Comparatively, in the SRIC micrographs, shVim-hMSCs have larger areas of dark contrast, indicating the cell membrane is closer to the substrate surface. These dark regions correspond to areas of the cell without vimentin, suggesting that with decreased vimentin the MSC cell surface is closer to the substrate surface and may have increased regions of surface adhesion. Interestingly, the immunofluorescence for focal adhesions, as visualized through vinculin, does not show co-localization with these SRIC-based adhesions or regions of dark contrast.

However, we observed increased staining for actin in these areas, suggesting a role for actin. Perhaps evaluation of other focal adhesion components may help clarify this finding. Previously vimentin decrease has been be shown to cause decreases in focal adhesion size as measured through αVβ3 integrin staining [105]. Similarly, investigation of alternative focal adhesion proteins, such as paxillin, may help to clarify this further [185]. However, it is certainly possible that a decrease in vimentin IFs may cause a decrease in the distance between the cell membrane and substrate surface that is independent of cellular adhesive structures. In either case, our study implies a complex relationship between vimentin, focal adhesion contacts, SIRC-based surface closeness that must be further clarified in the future.

The disruption of F-actin in GFP-vimentin hMSCs and shLacZ-hMSCs revealed vimentin-positive extensions remaining when the cell body retracted. The cellular extensions were not active pseudopodia, but remnants after the cell body retracted. As the shVim-hMSCs lacked these vimentin-positive extensions after actin disruption, we postulate that vimentin might be necessary for retaining cellular morphology in adhered hMSCs, while active pseudopodia enable the cell to spread further. However, in the transwell assay in which MSCs extend projections through narrow pores, we observed a similar result; shvim-hMSCs lacked vimentin-positive cellular projections, which shows that vimentin was also necessary to actively form cell projections.

It is well established that vimentin deficiency impairs cellular migration in a variety of cell types[87,113,114,120,132,184,185]. Increasingly, studies have shown that vimentin is necessary for the formation of filopodial structures during adhesion and early spreading on 2D surfaces[107]. Similarly, vimentin has been found to be needed for other types of cellular extensions as well such as for early neurite extension in hippocampal neurons[188] and lamellipodia formation for

epithelial lens repair[185]. Our results support this assertion and demonstrate that vimentin IFs may be necessary for the formation of these long protrusions in MSCs.

While migration of cancer cells is likely aberrant and involving other factors, there is increasing evidence in this research area supporting vimentin's involvement in the formation of lengthy cellular extensions as we observed. Invadopodia formation and extension in breast cancer and colorectal cancer cells lines both required vimentin for elongation[181]. Similarly, actin-independent tubulin microtentacles on detached breast carcinoma cells were found to contain vimentin[189]. Disruption of vimentin with phosphatase inhibitors in these cells as well as the use of vimentin negative cancer cells resulted in a decrease in the number of microtentacles. It has been proposed that vimentin provides stability for the formation of longer microtentacles, or cellular extensions, compared to the shorter, less stable vimentin-negative microtentacles of less invasive cancer cells[189].

Our study is primarily limited by the use of RNAi to decrease vimentin networks rather than to ablate all vimentin expression. Specifically, MSCs completely lacking a vimentin network may yield larger effects in protrusion formation and extension[189]. In addition, we chose to examine the formation of cellular protrusions using small pored transwell inserts. Examining transmigration through a variety of pore sizes as well as alternative culture and test conditions such as confined migration scenarios [190], gel degradation experiments [181], and transmigration through cell layers [191] may reveal more intricacies about vimentin IF's role in protrusive structures for MSC migration. Further investigation into the relationship between vimentin, F-actin, and microtubules will help to clarify the formation, extension, and maintenance of these protrusive structures. Our results showed that shLacZ-hMSCs' extensions contained both vimentin and F-Actin. Closer to the transwell pore and the origin of the extension, vimentin appears to be located in the interior of these protrusions with actin primarily located

in the outer regions. Closer to the protrusion end, vimentin and actin appear more interspersed. It is possible that in addition to potentially playing a structural role, vimentin may be involved in initial contact and adhesion. Comparatively, microtubules have been found to be needed for protrusion elongation [181] and microtentacles are dependent on a microtubule network [189]. However, the study of microtubules and other cytoskeletal structures are outside of the scope of this paper.

This study primarily demonstrates that vimentin IFs are needed for the formation and maintenance of protrusive structures in hMSCs. Further, our observations also suggest that vimentin IFs are involved in the organization of cellular adhesions and proximity to substrate surfaces. Both the capacities to adhere and form pseudopodia are critical cellular functions, and greater understanding of the mechanisms involved in these behaviors in MSCs is increasingly relevant as MSCs continue to be investigated for therapeutic purposes.

Appendix B: Layered Alginate Constructs: A Platform for Co-culture of Heterogeneous Cell Populations[4]

In addition to work described above, a dual-layered alginate hydrogel system was developed for potential co-culture, however, it was ultimately not implemented for studying the role of vimentin in MSCs. Included in this appendix is the written portion of the published Journal of Visualized Experiments article describing the method developed.

B.1 Introduction

Compressive load bearing tissues such as articular cartilage or intervertebral discs consist of heterogeneous tissue regions that are critical for both biomechanical function and appropriate mechano-transduction in the tissue. Not only is cellular organization and function distinct in different regions, but the extracellular matrices (ECM) are also varied in composition and orientation. For example, articular cartilage consists of three primary zones with varying cell morphology, mechanical function, and ECM. Differences in their ECM lead to differential load bearing responsibilities; the superficial layer is primarily involved in tensile response to load, while the middle and deep zones are mainly accountable for response to compression [192]. Similarly, in the intervertebral disc, a gel-like nucleus pulposus is surrounded by a lamellar annulus fibrosis and the cells within these two distinct areas experience different

[4] This work was published in the Journal of Visualized Experiments and is reproduced here with permission from the publisher.
Sharma, P., Twomey, J. D., Patkin, M., Hsieh, A. H. Layered Alginate Constructs: A Platform for Co-culture of Heterogeneous Cell Populations. *J. Vis. Exp.* (114), e54380, doi:10.3791/54380 (2016).

types of biophysical stimuli [193]. In these types of tissues, cells and the extracellular matrices within the tissue layers interact with each other as the tissue undergoes and responds to mechanical forces.

Recapitulation of such heterogeneous tissue structures remains a challenge in tissue engineering and regenerative medicine, and our understanding of their biological significance is limited. There is a need for culturing platforms for analyzing stratified tissues as well as co-cultures of different populations of cells within one construct. In articular cartilage tissue engineering, scaffold-less layered constructs have been constructed by harnessing the ability of zonal chondrocytes to deposit varied ECM to mimic the different layers of this tissue [194,195]. However, layered hydrogel constructs provide an opportunity for investigating the interaction of diverse types of cell populations that lack the ability to form a robust tissue independently. For example, different populations of mesenchymal stem cells can be co-cultured within layered constructs. Such layered scaffolds have been used with both chondrocytes and differentiating mesenchymal stem cells for improved tissue engineering [196]. Not only can different cell populations be co-cultured in similar hydrogel layers, but single cell type can also be cultured within layers that have been manipulated to have varying stiffness or biochemical content to elicit different responses from cells [197,198].

Many different biomaterial hydrogels have been used to layer cell populations for cartilage tissue engineering such as those using polyethylene glycol or poly vinyl alcohol bases [198–200]. However, alginate hydrogels are one of the simplest biomaterials

from which to create layered scaffolds for studying heterogeneous cell populations in co-culture. While agarose hydrogels are also easily formed, alginate hydrogels have the added benefit of allowing easy isolation of cells from the 3-D construct for analysis of individual cells as has been described previously [126]. In previous studies, bi-layered alginate hydrogels have been formed in thin sheets and from these sheets, sections were sliced (e.g. using a biopsy punch) for particular applications such as for analysis of biochemical content or interfacial shear properties [201,202]. Another method for forming thin alginate sheets has been described with the potential for stratification into multiple layers, but still would require alteration to the hydrogel for use in mechanical testing [203].

Here, we present a method for reproducibly creating bi-layered alginate hydrogel discs for use in co-culturing different populations of cells. This alginate disc platform possesses several advantages. Primarily, the reproducible shape and small size is conducive for mechanical stimulation of the embedded cells without requiring a biopsy punch or other physical alteration to the hydrogel for many applications. Additionally, cell viability remains high during the layering process and after gel formation a clear separation of the two cell populations within the gel is visible with no initial overlapping region.

B.2 Protocol

B.2.1. Preparation for Formation of Alginate discs

B.2.1.1 Prepare a 4% (w/v) alginate solution in 1x Dulbecco's Phosphate Buffered Saline without added calcium chloride or magnesium chloride and place in a 37°C water bath. Concentrations of the alginate solution can vary, but 1-4% (w/v) alginate solutions are recommended.

B.2.1.2 Mix the alginate solution at a ratio of 1:1 with warm cell culture media base (e.g. Dulbecco's Modified Eagle Medium) for the desired cell type. The alginate concentration is now half of the original concentration, i.e. 2% (w/v). Sterilize alginate/media solution using sterile 0.2 µm nylon syringe filters.

B.2.1.3 Prepare a bath of sterile 102 mM calcium chloride dihydrate in sterile water with enough solution to submerge molds (~ 200-300 mL).

B.2.1.4 Collect the sterile "gel formation mold" (6 mm diameter x 3 mm tall cylindrical wells in a 3 in x 3 in aluminum plate, see Figure 1) and endplates (Bottom: one 3 in x 3 in aluminum plate, Top: one 1.5 in x 3 in aluminum plate) and prepare molds as follows:

B.2.1.4.1 Cut thick filter paper (blotter filter paper) and the cell microsieve membrane (10 µm pore size) to the sizes of the top and bottom endplates and place them in the calcium chloride bath until saturated, approximately 1 min. If desired, sterilize the thick filter paper and the microsieve membrane via autoclave or ultraviolet light for 30 min prior to use.

B.2.1.4.2 Set-up one half (the bottom half) of the mold construct.

B.2.1.4.2.1 Place the following items atop one another in the following order and smoothen using a sterile spatula: large endplate (3 in x 3 in), thick filter paper, and then the microsieve membrane.

B.2.1.4.2.2 Invert and press the mold onto a stack of paper towels to ensure loss of excess calcium chloride solution.

B.2.1.4.2.3 Place the "gel formation mold" with the cylindrical wells on top of the cell microsieve membrane and gently fasten the mold together on two sides using binder clips on the left and right sides. Make sure to leave enough room for the top endplate (1.5 in x 3 in) to cover the wells completely later.

B.2.1.4.3 Set-up the second half (the top half) of the mold construct.

B.2.1.4.3.1) Place the following items atop one another in the following order and smoothen: small endplate, thick filter paper, microsieve membrane.

B.2.1.4.3.2) Invert and press this half of the mold onto a stack of paper towels to ensure loss of excess calcium chloride solution. Do not fasten this half of the mold using binder clips at this time.

B.2.1.5) Culture cells as recommended per manufacturer's instructions. Harvest the desired cells to embed in the layered alginate hydrogels. The recommended cell density is 1-2 x 10^6 cells/ml, but this can be varied depending on desired experiments.

Note: When using this method for making layers with different cell types, make sure to culture two cell types in parallel for layering. Mesenchymal stem cells (MSCs)

seeded at a cell density of 1 x 10^6 cells/ml in six discs will be used as an example for the following protocol. Cell number and disc number can be scaled for experiments as needed.

B.2.1.5.1) Two to three weeks prior to embedding, seed mesenchymal stem cells at a cell density of 3000-5000 cells/cm^2 in 10 ml of basal growth media (Dulbecco's Modified Eagle Medium, 10% Fetal Bovine Serum, 2% L-Glutamine, 1% Non-essential Amino Acids, 1% Penicillin/Streptomycin) in T-75 flasks.

B.2.1.5.2) Remove spent media every 2-3 days and replace with 10 ml of basal growth media until the cells are 80-90% confluent.

B.2.1.5.3) To harvest cells, remove spent media, and pipette 3 ml of 1x Dulbecco's Phosphate Buffered Saline without added calcium chloride or magnesium chloride to rinse cells. Remove this solution, pipette 3 ml of 0.25% Trypsin-EDTA onto cells growing in T-75 flasks, and incubate for 5 min at 37 ^oC. After cells have lifted from the adherent surface, add 6-9 ml of basal growth media.

B.2.1.5.4) Centrifuge MSCs at 600 x g for 5 min at room temperature, aspirate the supernatant, and re-suspend in 1-5 ml of basal growth media. Count the cells using a hemocytometer using device instructions.

B.2.1.5.5) Remove 1 x 10^6 cells from the total cell resuspension, centrifuge using the same conditions, and aspirate the supernatant.

B.2.2. Formation of Cell Seeded Alginate Discs

B.2.2.1) Re-suspend the cell pellet with 1 ml of the sterile alginate/media solution to achieve a cell density of 1 x 10^6 cells/ml. The cell-alginate mixture will be homogenously cloudy in appearance when cells are mixed in appropriately.

B.2.2.2) Pipette 130 µl of the cell-alginate mixture into six 6 mm diameter x 3 mm tall wells in the bottom half of the mold construct dropwise, so as not to create any bubbles. A slight convex meniscus should be visible above the edge of each well.

B.2.2.3) Carefully smoothen the top half of the mold construct using a sterile spatula and turn it over, so that the cell microsieve membrane is on top of the wells. Place the mold construct on top of the wells, making sure to cover the wells containing the cell and alginate mixture completely.

B.2.2.4) Lift the loaded mold construct and, while pressing down firmly on the center, binder clip the remaining two sides (top and bottom) to fasten the top and bottom halves of the mold construct. The cell-alginate solutions should be securely nestled in the wells at this time.

B.2.2.5) Immerse fastened mold construct in the 102 mM calcium chloride bath, making sure that the entire construct is submerged. Incubate in the cell culture hood at room temperature for 90 min.

B.2.2.6) At the end of the 90 min, remove the mold construct from the 102 mM calcium chloride bath and place on a stack of paper towels in the cell culture hood. Remove all four binder clips and separate the two halves of the mold construct.

Hydrogels formed in the wells should not have any bubbles and should fill the wells completely.

B.2.2.7) Using a spatula, carefully trace the edge of the wells containing the hydrogels to carefully loosen and wedge out the hydrogels. After removing the hydrogels from the mold construct, drop the hydrogels directly into a bath of 1x Dulbecco's Phosphate Buffered Saline with calcium chloride and magnesium chloride. Cover the gels completely to wash off the excess calcium chloride solution for 1-5 min.

B.2.2.8) Transfer the hydrogels into basal growth media solution in desired dish (e.g. 6 well plates) that completely covers the hydrogels. Incubate for at least 1 hr in the cell culture incubator at 37 ^{o}C and 5% CO_2 before continuing to the layering step.

Note: Hydrogels containing cells can be kept in the cell culture incubator indefinitely at this time until layering of gels with another cell population is desired, provided that media changes are completed every 2-3 days.

B.2.3. Layering of alginate discs

B.2.3.1) During the last half hour of the 1 hr incubation, collect and prepare sterile molds and solution for annealing the gels.

B.2.3.1.1) Prepare the "cutting mold" by fastening a mold that has wells half of the height of the "gel formation mold" (6 mm diameter x 1.5 mm tall wells in a 3 in x 3 in aluminum plate) to an endplate (3 in x 3 in aluminum plate) using binder clips on the left and right sides.

B.2.3.1.2) Prepare the “annealing mold” by fastening a mold that is 3 mm larger in diameter than the “gel formation mold” (9 mm diameter x 3 mm tall wells in a 3 in x 3 in aluminum plate) to an endplate (3 in x 3 in aluminum plate) using binder clips on the left and right sides.

B.2.3.1.3) Prepare a solution of 100 mM sodium citrate/30 mM EDTA (Sodium citrate dihydrate, Ethylenediaminetetraacetic acid tetrasodium salt dihydrate) in sterile water.

B.2.3.2) Remove gels of desired cell populations (in this example, two discs with hMSCs) from the media in the dish, and place into the “cutting mold” wells. Each gel should fit snugly into the wells with half of the gel protruding above the mold.

B.2.3.3) Using a scalpel, slice the gel along the surface of the mold (this will cut the hydrogel in half). Flip the top half of the gel and place it into an open mold well. The half of the gel should also fit snugly into the mold well, but now both half gels should be the height of the mold with the cut inner surface visible. Repeat with second gel.

Note: Warning: Only the inner cut surfaces will form layered discs. Using the outer surfaces will result in the halves separating. It is suspected that texture from the microsieve membrane transferred onto the gel surface prevents success of the annealing process.

B.2.3.4) Place a piece of dry cell microsieve membrane on top of the wells, making sure that the microsieve membrane is in contact with all of the gel halves to be

annealed and covering them entirely. Place thick filter paper on top of the microsieve membrane, making sure to cover the gels completely.

B.2.3.5) Pipette a solution of 100 mM sodium citrate/30 mM EDTA (Sodium citrate dihydrate, Ethylenediaminetetraacetic acid tetrasodium salt dihydrate) onto the thick filter paper until it is saturated. Approximately 750 µl is sufficient for four wells.

B.2.3.6) Incubate the gels for 1 min at room temperature. Then, remove the cell microsieve membrane and thick filter paper and discard them. Remove the binder clips and open the mold.

B.2.3.7) For each annealed gel, transfer one sodium citrate/EDTA-treated half of the hydrogel to the prepared "annealing mold" with the cut surface facing upwards. This will be one half of the annealed construct.

B.2.3.8) Using a spatula, lift and place a second sodium citrate/EDTA-treated half-gel (may contain a different cell type) onto the gel already in the "annealing mold", flipping this second half-gel so that the cut surface is in contact with the cut surface of the gel already in the "annealing mold".

B.2.3.9) Press gently down on the two gels using a spatula to remove any bubbles between to the two gels. Also, reposition the gels as needed to make sure that they are directly on top of one another.

B.2.3.10) Gently lift the "annealing mold" and submerge it in the 102 mM calcium chloride bath for 30 min. Do not cover the wells with an endplate.

B.2.3.11) After the 30min incubation, remove the “annealing mold” and place it onto paper towels. Remove the binder clips and separate the mold from the endplate.

B.2.3.12) Using a spatula, collect the annealed gels and place them into a 1x Dulbecco’s Phosphate Buffered Saline with calcium chloride and magnesium chloride bath to wash the gels. Subsequently, transfer annealed hydrogels to cell culture media in a desired dish (e.g. 6-well plate) for culture.

B.3 Representative Results:

Figure B.1 depicts the formation and layering of the alginate hydrogels. Completed bi-layered gels exhibit a complete initial separation of cell populations as shown in Figure B.2. Cell viability of human mesenchymal stem cells embedded within these hydrogels and layered remains high and comparable to the bulk hydrogels as shown in Figure B.3. Viability was assessed after annealing, slicing the gels vertically to access the center and then staining the live cells in the annealed gels with a live cell tracker, CMFDA (green) and the dead cells (red) with Ethidium homodimer-1 using the manufacturer’s instructions. Confocal Z-stacks were taken of the cut surface using a fluorescence microscope approximately 100μm into the gel. These images were projected into one 2D image. Live and dead cells were then quantified using the particle analyzer feature in the ImageJ software.

We wanted to verify that these layered hydrogels, lacking cells, would be able to withstand cyclic compression, similar to that needed to induce a chondrogenic response. We found that the hydrogels do remain intact after seven days in culture and subsequent unconfined cyclic compression for 4 hr at 1 Hz from 0-10% strain.

However, after isolating the peak stress from each cycle and analyzing the trends over the four hour stimulation, the trends indicate that the layered hydrogels have a different response to the cyclic compression compared to the bulk, non-layered, hydrogels. Cyclic compression over four hours resulted in significantly different ($p = 0.03$) peak stress trends between layered and non-layered gels (Figure B.4). Statistics were completed using the Student's T-test ($\alpha = 0.05$).

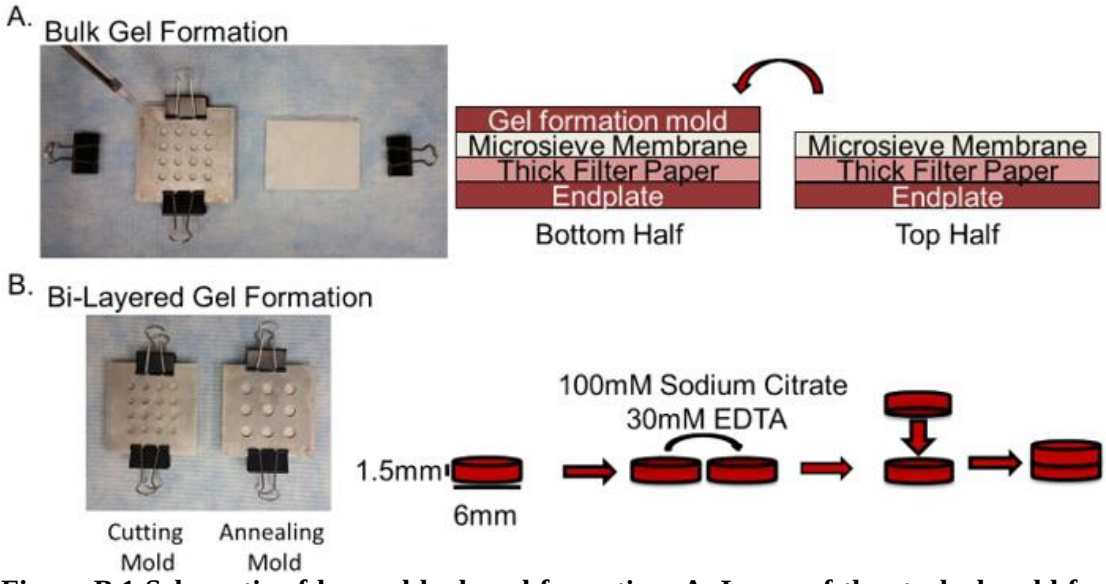

Figure B.1 Schematic of layered hydrogel formation. A. Image of the stacked mold for the addition of 2% alginate+cell mixture with a depiction of the stacking order for the bottom and top mold halves. B. Schematic depicting procedure for layering of the gel.

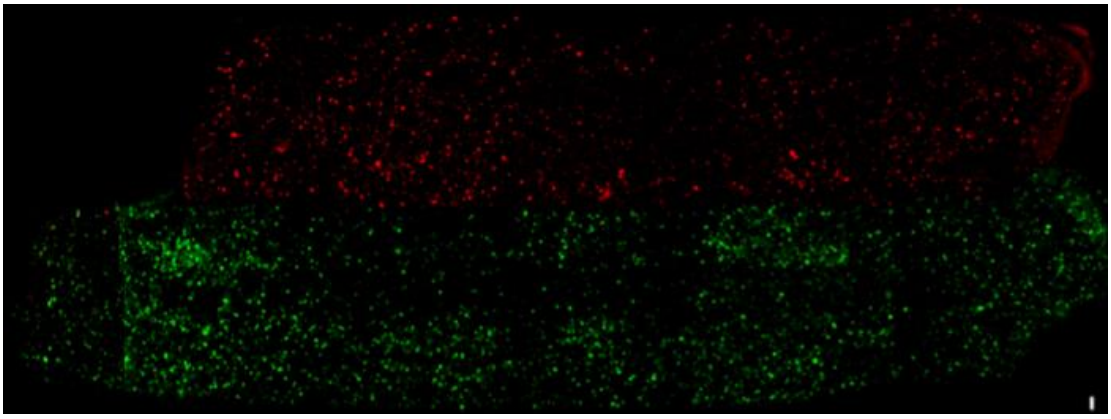

Figure B.2 Representative separation of cell populations in layered hydrogel. Model cell line 293FT HEK cells were either stained with live cell tracker CMFDA (green) or CMTPX (red). Each of these cell groups were embedded in 2% (w/v) alginate discs, and then halves of these discs were layered together. A piece was cut from the CMTPX side to identify it during imaging. Scale bar = 100µm.

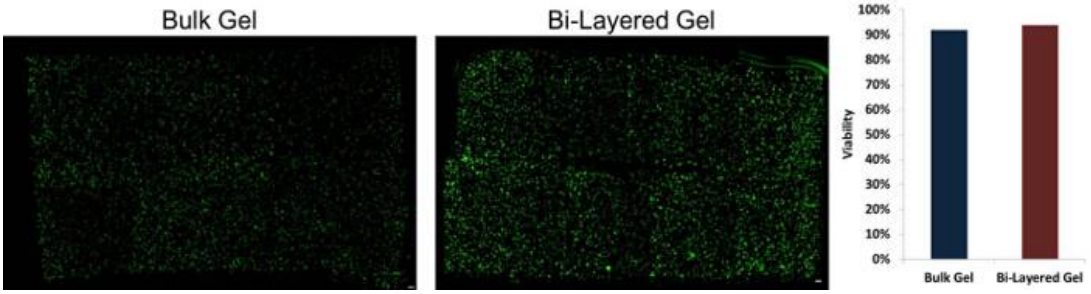

Figure B.3 High cell viability within layered hydrogel after layering process is complete. Human mesenchymal stem cells embedded in bulk and bi-layered hydrogels were stained with live cell (green) tracker CMFDA and dead cells (red) were stained with Ethidium homodimer-1. Viability remained high for both hydrogel groups after the layering process. Scale bar = 100µm.

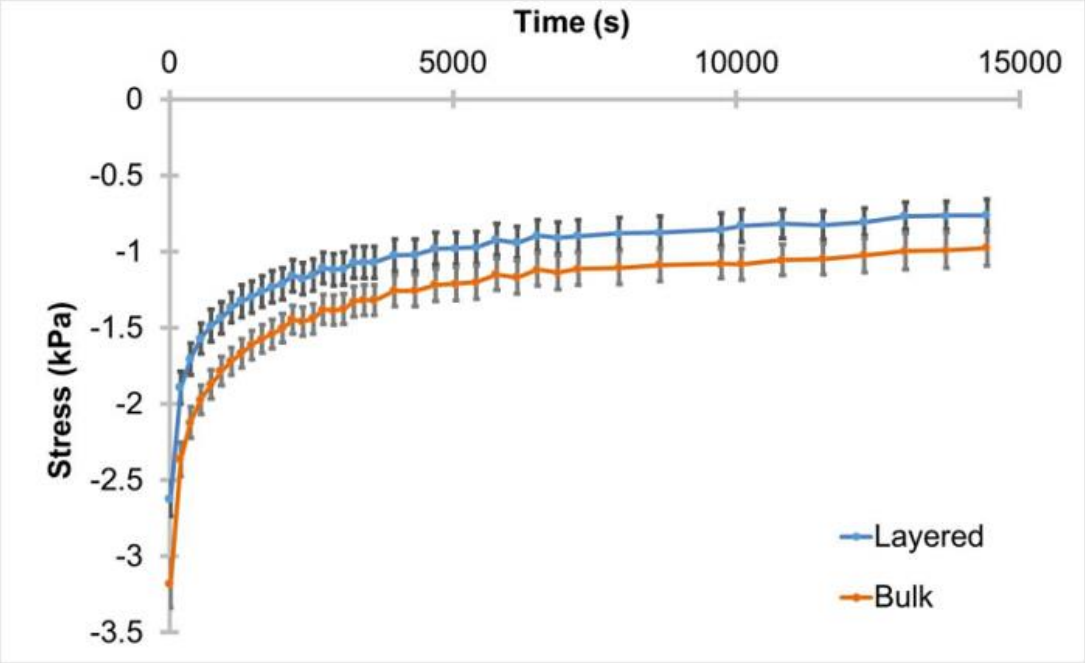

Figure B.4 Significantly different trends of layered hydrogel cyclic compression response to cyclic compression. Hydrogels were incubated in a cell culture incubator for seven days and subsequently subjected to 0-10% unconfined cyclic compression for four hours at 1Hz. Peak stresses (± SEM) for each cycle were isolated and the trends over the loading period analyzed. Trends under unconfined cyclic compression from 0-10% strain for layered (n = 9) and bulk (n = 8) gels are significantly different (p = 0.03).

B.4 Discussion

Here, we describe a protocol for the formation of layered alginate hydrogel discs for studying co-cultures of multiple cell populations, such as those in physiologically layered tissues, e.g. cartilage. Layered structures, such as the described culture platform, can be used to examine the interplay between two distinct cell populations subjected to the same culture environment or under load.

Alginate is an anionic linear polysaccharide that has been found to be biocompatible and has been successfully used for cartilage biology and tissue engineering research [44,202]. Alginate hydrogels are formed using divalent cations for crosslinking, e.g. calcium ions. These crosslinks can be undone by removing the cations using a chelator such as sodium citrate and this process has been used previously to isolate chondrocytes that have been cultured in the gels [194,195,202]. Similarly, the same principle has also been successfully applied for adhering alginate sheets in bilayers or even clusters of alginate beads together [201,202,204]. The platform described here relies on this same process, but is used to form small disc-shaped layered hydrogels. This is a two-step process in which first, alginate discs are formed using molds submerged in a calcium-rich bath. These are then sliced in half and treated with a calcium chelating solution to locally release the calcium ions from the crosslinked alginate. By placing these treated surfaces together and re-immersing the discs in a calcium-rich solution, crosslinks are reformed, making bi-layered constructs. These small layered gels eliminate the need for biopsy punches to generate easy-to-culture samples compatible with assays and experiments such as mechanical testing, as shown in Figure B.4, thereby minimizing waste of oftentimes precious cells as well as fabrication materials.

As shown in Figure B.3, this process of forming and layering the hydrogels resulted in similarly high viability as the control or bulk hydrogels indicating that this procedure is not overly taxing to the cell population despite the length and absence of replenishing nutrients. The lack of an initial overlapping region in the gel allows physical separation during initial co-culture and the ability to observe changes to that

interface over time. Studies have shown that over long culture periods this interface may lose definition due to cellular cross-infiltration and extracellular matrix deposition [201]. While the initial layered disc does not contain any adhesion molecules, as extracellular matrix is deposited, there is also a potential for investigating the merging of cell populations and the changing interface between the layers.

These bi-layer discs can be used easily for dynamic compression stimulation. We were able to confirm that these hydrogels withstand dynamic compression without separation of the halves. However, during this process, peak load exhibited by the layered hydrogels during the four hour cyclic compression were found to be significantly different from the non-layered, bulk, hydrogels. This result suggests complex, non-linear strain transfer between the layers and reveals a need for a physically layered control gel, e.g. bi-layered hydrogel with the same cell population/condition in each layer, an important detail to note when planning the experimental design for studies involving mechanical loading. Better understanding of the observed differences could be achieved through computational modeling of spatial mechanics within these gels. Not only would such analyses help clarify the strain distribution and transfer between the layers, but it would also be instrumental for interpreting cellular behavior in these layered gels, especially with layers of varying mechanical properties.

This is a versatile culture system that can be used for physical separation of cell populations during co-culture as described. Additionally, it can also be used as a base structure for further development. Changes to the existing structure could include increasing the number of layers, changing the sizes or the relative stiffness of the

layers, and incorporating additional extracellular matrix components into one or more of the layers. However, these expansions will require careful evaluation. In addition to changes in the distribution of forces throughout the discs, increasing the size and number of layers could lead to decreases in cell viability in the center of the gels and physical instability during mechanical stimulation. Further, large additions of extracellular matrix and stimulating proteins or alterations to the alginate to provide adhesion moieties may interfere with gel formation and annealing processes.

This culture platform was developed for research applications for investigating the relationships between different cell populations in 3D culture. Thus, it is limited by its lack of scalability for clinical applications. Alternative methods for creating layered hydrogels, such as 3D printing, may ultimately be more clinically relevant due to anticipated future scalability advances, control over microstructure in the disc interior, and customizability of macroscale geometric features. For research applications, as presented here, the alginate discs do not independently provide adhesion moieties for cells, which could limit its application to other cells types. The comparable alternative to alginate when considering ease of use is agarose, which suffers from similar limitations. Further, it requires the use of enzymes to release cells for downstream analysis, while alginate crosslinks can be safely removed using calcium chelating agents. Primarily, this culture platform will help with improving the understanding of relationships between cell populations in hydrogels and potentially the effects of mechanical stimulation of these co-cultures. This understanding will then inform the development of therapies for heterogeneous

tissues, especially loading bearing tissues such as articular cartilage or intervertebral discs.

References

1. Squillaro, T., Peluso, G. & Galderisi, U. Clinical Trials With Mesenchymal Stem Cells: An Update. *Cell Transplant.* **25,** 829–848 (2016).
2. Trounson, A. & McDonald, C. Stem Cell Therapies in Clinical Trials: Progress and Challenges. *Cell Stem Cell* **17,** 11–22 (2015).
3. Polymeri, A., Giannobile, W. V. & Kaigler, D. Bone Marrow Stromal Stem Cells in Tissue Engineering and Regenerative Medicine. *Horm. Metab. Res.* **48,** 700–713 (2016).
4. Vinatier, C. & Guicheux, J. Cartilage tissue engineering: From biomaterials and stem cells to osteoarthritis treatments. *Ann. Phys. Rehabil. Med.* **59,** 139–144 (2016).
5. Athanasiou, K. A., Darling, E. M. & Hu, J. C. Articular Cartilage Tissue Engineering. *Synth. Lect. Tissue Eng.* **1,** 1–182 (2009).
6. Vinatier, C., Mrugala, D., Jorgensen, C., Guicheux, J. & Noël, D. Cartilage engineering: a crucial combination of cells, biomaterials and biofactors. *Trends Biotechnol.* **27,** 307–314 (2009).
7. Martel-Pelletier, J., Boileau, C., Pelletier, J.-P. & Roughley, P. J. Cartilage in normal and osteoarthritis conditions. *Best Pract. Res. Clin. Rheumatol.* **22,** 351–384 (2008).
8. Barbour, K. E. *et al.* Prevalence of Doctor-Diagnosed Arthritis and Arthritis-Attributable Activity Limitation — United States, 2010–2012. (2013). Available at: https://www.cdc.gov/mmwr/preview/mmwrhtml/mm6244a1.htm. (Accessed: 4th August 2017)

9. Goldring, M. B. & Goldring, S. R. Osteoarthritis. *J. Cell. Physiol.* **213,** 626–634 (2007).

10. Alexopoulos, L. G., Haider, M. A., Vail, T. P. & Guilak, F. Alterations in the Mechanical Properties of the Human Chondrocyte Pericellular Matrix With Osteoarthritis. *J. Biomech. Eng.* **125,** 323 (2003).

11. Haudenschild, D. R. *et al.* Vimentin contributes to changes in chondrocyte stiffness in osteoarthritis. *J. Orthop. Res.* **29,** 20–25 (2011).

12. Wyles, C. C., Houdek, M. T., Behfar, A. & Sierra, R. J. Mesenchymal stem cell therapy for osteoarthritis: current perspectives. *Stem Cells Cloning Adv. Appl.* **8,** 117–124 (2015).

13. Jo, C. H. *et al.* Intra-Articular Injection of Mesenchymal Stem Cells for the Treatment of Osteoarthritis of the Knee: A Proof-of-Concept Clinical Trial. *STEM CELLS* **32,** 1254–1266 (2014).

14. Orozco, L. *et al.* Treatment of Knee Osteoarthritis With Autologous Mesenchymal Stem Cells: A Pilot Study. *Transplant. J.* **95,** 1535–1541 (2013).

15. Murphy, J. M., Fink, D. J., Hunziker, E. B. & Barry, F. P. Stem cell therapy in a caprine model of osteoarthritis. *Arthritis Rheum.* **48,** 3464–3474 (2003).

16. Chen, F. H. & Tuan, R. S. Mesenchymal stem cells in arthritic diseases. *Arthritis Res. Ther.* **10,** 223 (2008).

17. Orozco, L. *et al.* Treatment of Knee Osteoarthritis With Autologous Mesenchymal Stem Cells: Two-year Follow-up Results. *Transplantation* **97,** (2014).

18. Wei, C.-C., Lin, A. B. & Hung, S.-C. Mesenchymal Stem Cells in Regenerative Medicine for Musculoskeletal Diseases: Bench, Bedside, and Industry. *Cell Transplant.* **23,** 505–512 (2014).

19. Huang, B. J., Hu, J. C. & Athanasiou, K. A. Cell-based tissue engineering strategies used in the clinical repair of articular cartilage. *Biomaterials* **98,** 1–22 (2016).

20. Bhardwaj, N., Devi, D. & Mandal, B. B. Tissue-engineered cartilage: the crossroads of biomaterials, cells and stimulating factors. *Macromol. Biosci.* **15,** 153–182 (2015).

21. Dimmeler, S., Ding, S., Rando, T. A. & Trounson, A. Translational strategies and challenges in regenerative medicine. *Nat. Med.* **20,** 814–821 (2014).

22. Lee, W. Y. & Wang, B. Cartilage repair by mesenchymal stem cells: Clinical trial update and perspectives. *J. Orthop. Transl.* **9,** 76–88 (2017).

23. Filardo, G. *et al.* Mesenchymal stem cells for the treatment of cartilage lesions: from preclinical findings to clinical application in orthopaedics. *Knee Surg. Sports Traumatol. Arthrosc. Off. J. ESSKA* **21,** 1717–1729 (2013).

24. Kang, S. K., Shin, I. S., Ko, M. S., Jo, J. Y. & Ra, J. C. Journey of Mesenchymal Stem Cells for Homing: Strategies to Enhance Efficacy and Safety of Stem Cell Therapy. *Stem Cells Int.* **2012,** e342968 (2012).

25. Chapel, A. *et al.* Mesenchymal stem cells home to injured tissues when co-infused with hematopoietic cells to treat a radiation-induced multi-organ failure syndrome. *J. Gene Med.* **5,** 1028–1038 (2003).

26. Sasaki, M. *et al.* Mesenchymal Stem Cells Are Recruited into Wounded Skin and Contribute to Wound Repair by Transdifferentiation into Multiple Skin Cell Type. *J. Immunol.* **180,** 2581–2587 (2008).

27. Engler, A. J., Sen, S., Sweeney, H. L. & Discher, D. E. Matrix Elasticity Directs Stem Cell Lineage Specification. *Cell* **126,** 677–689 (2006).

28. Chen, W. L. K., Likhitpanichkul, M., Ho, A. & Simmons, C. A. Integration of statistical modeling and high-content microscopy to systematically investigate cell–substrate interactions. *Biomaterials* **31,** 2489–2497 (2010).

29. Rowlands, A. S., George, P. A. & Cooper-White, J. J. Directing osteogenic and myogenic differentiation of MSCs: interplay of stiffness and adhesive ligand presentation. *Am. J. Physiol. - Cell Physiol.* **295,** C1037–C1044 (2008).

30. Curran, J. M., Chen, R. & Hunt, J. A. The guidance of human mesenchymal stem cell differentiation in vitro by controlled modifications to the cell substrate. *Biomaterials* **27,** 4783–4793 (2006).

31. Salasznyk, R. M., Williams, W. A., Boskey, A., Batorsky, A. & Plopper, G. E. Adhesion to Vitronectin and Collagen I Promotes Osteogenic Differentiation of Human Mesenchymal Stem Cells. *BioMed Res. Int.* **2004,** 24–34 (2004).

32. Hidalgo-Bastida, L. A. & Cartmell, S. H. Mesenchymal Stem Cells, Osteoblasts and Extracellular Matrix Proteins: Enhancing Cell Adhesion and Differentiation for Bone Tissue Engineering. *Tissue Eng. Part B Rev.* **16,** 405–412 (2010).

33. Trappmann, B. *et al.* Extracellular-matrix tethering regulates stem-cell fate. *Nat. Mater. Lond.* **11,** 642–9 (2012).

34. McBeath, R., Pirone, D. M., Nelson, C. M., Bhadriraju, K. & Chen, C. S. Cell Shape, Cytoskeletal Tension, and RhoA Regulate Stem Cell Lineage Commitment. *Dev. Cell* **6,** 483–495 (2004).

35. Zhang, D. & Kilian, K. A. The effect of mesenchymal stem cell shape on the maintenance of multipotency. *Biomaterials* **34,** 3962–3969 (2013).

36. Kilian, K. A., Bugarija, B., Lahn, B. T. & Mrksich, M. Geometric cues for directing the differentiation of mesenchymal stem cells. *Proc. Natl. Acad. Sci.* **107,** 4872–4877 (2010).

37. Tee, S.-Y., Fu, J., Chen, C. S. & Janmey, P. A. Cell shape and substrate rigidity both regulate cell stiffness. *Biophys. J.* **100,** L25-27 (2011).

38. Mendez, M. G., Restle, D. & Janmey, P. A. Vimentin Enhances Cell Elastic Behavior and Protects against Compressive Stress. *Biophys. J.* **107,** 314–323 (2014).

39. Lv, H. *et al.* Mechanism of regulation of stem cell differentiation by matrix stiffness. *Stem Cell Res. Ther.* **6,** (2015).

40. Park, J. S. *et al.* The effect of matrix stiffness on the differentiation of mesenchymal stem cells in response to TGF-β. *Biomaterials* **32,** 3921–3930 (2011).

41. Johnstone, B., Hering, T. M., Caplan, A. I., Goldberg, V. M. & Yoo, J. U. In VitroChondrogenesis of Bone Marrow-Derived Mesenchymal Progenitor Cells. *Exp. Cell Res.* **238,** 265–272 (1998).

42. Mackay, A. M. *et al.* Chondrogenic differentiation of cultured human mesenchymal stem cells from marrow. *Tissue Eng.* **4,** 415–428 (1998).

43. Huang, A. H., Farrell, M. J. & Mauck, R. L. Mechanics and mechanobiology of mesenchymal stem cell-based engineered cartilage. *J. Biomech.* **43,** 128–136 (2010).

44. Xu, J. *et al.* Chondrogenic Differentiation of Human Mesenchymal Stem Cells in Three-Dimensional Alginate Gels. *Tissue Eng. Part A* **14,** 667–680 (2008).

45. Awad, H. A., Quinn Wickham, M., Leddy, H. A., Gimble, J. M. & Guilak, F. Chondrogenic differentiation of adipose-derived adult stem cells in agarose, alginate, and gelatin scaffolds. *Biomaterials* **25,** 3211–3222 (2004).

46. Erickson, G. R. *et al.* Chondrogenic potential of adipose tissue-derived stromal cells in vitro and in vivo. *Biochem. Biophys. Res. Commun.* **290,** 763–769 (2002).

47. Wagner, D. R. *et al.* Hydrostatic Pressure Enhances Chondrogenic Differentiation of Human Bone Marrow Stromal Cells in Osteochondrogenic Medium. *Ann. Biomed. Eng.* **36,** 813–820 (2008).

48. Steward, A. J. *et al.* Cell–matrix interactions regulate mesenchymal stem cell response to hydrostatic pressure. *Acta Biomater.* **8,** 2153–2159 (2012).

49. Huang, C. *et al.* Effects of cyclic compressive loading on chondrogenesis of rabbit bone-marrow derived mesenchymal stem cells. *Stem Cells* **22,** 313–323 (2004).

50. Mauck, R. L., Byers, B. A., Yuan, X. & Tuan, R. S. Regulation of Cartilaginous ECM Gene Transcription by Chondrocytes and MSCs in 3D Culture in Response to Dynamic Loading. *Biomech. Model. Mechanobiol.* **6,** 113–125 (2006).

51. Delaine-Smith, R. M. & Reilly, G. C. Mesenchymal stem cell responses to mechanical stimuli. *Muscles Ligaments Tendons J.* **2,** 169–180 (2012).

52. Mathieu, P. S. & Loboa, E. G. Cytoskeletal and Focal Adhesion Influences on Mesenchymal Stem Cell Shape, Mechanical Properties, and Differentiation Down Osteogenic, Adipogenic, and Chondrogenic Pathways. *Tissue Eng. Part B Rev.* **18,** 436–444 (2012).

53. Yu, H. *et al.* Mechanical behavior of human mesenchymal stem cells during adipogenic and osteogenic differentiation. *Biochem. Biophys. Res. Commun.* **393,** 150–155 (2010).

54. González-Cruz, R. D., Fonseca, V. C. & Darling, E. M. Cellular mechanical properties reflect the differentiation potential of adipose-derived mesenchymal stem cells. *Proc. Natl. Acad. Sci. U. S. A.* **109,** E1523–E1529 (2012).

55. Lee, J.-H., Park, H.-K. & Kim, K. S. Intrinsic and extrinsic mechanical properties related to the differentiation of mesenchymal stem cells. *Biochem. Biophys. Res. Commun.* **473,** 752–757 (2016).

56. Yourek, G., Hussain, M. A. & Mao, J. J. Cytoskeletal changes of mesenchymal stem cells during differentiation. *ASAIO J. Am. Soc. Artif. Intern. Organs 1992* **53,** 219–228 (2007).

57. Tse, J. R. & Engler, A. J. Stiffness Gradients Mimicking In Vivo Tissue Variation Regulate Mesenchymal Stem Cell Fate. *PLOS ONE* **6,** e15978 (2011).

58. O'Conor, C. J., Case, N. & Guilak, F. Mechanical regulation of chondrogenesis. *Stem Cell Res. Ther.* **4,** 61 (2013).

59. Meyer, E. G., Buckley, C. T., Steward, A. J. & Kelly, D. J. The effect of cyclic hydrostatic pressure on the functional development of cartilaginous tissues engineered using bone marrow derived mesenchymal stem cells. *J. Mech. Behav. Biomed. Mater.* **4,** 1257–1265 (2011).

60. Angele, P. *et al.* Cyclic hydrostatic pressure enhances the chondrogenic phenotype of human mesenchymal progenitor cells differentiated in vitro. *J. Orthop. Res. Off. Publ. Orthop. Res. Soc.* **21,** 451–457 (2003).

61. Carroll, S. F., Buckley, C. T. & Kelly, D. J. Cyclic hydrostatic pressure promotes a stable cartilage phenotype and enhances the functional development of cartilaginous grafts engineered using multipotent stromal cells isolated from bone marrow and infrapatellar fat pad. *J. Biomech.* **47,** 2115–2121 (2014).

62. Miyanishi, K. *et al.* Effects of hydrostatic pressure and transforming growth factor-β 3 on adult human mesenchymal stem cell chondrogenesis in vitro. *Tissue Eng.* **12,** 1419–1428 (2006).

63. Miyanishi, K. *et al.* Dose-and time-dependent effects of cyclic hydrostatic pressure on transforming growth factor-β3-induced chondrogenesis by adult human mesenchymal stem cells in vitro. *Tissue Eng.* **12,** 2253–2262 (2006).

64. Vinardell, T. *et al.* Hydrostatic pressure acts to stabilise a chondrogenic phenotype in porcine joint tissue derived stem cells. *Eur. Cell. Mater.* **23,** 121-132; discussion 133-134 (2012).

65. Li, Y. J. *et al.* Oscillatory fluid flow affects human marrow stromal cell proliferation and differentiation. *J. Orthop. Res. Off. Publ. Orthop. Res. Soc.* **22,** 1283–1289 (2004).

66. Zhong, W., Zhang, W., Wang, S. & Qin, J. Regulation of Fibrochondrogenesis of Mesenchymal Stem Cells in an Integrated Microfluidic Platform Embedded with Biomimetic Nanofibrous Scaffolds. *PLOS ONE* **8,** e61283 (2013).

67. Riehl, B. D., Lee, J. S., Ha, L. & Lim, J. Y. Fluid-flow-induced mesenchymal stem cell migration: role of focal adhesion kinase and RhoA kinase sensors. *J. R. Soc. Interface* **12,** 20141351 (2015).

68. Riddle, R. C., Taylor, A. F., Genetos, D. C. & Donahue, H. J. MAP kinase and calcium signaling mediate fluid flow-induced human mesenchymal stem cell proliferation. *Am. J. Physiol. - Cell Physiol.* **290,** C776–C784 (2006).

69. Glossop, J. R. & Cartmell, S. H. Effect of fluid flow-induced shear stress on human mesenchymal stem cells: Differential gene expression of IL1B and MAP3K8 in MAPK signaling. *Gene Expr. Patterns* **9,** 381–388 (2009).

70. Fahy, N., Alini, M. & Stoddart, M. J. Mechanical stimulation of mesenchymal stem cells: Implications for cartilage tissue engineering. *J. Orthop. Res.* n/a-n/a doi:10.1002/jor.23670

71. Chamberlain, G., Smith, H., Rainger, G. E. & Middleton, J. Mesenchymal stem cells exhibit firm adhesion, crawling, spreading and transmigration across aortic endothelial cells: effects of chemokines and shear. *PloS One* **6,** e25663 (2011).

72. Blain, E. J. Involvement of the cytoskeletal elements in articular cartilage homeostasis and pathology. *Int. J. Exp. Pathol.* **90,** 1–15 (2009).

73. Lim, Y. B. *et al.* Disruption of actin cytoskeleton induces chondrogenesis of mesenchymal cells by activating protein kinase C-alpha signaling. *Biochem. Biophys. Res. Commun.* **273,** 609–613 (2000).

74. Woods, A., Wang, G. & Beier, F. RhoA/ROCK Signaling Regulates Sox9 Expression and Actin Organization during Chondrogenesis. *J. Biol. Chem.* **280,** 11626–11634 (2005).

75. Titushkin, I. A. & Cho, M. R. Controlling cellular biomechanics of human mesenchymal stem cells. in *Annual International Conference of the IEEE Engineering in Medicine and Biology Society, 2009. EMBC 2009* 2090–2093 (2009). doi:10.1109/IEMBS.2009.5333949

76. Pan, W. *et al.* Viscoelastic Properties of Human Mesenchymal Stem Cells. in *Engineering in Medicine and Biology Society, 2005. IEEE-EMBS 2005. 27th Annual International Conference of the* 4854–4857 (2005). doi:10.1109/IEMBS.2005.1615559

77. Ridge, K. M. *et al.* Chapter Fourteen - Methods for Determining the Cellular Functions of Vimentin Intermediate Filaments. in *Methods in Enzymology* (ed. Liem, M. B. O. and R. K. H.) **568,** 389–426 (Academic Press, 2016).

78. Satelli, A. & Li, S. Vimentin in cancer and its potential as a molecular target for cancer therapy. *Cell. Mol. Life Sci.* **68,** 3033–46 (2011).

79. Eriksson, J. E. *et al.* Introducing intermediate filaments: from discovery to disease. *J. Clin. Invest.* **119,** 1763–1771 (2009).

80. Lowery, J., Kuczmarski, E. R., Herrmann, H. & Goldman, R. D. Intermediate Filaments Play a Pivotal Role in Regulating Cell Architecture and Function. *J. Biol. Chem.* **290,** 17145–17153 (2015).

81. Robert, A., Hookway, C. & Gelfand, V. I. Intermediate filament dynamics: What we can see now and why it matters. *BioEssays* **38,** 232–243 (2016).

82. Colucci-Guyon, E. *et al.* Mice lacking vimentin develop and reproduce without an obvious phenotype. *Cell* **79,** 679–694 (1994).

83. Eckes, B. *et al.* Impaired wound healing in embryonic and adult mice lacking vimentin. *J. Cell Sci.* **113 (Pt 13),** 2455–2462 (2000).

84. Terzi, F. *et al.* Reduction of renal mass is lethal in mice lacking vimentin. Role of endothelin-nitric oxide imbalance. *J. Clin. Invest.* **100,** 1520–1528 (1997).

85. Colucci-Guyon, E., Giménez Y Ribotta, M., Maurice, T., Babinet, C. & Privat, A. Cerebellar defect and impaired motor coordination in mice lacking vimentin. *Glia* **25,** 33–43 (1999).

86. Shen, W.-J. *et al.* Ablation of Vimentin Results in Defective Steroidogenesis. *Endocrinology* **153,** 3249–3257 (2012).

87. McInroy, L. & Määttä, A. Down-regulation of vimentin expression inhibits carcinoma cell migration and adhesion. *Biochem. Biophys. Res. Commun.* **360,** 109–114 (2007).

88. Liu, C.-Y., Lin, H.-H., Tang, M.-J. & Wang, Y.-K. Vimentin contributes to epithelial-mesenchymal transition cancer cell mechanics by mediating cytoskeletal organization and focal adhesion maturation. *Oncotarget* **6,** 15966–15983 (2015).

89. Herrmann, H. & Aebi, U. Intermediate filaments and their associates: multi-talented structural elements specifying cytoarchitecture and cytodynamics. *Curr. Opin. Cell Biol.* **12,** 79–90 (2000).

90. Juarez, M. *et al.* Identification of novel antiacetylated vimentin antibodies in patients with early inflammatory arthritis. *Ann. Rheum. Dis.* annrheumdis-2014-206785 (2015). doi:10.1136/annrheumdis-2014-206785

91. Mahammad, S. *et al.* Giant axonal neuropathy–associated gigaxonin mutations impair intermediate filament protein degradation. *J. Clin. Invest.* **123,** 1964–1975 (2013).

92. Capín-Gutiérrez, N., Talamás-Rohana, P., González-Robles, A., Lavalle-Montalvo, C. & Kourí, J. B. Cytoskeleton disruption in chondrocytes from a rat osteoarthrosic (OA) -induced model: its potential role in OA pathogenesis. *Histol. Histopathol.* **19,** 1125–1132 (2004).

93. Lambrecht, S., Verbruggen, G., Verdonk, P. C. M., Elewaut, D. & Deforce, D. Differential proteome analysis of normal and osteoarthritic chondrocytes reveals distortion of vimentin network in osteoarthritis. *Osteoarthritis Cartilage* **16,** 163–173 (2008).

94. Trickey, W. R., Vail, T. P. & Guilak, F. The role of the cytoskeleton in the viscoelastic properties of human articular chondrocytes. *J. Orthop. Res. Off. Publ. Orthop. Res. Soc.* **22,** 131–139 (2004).

95. Rollín, R. *et al.* Differential proteome of bone marrow mesenchymal stem cells from osteoarthritis patients. *Osteoarthritis Cartilage* **16,** 929–935 (2008).

96. Janmey, P. A., Euteneuer, U., Traub, P. & Schliwa, M. Viscoelastic properties of vimentin compared with other filamentous biopolymer networks. *J. Cell Biol.* **113,** 155–160 (1991).

97. Charrier, E. E. & Janmey, P. A. Mechanical properties of intermediate filament proteins. *Methods Enzymol.* **568,** 35–57 (2016).

98. Conway, D. E. *et al.* Fluid Shear Stress on Endothelial Cells Modulates Mechanical Tension across VE-Cadherin and PECAM-1. *Curr. Biol.* **23,** 1024–1030 (2013).

99. Helmke, B. P., Goldman, R. D. & Davies, P. F. Rapid Displacement of Vimentin Intermediate Filaments in Living Endothelial Cells Exposed to Flow. *Circ. Res.* **86,** 745–752 (2000).

100. Henrion, D. *et al.* Impaired flow-induced dilation in mesenteric resistance arteries from mice lacking vimentin. *J. Clin. Invest.* **100,** 2909–2914 (1997).

101. Steward, A. J., Wagner, D. R. & Kelly, D. J. The pericellular environment regulates cytoskeletal development and the differentiation of mesenchymal stem cells and determines their response to hydrostatic pressure. *Eur Cell Mater* **25,** 167–178 (2013).

102. Durrant, L. A., Archer, C. W., Benjamin, M. & Ralphs, J. R. Organisation of the chondrocyte cytoskeleton and its response to changing mechanical conditions in organ culture. *J. Anat.* **194,** 343–353 (1999).

103. Henson, F. M. & Vincent, T. A. Alterations in the vimentin cytoskeleton in response to single impact load in an in vitro model of cartilage damage in the rat. *BMC Musculoskelet. Disord.* **9,** 94 (2008).

104. Gonzales, M. *et al.* Structure and Function of a Vimentin-associated Matrix Adhesion in Endothelial Cells. *Mol. Biol. Cell* **12,** 85–100 (2001).

105. Tsuruta, D. The vimentin cytoskeleton regulates focal contact size and adhesion of endothelial cells subjected to shear stress. *J. Cell Sci.* **116,** 4977–4984 (2003).

106. Kreis, S., Schönfeld, H.-J., Melchior, C., Steiner, B. & Kieffer, N. The intermediate filament protein vimentin binds specifically to a recombinant integrin α2/β1 cytoplasmic tail complex and co-localizes with native α2/β1 in endothelial cell focal adhesions. *Exp. Cell Res.* **305,** 110–121 (2005).

107. Kim, H. *et al.* Filamin A is required for vimentin-mediated cell adhesion and spreading. *Am. J. Physiol. - Cell Physiol.* **298,** C221–C236 (2010).

108. Kim, H. *et al.* Regulation of cell adhesion to collagen via β1 integrins is dependent on interactions of filamin A with vimentin and protein kinase C epsilon. *Exp. Cell Res.* **316,** 1829–1844 (2010).

109. Bhattacharya, R. *et al.* Recruitment of vimentin to the cell surface by β3 integrin and plectin mediates adhesion strength. *J Cell Sci* **122,** 1390–1400 (2009).

110. Homan, S. M., Martinez, R., Benware, A. & LaFlamme, S. E. Regulation of the Association of α6β4 with Vimentin Intermediate Filaments in Endothelial Cells. *Exp. Cell Res.* **281,** 107–114 (2002).

111. Guo, M. *et al.* The Role of Vimentin Intermediate Filaments in Cortical and Cytoplasmic Mechanics. *Biophys. J.* **105,** 1562–1568 (2013).

112. Wang, N. & Stamenović, D. Contribution of intermediate filaments to cell stiffness, stiffening, and growth. *Am. J. Physiol.-Cell Physiol.* **279,** C188–C194 (2000).

113. Eckes, B. *et al.* Impaired mechanical stability, migration and contractile capacity in vimentin-deficient fibroblasts. *J. Cell Sci.* **111,** 1897–1907 (1998).

114. Mendez, M. G., Kojima, S.-I. & Goldman, R. D. Vimentin induces changes in cell shape, motility, and adhesion during the epithelial to mesenchymal transition. *FASEB J.* **24,** 1838–1851 (2010).

115. Lu, Y.-B. *et al.* Reactive glial cells: increased stiffness correlates with increased intermediate filament expression. *FASEB J.* **25,** 624–631 (2011).

116. Brown, M. J., Hallam, J. A., Colucci-Guyon, E. & Shaw, S. Rigidity of Circulating Lymphocytes Is Primarily Conferred by Vimentin Intermediate Filaments. *J. Immunol.* **166,** 6640–6646 (2001).

117. Gladilin, E., Gonzalez, P. & Eils, R. Dissecting the contribution of actin and vimentin intermediate filaments to mechanical phenotype of suspended cells using high-throughput deformability measurements and computational modeling. *J. Biomech.* **47,** 2598–2605 (2014).

118. Chahine, N. O. *et al.* Effect of Age and Cytoskeletal Elements on the Indentation-Dependent Mechanical Properties of Chondrocytes. *PLoS ONE* **8,** e61651 (2013).

119. Ofek, G., Wiltz, D. C. & Athanasiou, K. A. Contribution of the Cytoskeleton to the Compressive Properties and Recovery Behavior of Single Cells. *Biophys. J.* **97,** 1873–1882 (2009).

120. Havel, L. S., Kline, E. R., Salgueiro, A. M. & Marcus, A. I. Vimentin regulates lung cancer cell adhesion through a VAV2–Rac1 pathway to control focal adhesion kinase activity. *Oncogene* **34,** 1979–1990 (2015).

121. Bershadsky, A. D., Tint, I. S. & Svitkina, T. M. Association of intermediate filaments with vinculin-containing adhesion plaques of fibroblasts. *Cell Motil. Cytoskeleton* **8,** 274–283 (1987).

122. Burgstaller, G., Gregor, M., Winter, L. & Wiche, G. Keeping the Vimentin Network under Control: Cell–Matrix Adhesion–associated Plectin 1f Affects Cell Shape and Polarity of Fibroblasts. *Mol. Biol. Cell* **21,** 3362–3375 (2010).

123. Blain, E. J., Gilbert, S. J., Hayes, A. J. & Duance, V. C. Disassembly of the vimentin cytoskeleton disrupts articular cartilage chondrocyte homeostasis. *Matrix Biol.* **25,** 398–408 (2006).

124. Bobick, B. E., Tuan, R. S. & Chen, F. H. The intermediate filament vimentin regulates chondrogenesis of adult human bone marrow-derived multipotent progenitor cells. *J. Cell. Biochem.* n/a-n/a (2009). doi:10.1002/jcb.22419

125. Boraas, L. C. & Ahsan, T. Lack of vimentin impairs endothelial differentiation of embryonic stem cells. *Sci. Rep.* **6,** (2016).

126. Vigfúsdóttir, Á. T., Pasrija, C., Thakore, P. I., Schmidt, R. B. & Hsieh, A. H. Role of Pericellular Matrix in Mesenchymal Stem Cell Deformation during Chondrogenic Differentiation. *Cell. Mol. Bioeng.* **3,** 387–397 (2010).

127. Rathje, L.-S. Z. *et al.* Oncogenes induce a vimentin filament collapse mediated by HDAC6 that is linked to cell stiffness. *Proc. Natl. Acad. Sci. U. S. A.* **111,** 1515–1520 (2014).

128. Plodinec, M. *et al.* The nanomechanical properties of rat fibroblasts are modulated by interfering with the vimentin intermediate filament system. *J. Struct. Biol.* **174,** 476–484 (2011).

129. Eckert, B. S. Alteration of intermediate filament distribution in PtK1 cells by acrylamide. *Eur. J. Cell Biol.* **37,** 169–174 (1985).

130. Chen, C. *et al.* Effects of vimentin disruption on the mechanoresponses of articular chondrocyte. *Biochem. Biophys. Res. Commun.* **469,** 132–137 (2016).

131. Goldman, R. D., Khuon, S., Chou, Y. H., Opal, P. & Steinert, P. M. The function of intermediate filaments in cell shape and cytoskeletal integrity. *J. Cell Biol.* **134,** 971–983 (1996).

132. Helfand, B. T. *et al.* Vimentin organization modulates the formation of lamellipodia. *Mol. Biol. Cell* **22,** 1274–1289 (2011).

133. Valgeirsdóttir, S. *et al.* PDGF induces reorganization of vimentin filaments. *J. Cell Sci.* **111 (Pt 14),** 1973–1980 (1998).

134. Sliva, K. & Schnierle, B. S. Selective gene silencing by viral delivery of short hairpin RNA. *Virol. J.* **7,** 248 (2010).

135. Afizah, H. & Hui, J. H. P. Mesenchymal stem cell therapy for osteoarthritis. *J. Clin. Orthop. Trauma* **7,** 177–182 (2016).

136. Guilak, F. Biomechanical factors in osteoarthritis. *Best Pract. Res. Clin. Rheumatol.* **25,** 815–823 (2011).

137. Fukui, N., Purple, C. R. & Sandell, L. J. Cell biology of osteoarthritis: The chondrocyte's response to injury. *Curr. Rheumatol. Rep.* **3,** 496–505 (2001).

138. Broom, N. D. & Myers, D. B. A study of the structural response of wet hyaline cartilage to various loading situations. *Connect. Tissue Res.* **7,** 227–237 (1980).

139. Urban, J. P. G. The Chondrocyte: A Cell Under Pressure. *Rheumatology* **33,** 901–908 (1994).

140. Wu, J. Z., Herzog, W. & Epstein, M. Modelling of location- and time-dependent deformation of chondrocytes during cartilage loading. *J. Biomech.* **32,** 563–572 (1999).

141. Guilak, F., Ratcliffe, A. & Mow, V. C. Chondrocyte deformation and local tissue strain in articular cartilage: A confocal microscopy study. *J. Orthop. Res.* **13,** 410–421 (1995).

142. Lee, D. A. & Bader, D. L. The development and characterization of anin vitro system to study strain-induced cell deformation in isolated chondrocytes. *Vitro Cell. Dev. Biol. - Anim.* **31,** 828–835

143. McCloy, R. A. *et al.* Partial inhibition of Cdk1 in G2 phase overrides the SAC and decouples mitotic events. *Cell Cycle* **13,** 1400–1412 (2014).

144. Lee, D. A. *et al.* Chondrocyte deformation within compressed agarose constructs at the cellular and sub-cellular levels. *J. Biomech.* **33,** 81–95 (2000).

145. Chen, Q., Suki, B. & An, K.-N. Dynamic mechanical properties of agarose gels modeled by a fractional derivative model. *J. Biomech. Eng.* **126,** 666–671 (2004).

146. Twomey, J. D., Thakore, P. I., Hartman, D. A., Myers, E. G. H. & Hsieh, A. H. Roles of type VI collagen and decorin in human mesenchymal stem cell biophysics during chondrogenic differentiation. *Eur. Cell. Mater.* **27,** 237-250; discussion 249-250 (2014).

147. Yourek, G., McCormick, S. M., Mao, J. J. & Reilly, G. C. Shear stress induces osteogenic differentiation of human mesenchymal stem cells. *Regen. Med.* **5,** 713–724 (2010).

148. Pazzano, D. *et al.* Comparison of chondrogensis in static and perfused bioreactor culture. *Biotechnol. Prog.* **16,** 893–896 (2000).

149. Murray, M. E., Mendez, M. G. & Janmey, P. A. Substrate stiffness regulates solubility of cellular vimentin. *Mol. Biol. Cell* **25,** 87–94 (2014).

150. Sharma, P., Bolten, Z. T., Wagner, D. R. & Hsieh, A. H. Deformability of Human Mesenchymal Stem Cells Is Dependent on Vimentin Intermediate Filaments. *Ann. Biomed. Eng.* **45,** 1365–1374 (2017).

151. Stroka, K. M. & Aranda-Espinoza, H. Neutrophils display biphasic relationship between migration and substrate stiffness. *Cell Motil. Cytoskeleton* **66,** 328–341 (2009).

152. Jackson, W. M., Jaasma, M. J., Tang, R. Y. & Keaveny, T. M. Mechanical loading by fluid shear is sufficient to alter the cytoskeletal composition of osteoblastic cells. *Am. J. Physiol. Cell Physiol.* **295,** C1007-1015 (2008).

153. Pavalko, F. M. *et al.* Fluid shear-induced mechanical signaling in MC3T3-E1 osteoblasts requires cytoskeleton-integrin interactions. *Am. J. Physiol. - Cell Physiol.* **275,** C1591–C1601 (1998).

154. Kim, J. *et al.* Vimentin filament controls integrin α5β1-mediated cell adhesion by binding to integrin through its Ser38 residue. *FEBS Lett.* **590,** 3517–3525 (2016).

155. Humphries, J. D., Byron, A. & Humphries, M. J. Integrin ligands at a glance. *J. Cell Sci.* **119,** 3901–3903 (2006).

156. Du, J. *et al.* Integrin activation and internalization on soft ECM as a mechanism of induction of stem cell differentiation by ECM elasticity. *Proc. Natl. Acad. Sci.* **108,** 9466–9471 (2011).

157. Boeuf, S. & Richter, W. Chondrogenesis of mesenchymal stem cells: role of tissue source and inducing factors. *Stem Cell Res. Ther.* **1,** 31 (2010).

158. DeLise, A. M., Fischer, L. & Tuan, R. S. Cellular interactions and signaling in cartilage development. *Osteoarthritis Cartilage* **8,** 309–334 (2000).

159. Woods, A., Wang, G., Dupuis, H., Shao, Z. & Beier, F. Rac1 Signaling Stimulates N-cadherin Expression, Mesenchymal Condensation, and Chondrogenesis. *J. Biol. Chem.* **282,** 23500–23508 (2007).

160. Bian, L., Guvendiren, M., Mauck, R. L. & Burdick, J. A. Hydrogels that mimic developmentally relevant matrix and N-cadherin interactions enhance MSC chondrogenesis. *Proc. Natl. Acad. Sci.* **110,** 10117–10122 (2013).

161. Schmitt, J. F., Hua, S. K., Zheng, Y., Po, J. H. H. & Hin, L. E. Sequential differentiation of mesenchymal stem cells in an agarose scaffold promotes a physis-like zonal alignment of chondrocytes. *J. Orthop. Res.* **30,** 1753–1759 (2012).

162. Mauck, R. L., Yuan, X. & Tuan, R. S. Chondrogenic differentiation and functional maturation of bovine mesenchymal stem cells in long-term agarose culture. *Osteoarthritis Cartilage* **14,** 179–189 (2006).

163. Huang, A. H., Yeger-McKeever, M., Stein, A. & Mauck, R. L. TENSILE PROPERTIES OF ENGINEERED CARTILAGE FORMED FROM

CHONDROCYTE- AND MSC-LADEN HYDROGELS. *Osteoarthr. Cartil. OARS Osteoarthr. Res. Soc.* **16,** 1074–1082 (2008).

164. Rocha, B. *et al.* Metabolic Labeling of Human Bone Marrow Mesenchymal Stem Cells for the Quantitative Analysis of their Chondrogenic Differentiation. *J. Proteome Res.* **11,** 5350–5361 (2012).
165. Li, Y. Y., Choy, T. H., Ho, F. C. & Chan, P. B. Scaffold composition affects cytoskeleton organization, cell–matrix interaction and the cellular fate of human mesenchymal stem cells upon chondrogenic differentiation. *Biomaterials* **52,** 208–220 (2015).
166. Ogura, T., Tsuchiya, A., Minas, T. & Mizuno, S. Methods of high integrity RNA extraction from cell/agarose construct. *BMC Res. Notes* **8,** (2015).
167. Kavalkovich, K. W., Boynton, R. E., Murphy, J. M. & Barry, F. Chondrogenic differentiation of human mesenchymal stem cells within an alginate layer culture system. *Vitro Cell. Dev. Biol.-Anim.* **38,** 457–466 (2002).
168. Hui, T. Y., Cheung, K. M. C., Cheung, W. L., Chan, D. & Chan, B. P. In vitro chondrogenic differentiation of human mesenchymal stem cells in collagen microspheres: Influence of cell seeding density and collagen concentration. *Biomaterials* **29,** 3201–3212 (2008).
169. Steward, A. J., Kelly, D. J. & Wagner, D. R. The role of calcium signalling in the chondrogenic response of mesenchymal stem cells to hydrostatic pressure. *Eur Cell Mater* **28,** 358–371 (2014).

170. Makihira, S. *et al.* Thyroid Hormone Enhances Aggrecanase-2/ADAM-TS5 Expression and Proteoglycan Degradation in Growth Plate Cartilage. *Endocrinology* **144,** 2480–2488 (2003).

171. Bau, B. *et al.* Relative messenger RNA expression profiling of collagenases and aggrecanases in human articular chondrocytes in vivo and in vitro. *Arthritis Rheum.* **46,** 2648–2657 (2002).

172. Johansson, N. *et al.* Collagenase-3 (MMP-13) is expressed by hypertrophic chondrocytes, periosteal cells, and osteoblasts during human fetal bone development. *Dev. Dyn.* **208,** 387–397 (1997).

173. Tavella, S., Raffo, P., Tacchetti, C., Cancedda, R. & Castagnola, P. N-CAM and N-Cadherin Expression during in Vitro Chondrogenesis. *Exp. Cell Res.* **215,** 354–362 (1994).

174. Takada, Y., Ye, X. & Simon, S. The integrins. *Genome Biol.* **8,** 215 (2007).

175. Kurtis, M. S., Schmidt, T. A., Bugbee, W. D., Loeser, R. F. & Sah, R. L. Integrin-mediated adhesion of human articular chondrocytes to cartilage. *Arthritis Rheum.* **48,** 110–118 (2003).

176. Loeser, R. F. Modulation of Integrin-Mediated Attachment of Chondrocytes to Extracellular Matrix Proteins by Cations, Retinoic Acid, and Transforming Growth Factor β. *Exp. Cell Res.* **211,** 17–23 (1994).

177. Murphy, J. M. *et al.* Reduced chondrogenic and adipogenic activity of mesenchymal stem cells from patients with advanced osteoarthritis. *Arthritis Rheum.* **46,** 704–713 (2002).

178. Orozco, L. *et al.* Intervertebral Disc Repair by Autologous Mesenchymal Bone Marrow Cells: A Pilot Study. *Transplantation* **92,** (2011).

179. Wynn, R. F. *et al.* A small proportion of mesenchymal stem cells strongly expresses functionally active CXCR4 receptor capable of promoting migration to bone marrow. *Blood* **104,** 2643–2645 (2004).

180. Son, B.-R. *et al.* Migration of Bone Marrow and Cord Blood Mesenchymal Stem Cells In Vitro Is Regulated by Stromal-Derived Factor-1-CXCR4 and Hepatocyte Growth Factor-c-met Axes and Involves Matrix Metalloproteinases. *STEM CELLS* **24,** 1254–1264 (2006).

181. Schoumacher, M., Goldman, R. D., Louvard, D. & Vignjevic, D. M. Actin, microtubules, and vimentin intermediate filaments cooperate for elongation of invadopodia. *J. Cell Biol.* **189,** 541–556 (2010).

182. Ridley, A. J. *et al.* Cell Migration: Integrating Signals from Front to Back. *Science* **302,** 1704–1709 (2003).

183. Huang, L. *et al.* Proteomic analysis of porcine mesenchymal stem cells derived from bone marrow and umbilical cord: implication of the proteins involved in the higher migration capability of bone marrow mesenchymal stem cells. *Stem Cell Res. Ther.* **6,** (2015).

184. Zhao, Y., Yan, Q., Long, X., Chen, X. & Wang, Y. Vimentin affects the mobility and invasiveness of prostate cancer cells. *Cell Biochem. Funct.* **26,** 571–577 (2008).

185. Menko, A. S. *et al.* A central role for vimentin in regulating repair function during healing of the lens epithelium. *Mol. Biol. Cell* **25,** 776–790 (2014).

186. Nieminen, M. *et al.* Vimentin function in lymphocyte adhesion and transcellular migration. *Nat. Cell Biol.* **8,** 156–162 (2006).

187. Barberis, L. *et al.* Leukocyte transmigration is modulated by chemokine-mediated PI3Kγ-dependent phosphorylation of vimentin. *Eur. J. Immunol.* **39,** 1136–1146 (2009).

188. Boyne, L. J., Fischer, I. & Shea, T. B. Role of vimentin in early stages of neuritogenesis in cultured hippocampal neurons. *Int. J. Dev. Neurosci.* **14,** 739–748 (1996).

189. Whipple, R. A. *et al.* Vimentin Filaments Support Extension of Tubulin-Based Microtentacles in Detached Breast Tumor Cells. *Cancer Res.* **68,** 5678–5688 (2008).

190. Paul, C. D., Hung, W.-C., Wirtz, D. & Konstantopoulos, K. Engineered Models of Confined Cell Migration. *Annu. Rev. Biomed. Eng.* **18,** 159–180 (2016).

191. Smith, H., Whittall, C., Weksler, B. & Middleton, J. Chemokines Stimulate Bidirectional Migration of Human Mesenchymal Stem Cells Across Bone Marrow Endothelial Cells. *Stem Cells Dev.* **21,** 476–486 (2011).

192. Sophia Fox, A. J., Bedi, A. & Rodeo, S. A. The Basic Science of Articular Cartilage. *Sports Health* **1,** 461–468 (2009).

193. Neidlinger-Wilke, C. *et al.* Mechanical loading of the intervertebral disc: from the macroscopic to the cellular level. *Eur. Spine J.* **23,** 333–343 (2013).

194. Klein, T. J. *et al.* Tissue engineering of stratified articular cartilage from chondrocyte subpopulations. *Osteoarthritis Cartilage* **11,** 595–602 (2003).

195. Han, E. *et al.* Shaped, Stratified, Scaffold-free Grafts for Articular Cartilage Defects. *Clin. Orthop.* **466,** 1912–1920 (2008).

196. Ng, K. W., Ateshian, G. A. & Hung, C. T. Zonal chondrocytes seeded in a layered agarose hydrogel create engineered cartilage with depth-dependent cellular and mechanical inhomogeneity. *Tissue Eng. Part A* **15,** 2315–2324 (2009).

197. Ng, K. W. *et al.* A layered agarose approach to fabricate depth-dependent inhomogeneity in chondrocyte-seeded constructs. *J. Orthop. Res. Off. Publ. Orthop. Res. Soc.* **23,** 134–141 (2005).

198. Nguyen, L. H., Kudva, A. K., Saxena, N. S. & Roy, K. Engineering articular cartilage with spatially-varying matrix composition and mechanical properties from a single stem cell population using a multi-layered hydrogel. *Biomaterials* **32,** 6946–6952 (2011).

199. Leone, G. *et al.* Continuous multilayered composite hydrogel as osteochondral substitute. *J. Biomed. Mater. Res. A* **103,** 2521–2530 (2015).

200. Lai, J. H., Kajiyama, G., Smith, R. L., Maloney, W. & Yang, F. Stem cells catalyze cartilage formation by neonatal articular chondrocytes in 3D biomimetic hydrogels. *Sci. Rep.* **3,** (2013).

201. Lee, C. S. D. *et al.* Integration of layered chondrocyte-seeded alginate hydrogel scaffolds. *Biomaterials* **28,** 2987–2993 (2007).

202. Gleghorn, J. P., Lee, C. S. D., Cabodi, M., Stroock, A. D. & Bonassar, L. J. Adhesive properties of laminated alginate gels for tissue engineering of layered structures. *J. Biomed. Mater. Res. A* **85A,** 611–618 (2008).

203. Gharravi, A. M. *et al.* Design and Fabrication of Anatomical Bioreactor Systems Containing Alginate Scaffolds for Cartilage Tissue Engineering. *Avicenna J. Med. Biotechnol.* **4,** 65–74 (2012).

204. Yeatts, A. B., Gordon, C. N. & Fisher, J. P. Formation of an aggregated alginate construct in a tubular perfusion system. *Tissue Eng. Part C Methods* **17,** 1171–1178 (2011).